UNIVERSITY OF VERONA

DEPARTMENT OF
Neurosciences, biomedicine and movement sciences

GRADUATE SCHOOL OF
Life and Health Sciences

DOCTORAL PROGRAM IN
Biomolecular Medicine
XXXV cycle / 2019-2022

WITH THE FINANCIAL CONTRIBUTION OF
University of Verona

TITLE OF THE DOCTORAL THESIS

TARGETING STAT3 SIGNALING WITH ESSENTIAL OILS: A POTENTIAL STRATEGY FOR ADJUVANT CANCER THERAPY

S.S.D BIO/10

Coordinator: **Prof.ssa Lucia de Franceschi**

Tutor: **Prof.ssa Sofia Giovanna Mariotto**

PhD candidate: **Muhammed Ashiq Thalappil**

MUHAMMED ASHIQ THALAPPIL

DOCTORAL THESIS

TARGETING STAT3 SIGNALING WITH ESSENTIAL OILS: A POTENTIAL STRATEGY FOR ADJUVANT CANCER THERAPY

07 MARCH 2023

Verona

ABSTRACT

STAT3 is signaling is aberrantly active in most of the solid and hematological cancers. Constitutive activation of STAT3 plays a critical role in regulating the hallmarks of cancer, therefore STAT3 is considered as a promising target for cancer therapy. There is a growing interest in exploring natural compounds as potential anticancer agents due to the toxic effects of synthetic anticancer drugs on healthy cells and the development of chemoresistance. Essential oils (EOs) are phyto-complexes that exhibit diverse anticancer effects. In this work, from a panel of EOs, we aimed to identify EOs with potential anti-STAT3 activity and anticancer effects in DU145 human prostate cancer cells that exhibit constitutive STAT3 activation. EOs of *Pinus mugo*, *Lavandula angustifolia*, *Pinus sylvestris*, and *Cupressus sempervirens* were selected as the most potent EOs in inhibiting constitutive STAT3 phosphorylation and inducing cytotoxicity. Notably, Pinus mugo EO (PMEO) showed low cytotoxicity in non-transformed human fibroblasts, suggesting the specificity to efficiently target cancer cells. The molecular mechanism of anti-STAT3 activity was further evaluated through spectrophotometric and fluorometric analyses, and the biological effect of STAT3 inhibition was analyzed by western blotting, qRT-PCR and flow cytometry and wound healing assay. PMEO treatment induced a rapid decline in glutathione (GSH) levels and an increase in reactive oxygen species (ROS) levels, leading to oxidative stress. Pre-treatment of cells with N-acetyl-cysteine (NAC), a cell permeable ROS scavenger, reversed the inhibitory action of PMEO on STAT3 phosphorylation, suggesting that the inhibition of STAT3 activation by PMEO is mediated by ROS. The suppression of the STAT3 signaling cascade reduced the expression of pro-proliferative and anti-apoptotic genes at mRNA and protein levels, leading to the inhibition of cell migration and apoptotic cell death. Additionally, a combination treatment revealed that PMEO acts synergistically with cisplatin in inducing cytotoxicity in cancer cells. Furthermore, a nanoformulation was developed by loading PMEO into PLGA nanoparticles (PMEO-NPs) to improve the efficiency of the EO. PMEO-NPs displayed sustained release of PMEO and effective uptake by MDA-MB-231 cells in vitro and exhibited more potent anticancer activities, including enhanced cytotoxicity through ROS generation, and increased apoptotic morphology in MDA-MB-231 cells. Moreover, both PMEO and PMEO-NPs effectively suppressed breast cancer stem cell markers, indicating their potential to combat cancer stemness and aggressiveness. Additionally, the results suggest the potential use of these EOs as adjuvant or complementary therapies to enhance the effectiveness of conventional chemotherapy in the treatment of aggressive cancer cells.

Contents

1. ABBREVIATIONS

H2DCFDA : 2'7'-dichlorodihydrofluorescein diacetate

DTNB : 5,5'-dithiobis(2-nitrobenzoic acid)

5-FU : 5-Flourouracil

v-Abl : Abelson murine leukemia virus

AO : Acridine orange

APRF : Acute-Phase Response Factor

ALDH1 : Aldehyde dehydrogenase 1

ALK : Anaplastic lymphoma kinase

ASOs : Antisense oligonucleotides

AhR : Aryl hydrocarbon receptor

bFGF : basic fibroblast growth factor

BSA : Bovine serum albumin

BCSC : Breast cancer stem cells

CSCs : Cancer stem cells

CPT1B : Carnitine palmitoyltransferase 1B

CML : Chronic myeloid leukemia

CNTF : Ciliary neurotrophic factor

CCD : Coiled-coil domain

CSEO : *Cupressus sempervirens* essential oil

TPGS : D-α-tocopheryl polyethylene glycol succinate

DATS : Diallyl trisulfide

DDR : DNA damage response

DBD : DNA-binding domain

DRI : Dose-reduction index

dsODNs : double stranded oligodeoxynucleotides

DMEM : Dulbecco's Modified Eagle Medium

EGF - Epidermal growth factor

EGFR: epidermal growth factor receptor

Etk: Epithelial and endothelial tyrosine kinase

EMT : Epithelial to Mesenchymal Transition

EOs : Essential oils

EtBr : Ethidium bromide

FAK : Focal adhesion kinase

FDA : Food and Drug Administration

FA : Fraction affected

GAS : Gamma activated sequence

GC-MS : Gas chromatography–mass spectrometry

GSC : Glioblastoma-derived stem cells

GSH : Glutathione reduced

GPCR : G-Protein coupled receptors

GQ-ODN : G-quadruplexes oligodeoxynucleotide

HBSS : Hanks' Balanced Salt Solution

HK2 : Hexokinase 2

HMGA1 : High Mobility Group A1

HDAC6 : Histone deacetylase 6

hTERT : Human telomerase reverse transcriptase

HIF-1α : Hypoxia inducible factor 1 alpha

IL-6R : IL-6 receptor

IGF-1 : insulin-like growth factor 1

ICAM-1 : intracellular adhesion molecule

KSHV : Kaposi's sarcoma-associated herpesvirus

LGL : Large granular lymphocytic

LMP1 : Latent membrane protein 1

LNEO : *Laurus nobilis* essential oil

LAEO : *Lavandula angustifolia* essential oil

LRG1 : Leucine-rich-alpha-2-glycoprotein 1

LIF - Leukaemia inhibitory factor

LD - Linker domain

LPS : Lipopolysaccharide

Lkb1 : Liver Kinase B1

Lck : Lymphocyte-specific protein tyrosine kinase

MEK : MAPK/ERK kinase

miRNAs : MicroRNAs

MUC1/4 : Mucin 1/4

MRP1 : Multidrug resistance protein 1

NAC : N-acetyl-l-cysteine

NRTKs : Non-receptor tyrosine kinases

NS5A : Non-structural protein 5A

NTD : N-terminal domain

NPM : Nucleophosmin

PRX : Peroxiredoxin

PMEO : *Pinus mugo* essential oil

PSEO : *Pinus sylvestris* essential oil

PDGF : Platelet-derived growth factor

PDGFA : Platelet-derived growth factor A

PMEO-NPs : PMEO loaded PLGA nanoparticles.

PDI : Polydispersity index

PEG-b-PCL : Polyethylene glycol-block-polycaprolactone

PLGA : Poly-lactic-co-glycolic acid

PVA : Polyvinyl alcohol

PVDF : Polyvinylidene difluoride

PIAS3 : Protein inhibitors of activated STAT3

PTPN9 : Protein tyrosine phosphatase nonreceptor type 9

PTPRD, PTPRT, PTPRK : Protein tyrosine phosphatase receptor-type D, T, and K

PTPs : Protein tyrosine phosphatases

PROTAC - Proteolysis targeting chimera

PDK1 : Pyruvate dehydrogenase kinase 1

PKM2 : Pyruvate kinase M2

RT-qPCR : Quantitative reverse transcription PCR

ROS : Reactive oxygen species

RTKs : Receptor tyrosine kinases

SEM : Scanning electron microscope

STAT3 : Signal Transducer and Activator of Transcription 3

siRNAs : Small interfering RNAs

SH2 : Src homology 2 domain

SHP1 and SHP2 - Src homology region 2 domain-containing phosphatase 1 and 2

SOD : Superoxide dismutase

SOCS : Suppressors of cytokine signaling

TC-PTP : T-cell protein tyrosine phosphatase

Trx : Thioredoxin

TrxR1 : Thioredoxin Reductase 1

TRAIL : TNF-related apoptosis-inducing ligand

TNM : Tumor size, lymph node involvement, and distant metastases

TAD : Transactivation domain

TEM : Transmission Electron microscope

TBST : Tris-buffered saline with 0.1% Tween 20

TAMs : Tumor associated macrophages

TME : Tumour microenvironment

TKI : Tyrosine kinase inhibitor

YAP : Yes-associated protein 1

TAZ : Transcriptional coactivator with PDZ-binding motif

uSTAT3: Unphosphorylated STAT3

2. INTRODUCTION

2.1. STAT3 Signaling Pathway

Transcription factors play crucial roles in cancer initiation, progression, and metastasis, making them attractive targets for cancer therapy. Among these transcription factors, Signal Transducer and Activator of Transcription 3 (STAT3) has been found to play crucial roles in cancer [1]. Constitutively active STAT3 has been identified as a pivotal driver of tumor progression, chemoresistance, and poor clinical prognosis in many types of cancer. As a result, STAT3 has emerged as a promising target for cancer therapy [1].

The discovery of STAT3 and the JAK-STAT pathway in general, is the culmination of series of landmark investigations by multiple laboratories. The discovery of Interferon by Alick Isaacs and Jean Lindenmann in 1957 initiated a series of landmark investigations that revolutionized the understanding of cell signaling pathways [2][3]. Cumulative results from studies by James E. Darnell, George R. Stark, and Andrew Wilks uncovered the JAK-STAT pathway and the roles of STAT1, STAT2, and JAK family protein-tyrosine kinases in interferon-dependent signaling. These findings established that cytokines and growth factors could activate STATs and led to the identification of the remaining members of the STAT family, including STAT3. In 1994, the Darnell group identified and described STAT3 as a 92 kDa protein activated in response to IL-6 and Epidermal growth factor (EGF). Earlier, in 1992, Wegenka et al had identified a protein called Acute-Phase Response Factor (APRF), which was rapidly activated by IL-6 through phosphorylation and bound to Gamma activated sequence (GAS) elements. Later, amino acid sequence analysis revealed that APRF is related to STAT3 [2].

In homeostatic conditions, STATs are transiently activated in response to extracellular signals such as cytokines, growth factors, and hormones. The precise function of the activated STAT transcription factors varies depending on the specific STAT protein and the context of the cellular response. Knockout studies in mice have demonstrated the essential role of specific STAT proteins in various normal physiological processes. Specifically, the absence of STAT1, STAT2, STAT4, and STAT6 resulted in compromised immune responses, increasing susceptibility to microbial and viral infections. Conversely, STAT3 knockout led to early embryonic lethality, and STAT5a and STAT5b knockouts were associated with a lack of mammary gland development and lactation [4].

It now well understood that STATs play a significant role in various normal cellular activities such as tissue growth, development, maintenance of homeostasis, and immune response. Conversely, dysregulation of STATs such as their hyperactivation can be causative of diseases including cancer. In particular, aberrant activation of STAT3 and STAT5 have been reported in many human cancers [5]. For instance, the activation of STAT5 plays a critical role in driving the progression of cancer in chronic myeloid leukaemia and TEL-JAK2-induced myeloproliferative disease [5]. However, dysregulation in STAT3 signaling is more frequent in cancers and constitutive activation of STAT3 have been linked to the oncogenic transformation in broad spectrum of solid and hematological cancers. Several studies have also linked constitutive STAT3 activation to poor prognosis in cancer patients.

2.1.1. Structure of STAT3

Structural studies have identified remarkable similarities in the domain architectures of the STAT family [6]. As depicted in the **figure 1**, the structure of STAT3 contain six functionally conserved domains, which are: (1) Src homology 2 (SH2) domain (SH2D) which recognizes and binds to specific phospho-tyrosine residues in the cell surface receptors and facilitate the dimerization, (2) transactivation domain (TAD) in the C-terminal that contains specific tyrosine residues which are phosphorylated upon interaction of ligands with their receptors, (3) N-terminal domain (NTD) which is responsible for protein-protein interactions that facilitate the formation of STAT dimers, (4) Coiled-coil (CCD) domain which is crucial for the interactions with regulatory proteins that maintain the stability of the STAT dimers (5) DNA-binding domain (DBD) which is necessary for the binding of the STAT dimers to specific target DNA sequences (6) a linker domain (LD) which links the DBD to the SH2D and plays an essential role in the flexibility of the STATs [6].
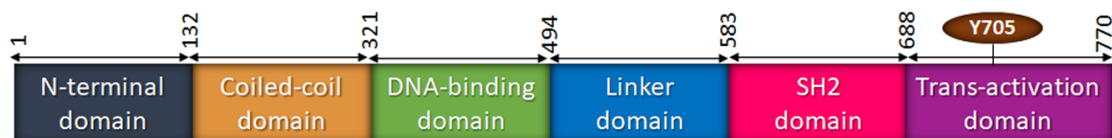
Figure 1. Structure of STAT3.

2.1.2. Canonical Pathway and the regulators Of STAT3 Activation

According to the canonical pathway, STAT3 can be activated by a broad spectrum of stimuli which include cytokines mainly belong to the IL-6 family including but not limited to IL-6, L-11, IL-22, IL-27, IL-31, Oncostatin M (OSM), Ciliary neurotrophic factor (CNTF), and leukaemia inhibitory factor (LIF).

Additionally, several growth factors, including epidermal growth factor (EGF), platelet-derived growth factor (PDGF), and insulin-like growth factor 1 (IGF-1), can activate STAT3 [6]. Chemokines such as Chemokine (C-C motif) ligand 5 (CCL5) and macrophage inflammatory protein)-1α (MIP) a are also reported to activate STAT3 through G-Protein coupled receptors (GPCR) in T cells [7]. Binding of these ligands to their cognate receptors activates the receptor, leading to the recruitment and activation JAKs (JAK1, JAK2, and TYK2). Activated JAKs then phosphorylate the tyrosine residues on the receptor, creating docking sites for STAT3. STAT3 is then recruited to the receptor, where it is also phosphorylated at the specific tyrosine 705 residue in the transactivation domains by JAKs This phosphorylation leads to the formation of STAT3 homodimers, which translocate to the nucleus and bind to specific DNA sequences to regulate the transcription of target genes. In addition to receptor tyrosine kinases (RTKs) and cytokine receptors, non-receptor tyrosine kinases (NRTKs) can also activate STAT3. NRTKs, such as Src and Abl, can directly phosphorylate and activate STAT3 independent of JAKs or receptors [7].

In normal non-transformed cells, the activation of STAT3 is a transient event that typically lasts from a few minutes to several hours. This activation is crucial for maintaining normal cellular events such as cell proliferation and proper immune responses [5]. Negative regulators of STAT3 play crucial role in maintaining the homeostasis of STAT3 activation. Wu et al. have recently published a comprehensive review of the negative regulators of STAT3 signaling [8]. They mainly include several proteins belonging to protein tyrosine phosphatases (PTPs), suppressors of cytokine signaling (SOCS) and protein inhibitors of activated STAT3 (PIAS3). PTPs can interact with STAT3 and inhibit of STAT3 signaling via directly dephosphorylating STAT3 at Y705. Examples of PTPs that target STAT3 include Protein tyrosine phosphatase receptor-type D, T, and K (PTPRD,PTPRT,PTPRK) and Src homology region 2 domain–containing phosphatase 1 and 2 (SHP1 and SHP2), Protein tyrosine phosphatase nonreceptor type 9 (PTPN9) and T-cell protein tyrosine phosphatase (TC-PTP). SOCS proteins, mainly SOCS1 and SOCS3, bind to activated cytokine receptors and inhibit the downstream signaling, ultimately blocking STAT3 activation. PIAS3, on the other hand, repress STAT3 transcriptional activity by blocking its DNA binding and coactivator recruitment. An illustration depicting the events in canonical activation of

STAT3 signaling and its regulators are presented in the **figure 2**. Dysregulation of these negative regulators lead to the constitutive activation of STAT3 signaling, which is a major contributing factor to cancer development. For instance, reduced levels of PIAS3 in glioblastoma tumour tissues is correlated with the elevated levels of phosphorylated STAT3 [9]. Moreover, it has been found that epigenetic silencing of SOCS1, SOC3 and SHP1 through hypermethylation is responsible for sustained STAT3 activation in several types of cancers including Lung cancer, Gastric cancer, Hepatocellular carcinoma, Cholangiocarcinoma, Head and neck squamous cell carcinoma, large cell lymphoma, chronic myeloid leukaemia, and multiple myeloma [10][11][12][13]. Moreover, various studies have shown that loss of function mutations in PTPs including PTPRT and PTPRD led to the constitutive activation of STAT3 in head and neck squamous cell carcinoma cells [14].

Somatic mutations in STAT3 have also been observed in various cancers, leading to abnormal activation and increased transcriptional activity. These mutations include those in the SH2 domains, resulting in constitutive phosphorylation and independent homodimerization. Hematological malignancies and diffuse large B cell lymphoma also exhibit activating mutations. Mutations in upstream activators like EGFR and JAK2-V617F contribute to persistent STAT3 activation in glioblastoma and myeloproliferative neoplasms[15][16][17].
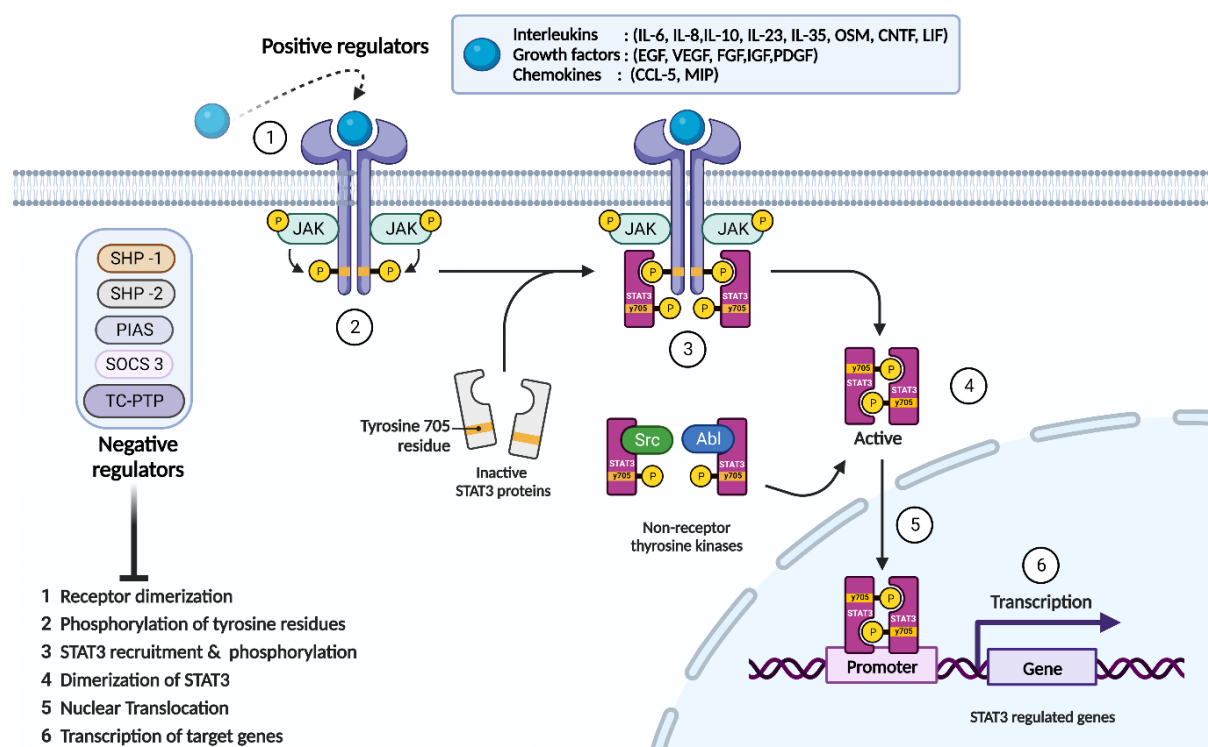
Figure 2. Overview of canonical pathway and the regulators of STAT3 activation. There are six key events in the STAT3 signaling cascade and STAT3 activation is tightly regulated by the activity of negative regulators.

2.1.3. Non Canonical STAT3 Pathways

Recent evidence suggests the presence alternative post-translational modifications for activating STAT3, termed as the noncanonical pathways [18]. Phosphorylation at S727 and acetylation at K685 are two such modifications with important implications in cancer. Initially, it was believed that the phosphorylation of S727 in STAT3 was dependent on prior activation of Y705 and was necessary for its full transactivation. However, recent findings indicate that STAT3 can also be activated through the S727 phosphorylation independent of Y705 phosphorylation [18]. This has been observed in certain cancer types such as chronic lymphocytic leukemia, prostate cancer and ER-negative breast cancer, where overexpression of pS727 is detected in tumor tissues without concurrent pY705 activation [18,19]. Predominant expression of pS727 STAT3 has been linked to radiation resistance in glioblastoma and serves as a predictive marker for poorer clinical outcomes [18]. Moreover, S727 phosphorylation on STAT3 is integral to mitochondrial localization of STAT3. Mitochondrial STAT3 has been shown to regulate metabolic changes and promote tumor growth in breast cancer [20]. Acetylation of the K685 residue, on the other hand, has been reported to induce STAT3 dimerization in the absence of phosphorylation, promote nuclear translocation of STAT3, and regulate the expression of STAT3 target genes to promote oncogenesis [20].

Emerging studies also report the presence of transcriptionally active STAT3 dimers in the absence of phosphorylation, signifying the role of unphosphorylated STAT3 (uSTAT3) in oncogenesis [21,22]. Furthermore, nuclear-localized uSTAT3 has been implicated in the regulation of gene expression through direct interactions with the STAT3 promoter and M67, a modified c-fos cis-inducible enhancer sequence[21]. Furthermore, it has been observed that the overexpression of uSTAT3, rather than pSTAT3 homodimers, leads to the transcription of specific mRNAs including Cyclin B1, E2F1, MRAS, and Met, which have been found to be highly expressed in various cancer types, including breast cancers and head and neck squamous cell carcinomas [21].

2.2. STAT3 Activation And The Hallmarks Of Cancer

In 2022 in the review the 'Hallmarks of Cancer: New Dimensions', Hanahan and Weinberg define the principal hallmarks of cancer, a set of fundamental characteristics that are acquired by cells as they transform into cancerous cells. Currently there are eight hallmarks to cancer, which are 1. Sustaining proliferative signaling, 2. Evading growth suppressors, 3. Resisting cell death, 4. Enabling replicative immortality, 5. Inducing angiogenesis, 6. Activating invasion and metastasis, 7. Reprogramming cellular energy metabolism and 8. Evading immune destruction. In addition, 'Tumor-promoting inflammation' and 'Genomic instability and mutations' have been described as two enabling characteristics to the eight fundamental hallmarks. Compelling evidence can be traced from the literature for the role of constitutively active STAT3 signaling in driving these cancer hallmarks as well as other challenges such as promoting cancer stem cells and development of chemoresistance [23]. An illustration summarising major genes regulated by STAT3 and the corresponding role STAT3 activation in mediating cancer hallmarks, enabling mechanisms such as genomic instability and replicative immortality, and in other major challenges such as chemoresistance, and promoting cancer stem cells is represented in the **figure 3**.

2.2.1. STAT3 Activation In Genome Instability, Replicative Immortality And Sustaining Proliferative Signaling

STAT3 directly regulates the transcription of several genes such as Cyclin D1, cyclin B, cdc2, c-Myc, PLK-1, and Pim1 that are involved in cell proliferation and the regulation of cell cycle progression [24]. The elevated expression of these genes through dysregulated STAT3 activation has been reported in various cancers. For instance, persistent STAT3 activation leading to the overexpression of Cyclin D1 has been shown to promote hyperproliferation of gastric and colon cancer cells [25]. Bollrath et al. demonstrated that hyperactivation of STAT3 through the gp130/IL-6/IL-11 axis serves as a crucial link between chronic inflammation and tumor promotion in enterocytes, leading to colitis-associated tumorigenesis.

They have identified that the hyperproliferation and increased cell survival resulting from STAT3 stimulation were due to the downregulation of key genes regulated by STAT3, including cyclin D1, c-Myc, Cdc2 and cyclin B1 [26]. Furthermore, Béguelin et al. has identified that progesterone receptor activated HER2 acts as a coactivator of STAT3, and their complex drive the activation of the cyclin D1 promoter, enhance Cyclin D1 expression and promote the proliferation of breast tumors *in vitro* and *in vivo* [27].

Replicative immortality is another of the hallmarks of cancer, which refers to the ability of cancer cells to divide and replicate indefinitely without undergoing senescence or apoptosis. Human telomerase reverse transcriptase (hTERT) which is frequently overexpressed in cancer cells is an enzyme that plays a crucial role in the maintenance of telomeres by adding new telomere repeats onto the ends of chromosomes, thereby preventing telomere shortening and enabling cells to divide indefinitely. According to Konnikova et al. constitutively active STAT3 directly regulates the expression of hTERT and drive replicative immortality in human cancer and primary cells [28]. Lastly, STAT3 plays a critical role in the DNA damage response (DDR) signaling network, which is essential for maintaining genome stability and defending against tumorigenesis. However, to promote cell proliferation and transformation, viral and cellular oncogenes must overcome the cell-cycle checkpoints induced by DDR. Koganti et al. demonstrated that STAT3 activated by Epstein-Barr virus infection triggers the activation of Caspase 7 which then cleaves Claspin, a protein that plays a crucial role in the DNA damage response pathway. This event impairs the ability of ATR to phosphorylate Chk1, which is indispensable for the activation of the intra-S phase checkpoint. Bypassing of this critical cell-cycle checkpoint promotes uncontrolled and tumorigenic cell proliferation [29].

2.2.2. STAT3 Activation And Resistance To Apoptosis

STAT3 mediates anti-apoptotic mechanisms by regulating the expression of several genes and promote the survival of cancer cells. Inhibition of the tumor suppressor genes p53 by activated STAT3 in multiple tumor cells is a major example [30]. STAT3 also regulates the expression of several anti-apoptotic proteins and growth suppressors like Bcl-2, Bcl-XL, Mcl-1, Survivin and XIAP. and contribute to cell survival via resistance to apoptosis. Grandis et al. has shown that EGFR mediated activation of STAT3 signaling blocks apoptosis in head and neck squamous cell carcinoma cells *in vitro* and *in vivo* [31]. Further, Rahaman et al. observed that glioblastoma multiforme cells with high levels of constitutively active STAT3 exhibit elevated expression of Bcl-2, Bcl-XL, and Mcl-1. Conversely, treatment with AG-490, an inhibitor of STAT3 activation, suppresses the expression of these proteins and induces apoptosis [32]. Whereas Gritsko et al. show that survivin as a direct downstream target of STAT3 and observed that sustained activation of STAT3 signaling induces the expression of survivin, which confers resistance to apoptosis in cells of breast cancer [33]. Moreover, in LGL leukemia it has been demonstrated that overexpression of v-Src activates STAT3, which in turn enhances the expression of Mcl-1, promoted the survival of Leukemic LGL-clones [34].

2.2.3. STAT3 Activation And Induction Of Tumour Angiogenesis

Many reports describe that constitutively activated STAT3 upregulates the transcription of Vascular endothelial growth factor (VEGF), one of the key mediators of angiogenesis in several human cancer cells including breast carcinoma, head and neck carcinoma and melanoma [35]. Moreover, STAT3 stimulates formation of tumor vascular capillaries and stimulated tumor angiogenesis in vivo [36]. Furthermore, in the hypoxic tumour microenvironment, STAT3 activation mediated by Hypoxia inducible factor 1 alpha (HIF-1α) promotes angiogenesis by increasing VEGF expression [35]. Interestingly, Kujawski et al. identified that activation of STAT3 signaling in the Myeloid-derived suppressor cells and macrophages isolated from mouse tumors induced angiogenesis in vitro by increasing the expression of angiogenic factors, including VEGF and bFGF (basic fibroblast growth factor). This finding signifies that besides to the tumor cells, STAT3 activation in the cells in TME can also contribute to induction of angiogenesis [37]. A recent finding by Shen et al. revealed that Yes-associated protein 1 (YAP)/Transcriptional coactivator with PDZ-binding motif (TAZ) nuclear translocation and activity stimulated by the activation of STAT3 signaling promoted tumor vascularization and angiogenesis in human colorectal carcinomas and melanoma cells [38]. Furthermore, He et al. reported that leucine-rich-alpha-2-glycoprotein 1 (LRG1) was overexpressed in gastric tumour tissues which was shown to promote tumour angiogenesis by activating Src-STAT3 signaling pathway [39].

2.2.4. STAT3 Activation In Promotion Of Tumour Invasion And Metastasis

Activated STAT3 regulate the expression of various genes involved in tumour Invasion to extracellular matrix, a key process responsible for in tumor progression and metastasis. these STAT3 is has been shown to upregulate the expression of various metalloproteinases (MMPs), family of proteins that facilitate cancer cell invasiveness by degrading extracellular matrix proteins. STAT3 has been demonstrated to directly regulate the expression of MMP-1 (also known as Collagenase 1) in T24 bladder cancer cells and colon cancer cells [40]. Xie et al. discovered that in highly metastatic clones of K-1735 melanoma cell line, activated STAT3 signaling directly regulates the expression of MMP-2 resulting in tumor invasion and metastasis [41]. Results from studies carried out in MCF-7 breast cancer cells further identified that expression of MMP-7 and MMP-9 are also induced by direct transcriptional activity of activated STAT3 [42][43]. Snyder et al. identified that Fascin, an actin binding protein, is implicated in driving the migration, invasion, and metastasis of tumor cells. Their investigation demonstrated that in both mouse (4T1) and human (MDA-MB231) breast cancer cells, Fascin is directly regulated by STAT3 in response to OSM and IL-6 [44].

Epithelial to Mesenchymal Transition (EMT) is a process by which epithelial cells, which are typically tightly interconnected and exhibit apical-basal polarity, acquire mesenchymal traits such as increased migratory capacity and resistance to apoptosis. STAT3 directly regulate the expression of multiple genes involved in EMT. Vimentin, a type III intermediate filament protein mainly expressed during EMT, has been found to be a direct transcriptional target of STAT3 in triple negative breast cancer cells MD-MBA-231 [40]. Downregulation of E-cadherin is another frequent driving factor of EMT in cancers [45]. Interestingly, STAT3 regulated the expression of proteins such as TWIST and ZEB1, that are transcriptional repressors of E-cadherin [45]. Moreover, Ma et al. recently reported that activated STAT3 promote the expression of estrogen-related receptor a (ERR-α) which concomitantly enhanced EMT, migration and invasion of MD-MBA-231 cells through the upregulation of ZEB1, N-cadherin, and vimentin and downregulation of E-cadherin [46]. STAT3 has been shown to regulate the expression of Rho-GTPase family proteins such as Cdc42 and RhoU that are involved in promoting the migration of various cancer cells [47][48]. Furthermore, Lim et al. have demonstrated that the expression of intracellular adhesion molecule (ICAM-1) stimulated by Src mediated STAT3 activation promotes poor prognosis by regulating EMT and angiogenesis in colorectal cancer [49].

2.2.5. STAT3 Activation In Promoting Immunosuppression

Several studies have demonstrated that STAT3 activation promote immunosuppression and pro-tumour inflammation. Activated STAT3 also mediate multiple levels of crosstalk between tumor cells and other cells in the tumour microenvironment (TME) leading to tumor-induced immunosuppression [50]. Constitutively active STAT3 promotes the expression of immunosuppressive factors such as VEGF, IL-6, and IL-10 in tumour cells that influence the immune cells in the TME to derive at an immunosuppressive environment [51]. For example, the immunosuppressive factors such as IL- 6, IL-10, and VEGF induced by STAT3 has been shown to suppress dendritic cell generation through reducing protein kinase C beta II (PKCβII) expression [51]. Likewise, IL-6 and IL-8 secreted by tumour cells has been reported to impair the cytotoxic function of NK cells through the activation of STAT3 pathway in oesophageal squamous cell carcinoma [52]. A study has found that tumour derived lactate act as an oncometabolite in the TME that drives macrophage M2-polarization by activating STAT3 and promote the proliferation of breast cancer cells [53]. In a similar note, M2 polarization stimulated by the activation of STAT3 signaling induced the resistance of prostate cancer cells to cytotoxic action of NK cells [54]. Consistent with these, in gastric tumour tissues IL-6 induced STAT3 activation was reported to drive M2 macrophage differentiation that exerted a pro-tumor function also correlated with the

low survival of the patients [55]. Exosome play critical roles in tumour promoting intracellular crosstalk. Interestingly, it has been reported that exosomes from glioblastoma-derived stem cells (GSC) contain various immunosuppressive components that trigger M2 macrophage polarization and PD-L1 expression through the activation of STAT3 signaling and promote tumour immunosuppression [56]. STAT3 activation in Cancer associated fibroblast cells also has been reported to promote immunosuppression in the TME. For instance, IL-6/IL-11 induced STAT3 activation in CAFs promotes colorectal tumour development and is correlated with poor prognosis [57]. Furthermore, IL-6 produced by hepatocellular carcinoma derived CAFs induced STAT3 activation in neutrophils and triggered the expressions of PDL1, IL8, CD66b, TNFα, and CCL2 fostering to an immunosuppressive environment [58]. Lastly, in breast cancer derived CAFs, upregulated expression of Histone deacetylase 6 (HDAC6) promoted immunosuppression through STAT3 mediated COX2 overexpression [59].

2.2.6. STAT3 Activation In Reprogramming Cellular Metabolism

Recently due to abundance of evidence, reprogramming of cellular energy metabolism has been inducted into the hallmarks of cancer stem cells. Cancer cells exhibit a metabolic phenomenon known as the "Warburg effect," in which they convert pyruvate into lactate even in the presence of oxygen, through a process called aerobic glycolysis [60]. This altered metabolism allows cancer cells to generate energy more quickly and maintain rapid cell proliferation, which is critical for their survival and growth. It has been demonstrated that STAT3 activation play crucial roles in regulating the metabolism of cancer cells and promoting the Warburg effect [61]. It has been found that Pyruvate kinase M2 (PKM2), Hypoxia inducible factor 1-α (HIF1-α), and STAT3 engage in a cyclic feedback loop activity to control cancer cell metabolism. PKM2 activates HIF1 alpha, which then increases the expression of genes involved in glycolysis and glucose uptake. Similarly, STAT3 activates HIF1 alpha, which also leads to more glucose uptake and glycolysis. Additionally, PKM2 can directly activate STAT3 by phosphorylation [62][60].

Moreover, a recent study reported that in liver precancerous lesions upregulated expression of pSTAT3 promotes the Warburg effect by inducing PKM2 [63]. Moreover, in triple negative breast cancer cells (MD-MBA-231), miR-155, a pro-inflammatory regulator that is known to link inflammation and cancer, has been demonstrated to induce STAT3 activation. This activated STAT3, in turn, directly regulates the expression of Hexokinase 2 (HK2), a glycolytic enzyme known to promote the Warburg effect [64]. Additionally, Qin et al. have demonstrated that STAT3 activation induces the upregulation of HIF1α and its downstream targets including lactate

dehydrogenase A (LDHA), and pyruvate dehydrogenase kinase 1 (PDK1) leading to increased glycolysis in myeloma cells [65].

2.2.7. STAT3 Activation In Promoting Cancer Stem Cells

Cancer stem cells (CSCs) are a small subpopulation of cancer cells within heterogeneous tumors that possess the unique ability to self-renew and differentiate into various cell types [66]. CSCs have also been found to exhibit metabolic reprogramming through Warburg effect and have been associated with cancer recurrence following chemotherapy or radiotherapy [66]. Several lines of evidence have established crucial role for STAT3 signaling in the induction of cancer stemness properties. Recently, RNAseq analysis of cancer stem-like cells derived from colorectal cancer cells HCT116 and HT29 identified that STAT3, along with platelet-derived growth factor A (PDGFA) is crucial for the survival and tumor-sphere formation of the cancer stem cells and pharmacological suppression of STAT3 activation using homoharringtonine significantly reduced the formation and survival of HT29-derived tumor-spheres [67].

Activated STAT3 can regulate the expression of stemness associated transcription factors such as SOX2, OCT4, NANOG and MYC [40]. Kim et al. showed that IL-6/AK1/STAT3 signaling activation engage to convert non-CSC like breast cancer cells to CSC like cells through the upregulation of OCT4 [68]. It has been shown that activated STAT3 was necessary for the growth and self-renewal of Glioblastoma stem cells. In contrast, transient inhibition of STAT3 led to growth arrest, impeded the formation of neurospheres and depleted the expression of GBM-SCs stemness markers of such as Olig2 and Nestin [69]. Further, it has been reported that transcriptional regulation of Carnitine palmitoyltransferase 1B (CPT1B) through Leptin-JAK2/STAT3 signaling regulated fatty acid oxidation which in turn induced chemoresistance and self-renewability in breast cancer stem cells [70]. In a similar note, a recent report has shown that a high levels of Aryl hydrocarbon receptor (AhR) is associated with an aggressive tumor phenotype and poor survival in non-small cell lung cancer cells and upregulation and activation of AhR have been found to enhance cancer stem-like properties through activated Jak2/STAT3 signaling pathway [71]. Won et al. have shown that in hepatocellular carcinoma, the upregulation of stemness marker CD133 was mediated to through STAT3 activation [72]. Consistent with this, STAT3 activation was also found to be responsible for the highly aggressive and malignant features *in vitro* and *in vivo* of CD133 expressing cancer stem-like cells isolated from Wilms' tumor cells (a rare kidney carcinoma that primarily affects children) [73].

2.2.8. STAT3 Activation In Chemoresistance

Cancer cells often evolve with several mechanisms to bypass the effects of chemotherapy drugs. Accumulating evidence points out STAT3 signaling as one of the major contributors to chemoresistance. In 2002, Real et al. reported that in metastatic breast cancer cells, overexpression of Bcl2 through STAT3 activation was responsible for the resistance to Taxol induced apoptosis [74]. Recently, tumor associated macrophages (TAMs) have been shown to induce resistance to Paclitaxel in breast cancer cells through activating IL-10/STAT3 signaling and concomitantly upregulating the expression of Bcl2 [75]. The resistance of oral squamous cell carcinoma cells to TPF (Cisplatin in combination with 5FU (5-fluorouracil) and docetaxel) was also demonstrated to be mediated by STAT3 activation and the downregulation of Mcl-1 [76]. Fang et al. have found that the overexpression of the long non-coding RNA (lncRNA) MALAT1 was associated with resistance to cisplatin in lung cancer cells. The authors further demonstrated that this resistance was mechanistically linked to the activation of STAT3, and the upregulation of proteins related to multidrug resistance, including MDR1 (also known as ABCB1 or P-gp) and multidrug resistance protein 1 (MRP1) [77]. A recent discovery revealed that exosomes derived from colorectal cancer cells resistant to 5-fluorouracil (5-FU) contained pSTAT3, and when taken up by otherwise 5-FU-sensitive CRCs, induced acquired resistance to the drug [78].

Multiple evidence also links feedback activation of STAT3 by various chemotherapy drugs in as a chemoresistance mechanisms in multiple cancer models. Resistance to Trastuzumab in HER2-positive breast and gastric cancers has been associated with a positive feedback loop mechanism activating STAT3, mediated by upstream mediators like fibronectin, EGF, and IL-6, as well as downstream effectors like mucins (MUC1/4) [79]. Likewise, melanoma cells have been shown to develop resistance to MAPK/ERK kinase (MEK) inhibitors through the feedback activation of Src/Focal adhesion kinase (FAK)/STAT3 signaling axis [80]. EGF/EGFR inhibitors are ideally supposed to suppress tumor growth by blocking STAT3 signaling activation. However, clinical findings suggest that tumors can become resistant to these inhibitors by upregulating STAT3 signaling activation through feedback mechanisms [81]. Likewise, Wen et al. found that inhibiting STAT3 activation with JAKi can synergistically increase the anti-tumor activity of gefitinib, another EGFR inhibitor, in human ovarian cancer cells [82]. Collectively, these findings point out the critical role of STAT3 activation in the development of chemoresistance and imply that targeting STAT3 activation can be a promising strategy for combating chemoresistance.
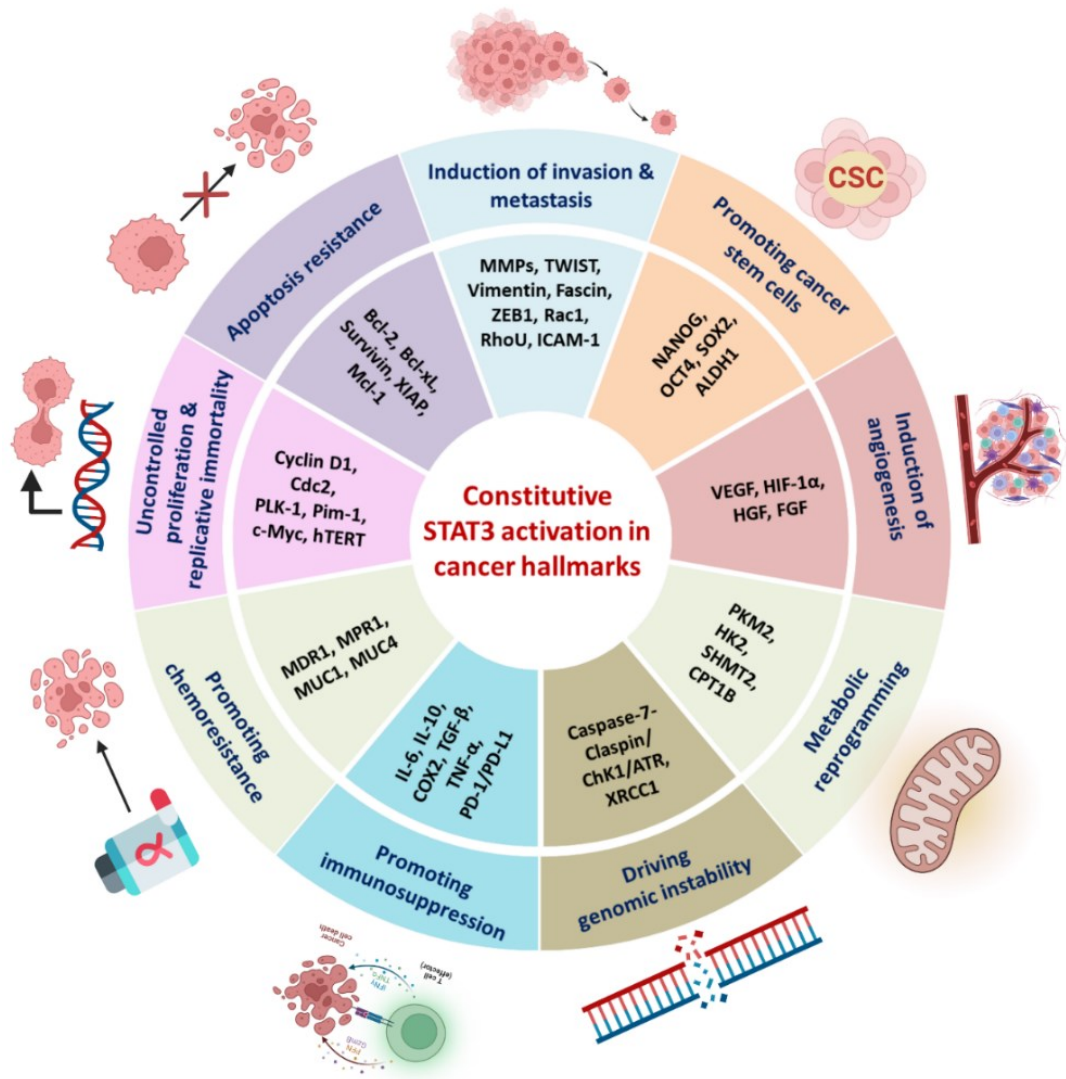
Figure 3: Major STAT3 target genes and the role of STAT3 activation underlying the cancer hallmarks and other challenges such as chemoresistance and promoting cancer stem cells.

2.3.   Targeting STAT3 Signaling For Cancer Therapy

Given the crucial involvement of STAT3 signaling in numerous aspects of cancer development and progression, targeting STAT3 signaling represents a promising approach for cancer therapy. Pharmacological strategies that specifically target STAT3 can be classified into various subclasses, which are discussed below and summarized in the **figure 4**.

2.3.1. Targeting Upstream Regulators Of STAT3

IL-6 widely overexpressed in most of the cancers, and we have discussed crucial role for IL-6 in the activation of STAT3 signaling pathway. Targeted inhibition of IL-6 or IL-6 receptor have been shown to efficiently suppress STAT3 activation and counteract tumour growth in various studies [83].

By far monoclonal antibodies specifically raised against them are the leading examples for the targeted inhibition IL-6 and IL-6R. For example, Siltuximab, is a recombinant human-mouse chimeric monoclonal antibody that is raised against IL-6 has been reported effectively suppress the activation and nuclear translocation of STAT3 [83]. As a result, the expression of STAT3 target genes such as Mcl-1, Bcl-XL, and Survivin were downregulated ovarian cancer cells [83]. Tocilizumab, on the other hand, is a recombinant monoclonal antibody designed to target the IL-6 receptor (IL-6R). FDA has approved Tocilizumab for patients with rheumatologic disorders, those with cytokine release syndrome resulting from chimeric antigen receptor T cell therapy, and certain hospitalized adults who have been diagnosed with COVID-19. Interestingly, Tocilizumab has demonstrated its effectiveness in suppressing prostate cancer growth and metastasis by inhibiting the activation of IL-6/STAT3 signaling, either alone or in combination with Stattic, which is a well-known STAT3 inhibitor [84]. Additionally, couple of other studies have demonstrated that Toclizumab could effectively overcome resistance to Tamoxifen and docetaxel through suppressing IL-6/STAT3 signaling pathway in breast cancer cells [85].

Pharmacological inhibition of the upstream kinases in the STAT3 signaling cascade has been reported to suppress STAT3 activation in several cancer models *in vitro* and *in vivo*. Several small molecule inhibitors have been investigated as upstream kinase inhibitors of STAT3. AZD1480, a JAK2 inhibitor, demonstrated efficient blockage of STAT3 signaling and suppressed cancer cell growth both *in vitro and in vivo* mouse models of head and neck squamous cell carcinoma and myeloma cells [86][87]. Similarly, Ruxolitinib, a JAK1/2 inhibitor approved by Food and Drug Administration (FDA) to treat inflammatory diseases, has been shown to overcome cisplatin resistance in non-small-cell lung cancer cells by inducing the activation of STAT3 signaling [87]. Dasatinib, targets multiple tyrosine kinases, including Src and Abl, has been found to have inhibitory effects on STAT3 phosphorylation in tumour tissues from Acute Myeloid Leukemia patients [88]. Likewise, AG490 is another broad-spectrum tyrosine kinase that can inhibit JAK2, EGFR, and JAK3, inhibited STAT3 phosphorylation and induced apoptosis in multiple human cancers acute such as lymphoblastic leukemia, glioblastoma, breast carcinoma, gastric carcinoma and hepatoma [25,89–92].

2.3.2. Targeting STAT3- SH2 Domain And Dimerization

The interaction between tyrosine residues on STAT3 receptors and the dimerization of activated STAT3 monomers both rely heavily on the STAT3 SH2 domain. This domain facilitates communication between tyrosine residues and plays a critical role in binding to phosphorylated tyrosine residues during dimerization.

Initially researchers have explored various Peptides and Peptidomimetics inhibitors of STAT3, such as those designed on the STAT3 SH2 domain sequence containing a tyrosine-phosphorylation site (PY*LKTK), have shown promising results in preventing the dimerization and translocation of STAT3 into the nucleus. These compounds have demonstrated proapoptotic and antitumor activity in cancer cells, making them a potential therapeutic option for cancer treatment. However, several limitations such poor membrane permeability and low cellular uptake and *in vivo* instability restricted their further progress. Circumventing these limitations, researchers then rationally designed several small molecules targeting the STAT3 SH2 domain, including Stattic, WB436B, OPB-31121, OPB-51602, HJC0416, HJC0152, S3I-201, SH-4-54 and STA-21 [51][93][1]. These molecules have shown efficacy in inhibiting STAT3 activation, dimerization, and nuclear translocation, as well as decreasing cell proliferation and inducing apoptosis in cancer cell lines [94]. Moreover, OPB-31121 and OPB-51602 are currently undergoing clinical trials [51].

2.3.3. Targeting DNA-Binding Activity Of STAT3

Inhibiting the DNA binding capacity will have significant antitumour effects as it downregulates the expression of STAT3 target genes. The first line of evidence in this regard was reported by Wolfrum et al., who showed that DBD-1, a peptide aptamer that recognize STAT3-DBD induced apoptosis in tumour cells by efficiently inhibiting the constitutive STAT3 signaling [95]. Turkson et al., developed platinum-containing compounds namely CPA-1 and CPA-7 that can regress the tumour growth *in vitro* and *in vivo* by selectively disrupting STAT3 signaling through impairing the DNA-Binding activity [96]. Other small molecules such as BBI608 (Napabucasin), (E)-2-methoxy-4-(3-(4-methoxyphenyl)prop-1-en-1-yl)phenol (MMPP), S3-54 are also reported to selectively disrupt the STAT3 DNA-binding activity and exert tumour suppressing activities [97][98][99].

Furthermore, double stranded oligodeoxynucleotide (dsODNs), which are types of synthetic DNA molecules have been designed to mimic cis regulatory elements STAT3 gene. They work by competing with active transcription factor dimers and block the induction of gene expression. Multiple reports have demonstrated that dsODNs impede STAT3 DNA binding and supress the growth of human cancer cells including lung cancer cells and of head and neck small cell carcinoma [100]. G-quadruplexes ODNs (GQ-ODNs) have also shown to inhibit STAT3 signaling by inhibiting the DNA-binding activity in multiple cancer cells including High Mobility Group A1 (HMGA1) transgenic T-cell leukemia, head and neck small cell carcinoma, breast cancer and prostate cancer [101,102].

2.3.4. Inhibitors Targeting STAT3 Expression

Another approach to targeting STAT3 is inhibiting its expression by targeting the mRNA. There are several strategies for targeting the mRNA and suppress the expression of a protein, including antisense oligonucleotides (ASOs), small interfering RNAs (siRNAs), and microRNAs (miRNAs). ASOs can selectively inhibit the translation of STAT3 mRNA by binding to single-stranded RNA sequences in a complementary fashion. Treatment with specific ASOs such as AZD9150 has been shown to reduce neovascularization, inhibit metastasis and growth of cancer cells and reduce chemoresistance [51][103]. Knockdown of STAT3 using small interfering RNA (siRNA) has been found to be effective in inhibiting the growth of tumours [104]. Furthermore, STAT3 inhibiting miRNAs are also being explored in addition to siRNAs and ASOs. For example, delivering miR-125b, which is downregulated in various malignant tumors, has been demonstrated to exerts antitumor functions in cutaneous squamous cell carcinoma by directly suppressing STAT3 expression [105]. Similarly, miRNA-124-3p inhibited the growth and metastasis of nasopharyngeal carcinoma cells by targeting STAT3 [106].

2.3.5. Pharmacological Degradation Of STAT3 Protein

Few novel methods are being explored for efficient degradation of STAT3 proteins in cancer cells. Targeted degradation of STAT3 by proteolysis targeting chimera (PROTAC) is an example for this. PROTACs are bifunctional molecules that can bind to bind to STAT3 and an E3 ubiquitin ligase. This complex then accelerates STAT3 ubiquitination and subsequent degradation by the proteasome system. SD-36 was the PROTAC degrader designed for targeted STAT3 degradation and has demonstrated growth inhibitory activity in leukemia and lymphoma cell lines [107].

Successively the same group developed SD-91, by modifying SD-36 and demonstrated highly selective and efficient targeted degradation of STAT3 [108]. Moreover, TSM-1 is a recently developed PROTAC degrader targeting STAT3. It was designed using toosendanin, tetracyclic plant triterpenoid and demonstrated to promote cell cycle arrest and apoptosis in epithelial tumor cells [108]. A recently published study by Kim et al. demonstrated STAT3 degradation in cancer cells by using a ROS generating metal chelator named KS10076. Mechanistically, KS10076 increased STAT3 ubiquitination followed by proteasome degradation. As a result, KS10076 promoted autophagic cell death and eliminated cancer stem cells in both *in vitro* and *in vivo* colon cancer models [109].
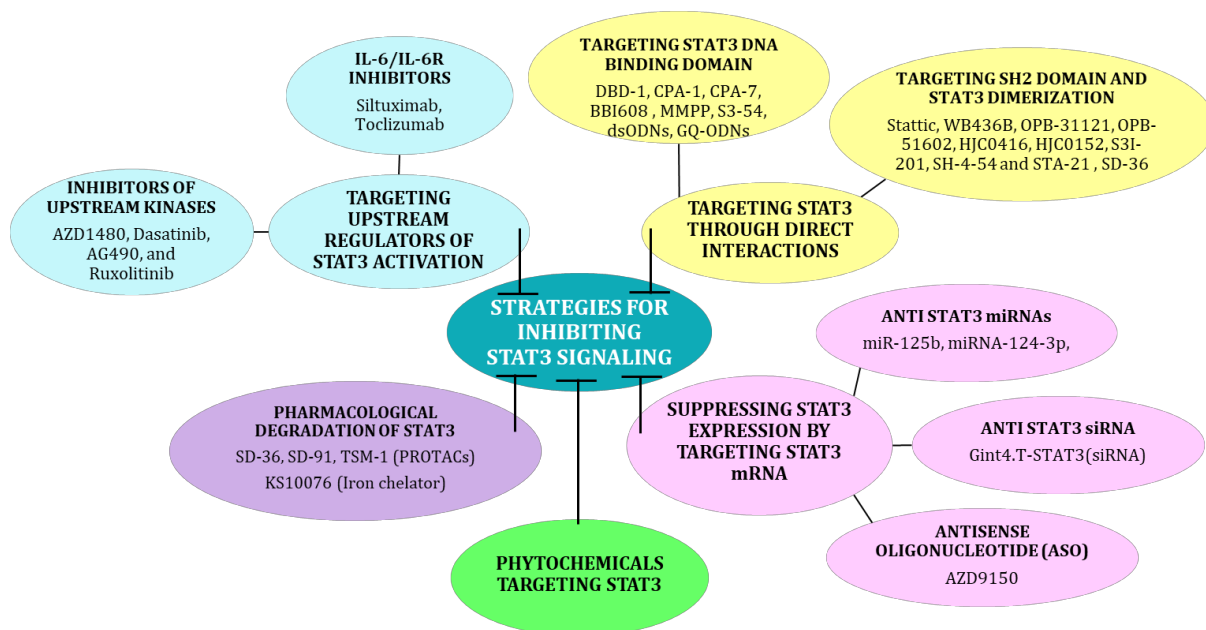
Figure 4: Strategies explored for inhibiting STAT3 signaling. STAT3 signaling can be suppressed by various strategies. Which include targeting through directly interacting with STAT3 protein domains such as the SH2 domain and DNA-binding domain, targeting upstream regulators of STAT3 activation such as IL-6/IL-6R and inhibitors of kinases upstream of STAT3, suppressing STAT3 expression by targeting STAT3 mRNA, and targeting STAT3 using phytochemicals.

2.4. Phytochemicals Targeting STAT3 Activation

Most of the strategies that we have discussed so far for inhibiting STAT3 signaling are synthetic in nature. While these approaches have shown considerable potential for cancer therapy, they also have certain limitations, such as high cost of research and development, toxicity on healthy cells, and the development of resistance. As an alternative, phytochemicals are being explored as anticancer agents. In the past several anticancer drugs were derived from phytochemicals. In fact, more than 60% of all anticancer drugs currently in clinical use are either phytochemicals or their derivatives. For example, Vincristine and Vinblastine, which are secondary metabolites from *Catharanthus roseus* (Madagascar periwinkle), and their analogues Vindesine and Vinorelbine are well known chemotherapy drugs. Additionally, Taxol (Paclitaxel), is a diterpenoid isolated from the bark of *Taxus baccata* or *Taxus brevifolia* (Pacific Yew tree) and its analogues Docetaxel (Taxotere) and Cabazitaxel (Jevtana) are drugs widely used chemotherapy drugs [110].

Phytochemicals have several advantages over synthetic drugs, including but not limited to high chemical diversity, multimodal mechanisms of action, low toxicity and evolutionary optimization [110]. Due to their structural diversity, phytochemicals exhibit unique bioactivities that are not found in synthetic drugs. Furthermore, their ability to modulate multiple signaling pathways gives them broad-spectrum activity.

Compared to synthetic drugs, phytochemicals have lower toxicity profiles, making them safer and more tolerable for patients [110]. Additionally, phytochemicals have evolved over several years in plants to optimize their biological activity, making them highly selective and competent [111]. Furthermore, biotechnology advancements have allowed synthesis of desired plant metabolites *in vitro* through efficient plant tissue culture techniques [112,113].

Several natural compounds isolated from plants have shown potent activity against STAT3 and are being investigated for their potential use in cancer treatment. As illustrated in the **figure 5**, studies have reported the potential of phytochemicals to inhibit STAT3 signaling through a variety of mechanisms that are described below.

2.4.1. Phytochemicals Directly Interacting With STAT3

Some phytochemicals, including Silibinin, Cryptotanshinone, and Garcinol have been shown to interact with STAT3 and exert anticancer effects. Silibinin has been shown to interact with STAT3 by directly binding to the SH2 and DNA-binding domains. These dual interactions led to the inhibition of activation, dimerization, nuclear translocation, DNA-binding, and transcriptional activity of STAT3 in non-small cell lung carcinoma cells[114]. Cryptotanshinone has been demonstrated to interact with STAT3 SH2 domain and impair its activation, which resulted in the downregulation of STAT3 downstream target proteins and growth arrest in multiple human cancer cells [115,116]. Furthermore, Garcinol has been reported to directly bind with STAT3 DNA-binding domain and inhibit the acetyltransferase activity of p300, which mediates STAT3 acetylation. As a result, Garcinol downregulated the expression of various STAT3 downstream target proteins, altered cell cycle progression, induced apoptosis *in vitro* in hepatocellular cancer cells and suppressed tumor growth *in vivo* [117].

2.4.2. Phytochemicals Targeting Upstream Regulators Of STAT3 Activation

Several phytochemicals have been reported to inhibit STAT3 signaling by regulating the upstream activators such as IL-6/IL-6R, EGF/EGFR and the kinases. Baicalein, a flavonoid has been demonstrated to suppress IL-6 production and inhibit STAT3 signaling which resulted in suppression of growth and metastatic potential of 4T1 breast cancer cells *in vitro* and *in vivo* [118]. Plumbagin, a quinoid derivative has been shown promising results in inducing apoptosis in pancreatic cancer cells *in vitro* and suppressing tumor growth *in vivo*. Its mechanism of action involves inhibiting STAT3 activation by reducing the level of EGFR protein and blocking the interaction between EGFR and STAT3 [119]. Withacnistin, a withanolide lactone has been shown to block EGF- and IL-6-stimulated binding of STAT3 to EGFR and gp130. This results in the

inhibition of invasiveness and induction of apoptosis in breast cancer cells. Moreover, Withacnistin caused breast tumour regression in an ErbB2-driven transgenic mouse model through downmodulation of STAT3 signaling [120]. Lastly, Lupeol, a dietary triterpenoid found in many fruits, has been reported to inhibit EGFR activation by directly binding to the EGFR tyrosine kinase, inhibit STAT3 activation and induce apoptosis in human non-small cell lung cancer cell [121].

Recently, sesquiterpene compound Germacrone and a lignin called Sesamin, have been reported to inhibit JAK2 phosphorylation and suppress STAT3 signaling to induce apoptosis in hepatocellular carcinoma cells [92][122]. Honokiol, another lignin compound also has been shown to suppress STAT3 signaling by reducing the JAK2 phosphorylation in oral cancer cells [123]. 6-Shogaol, one of the main constituents in Ginger, has been reported to reduce the levels of phosphorylated JAK2 and Src kinases in prostate cancer cells to suppress STAT3 activation and promote apoptosis *in vitro* and regress tumour growth *in vivo* [124]. Dioscin, a saponin found in many plants, was recently reported to suppress the growth of melanoma by reducing the Src activation and suppressing STAT3 signaling pathway [125]. Moreover, a recently published study showed that Gallic acid, a polyphenol compound can overcome acquired resistance to EGF receptor tyrosine kinase inhibitors in advanced non-small cell lung cancer cells by inhibiting Src-STAT3 signaling [103]. Various phytochemicals have also shown to suppress STAT3 signaling by upregulating the activity of STAT3 negative regulators. For example, Resveratrol upregulates the expression of PTPε and SHP2 tyrosine phosphatases and suppresses constitutive STAT3 activation and downregulated the expression of several STAT3 target genes to induce apoptosis renal cell carcinoma cells [126]. Likewise, Zerumbone upregulates the expression of SHP1 and suppresses STAT3 activation to induce cell cycle arrest and apoptosis *in vitro* and suppress tumour growth *in vivo* in HCC carcinoma [127].

Some phytochemicals are also reported to interact directly with PTPs and enhance STAT3 dephosphorylation activity. For instance, Phloretin directly interacts with SHP1, increased its phosphatase activity, and reduced the levels of pSTAT3 [128]. Through this mechanism, Phloretin overcame Sorafenib resistance and induced apoptosis in hepatocellular carcinoma cells *in vitro* and *in vivo* [128]. Similarly, Geranylnaringenin has been shown to directly interact with SHP2 and enhance its activity. This interaction suppress the activation of STAT3 signaling and inhibit the growth of DU145 cells both *in vitro* and *in vivo* through the downregulation of STAT3-targets such as cyclin A, cyclin D1, and survivin [129].

2.4.3. Phytochemicals Targeting STAT3 Activation Through Oxidative Stress

Oxidative stress is an imbalance between the production of reactive oxygen species (ROS) and the cell's antioxidant defence mechanisms such as the GSH/GSSG, N-acetyl-l-cysteine (NAC), Superoxide dismutase (SOD), Catalase , Peroxiredoxin (PRX) and thioredoxin (Trx) systems. Cancer cells have a higher demand for energy than non-transformed cells, leading to an imbalance between ROS production and elimination, resulting in relatively higher levels of ROS. Increasing the ROS levels of cancer cells further can overwhelm the antioxidant mechanisms and disrupt their ability to handle ROS, leading to apoptosis. As a result, cancer cells are also more susceptible to therapeutic agents that induce oxidative stress compared to normal cells [130]. Interestingly, studies suggest that many prooxidant phytochemicals possess the potential to inhibit STAT3 signaling through different ways as depicted in the **figure 6**. ROS generation induced by phytochemicals can inhibit the kinases upstream of STAT3 and as a result suppress the STAT3 signaling. For example, Carnosic acid induced ROS inactivated Src/STAT3 signaling pathway and induced apoptosis in human renal carcinoma cells [131]. Similarly, Sanguinarine mediated apoptosis in non-small cell lung cancer and multiple myeloma cells via generation of ROS and depletion of GSH that concomitantly inhibited JAK2 and suppressed JAK/STAT pathway [132].

Multiple studies have demonstrated that STAT3 is a redox sensitive protein. Some studies, including from our lab, have shown that oxidative stress induces redox modifications of cysteine residues on STAT3, such as S-nitrosylation and S-glutathionylation that impede STAT3 tyrosine phosphorylation and activation [133][134]. Studies from our lab have identified three sesquiterpene lactones Cynaropicrin, Dehydrocostuslactone and Costunolide that drive a rapid decline in the GSH/GSSG levels and an increase in ROS production. Oxidative stress induces S-glutathionylation on specific cysteine residues in STAT3 and impaired its tyrosine phosphorylation [135]. Moreover, one of these compounds Cynaropicrin has been demonstrated to induce apoptosis and enhance chemosensitivity of DU145 prostate adenocarcinoma cells to chemotherapeutic drugs including Cisplatin and Docetaxel [134]. Alantolactone, is also found to induce apoptosis and increase the sensitivity of A549 lung adenocarcinoma cells to doxorubicin by promoting S-glutathionylation of STAT3 and inhibiting tyrosine phosphorylation. [136]. R001, a natural substance from *Vernonia cinerea*, decreases glucose-6-phosphate dehydrogenase (G6PD) and Thioredoxin Reductase 1 (TrxR1) levels in breast cancer cells. This leads to modulation of NADPH and GSH levels, increased ROS generation, inhibited STAT3 activation and decreased expression of STAT3 target genes resulting in the suppression of tumor growth in vivo [137]. Likewise, Sugiol, inhibited the activity of Transketolase, (an enzyme which plays a critical for

generating NADPH), upregulated ROS generation leading to the inhibition of STAT3 signaling and suppressed growth of prostate cancer cells *in vitro* and *in vivo* [138].
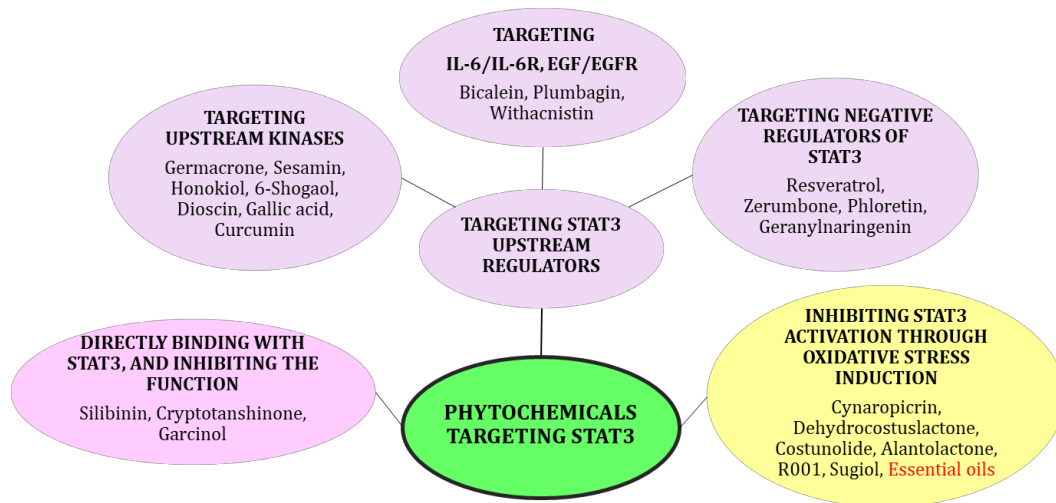
Figure 5: Mechanisms mediated by phytochemicals for inhibiting STAT3 activation. Phytochemicals have been reported to mediate an extensive spectrum of mechanisms for inhibiting STAT3 activation, including multimodal targeting of the upstream regulators, directly binding with STAT3 functional domains and inhibit their function and through enhancing oxidative stress.
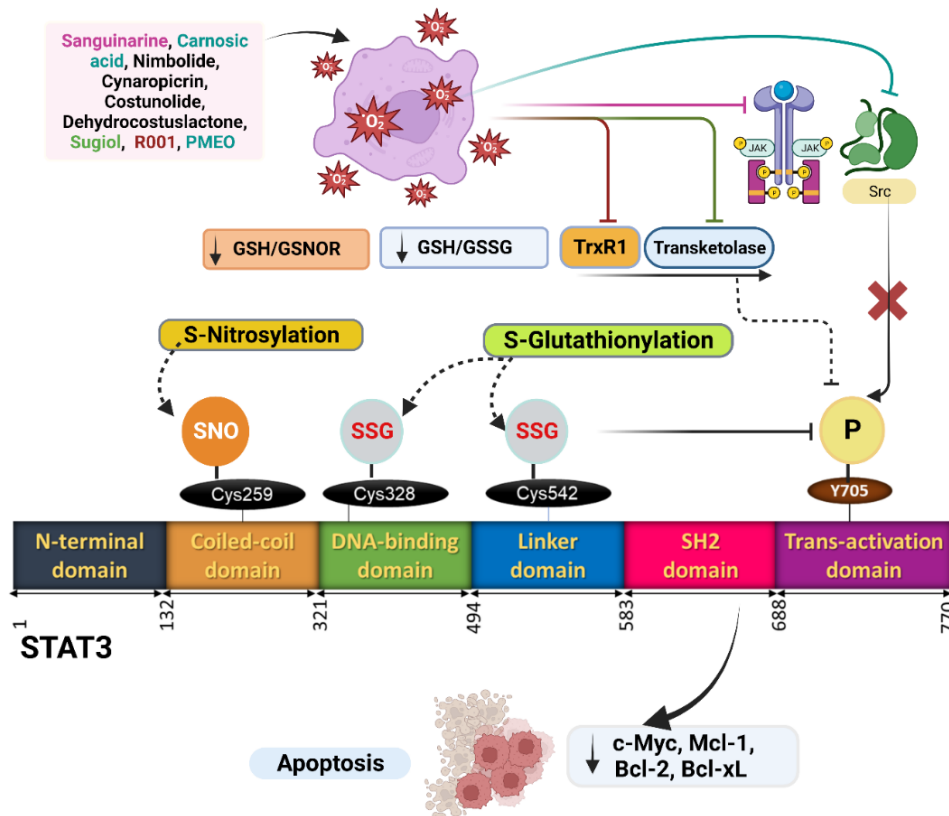
Figure 6: Mechanisms mediated by prooxidant phytochemicals to suppress STAT3 signaling. These mechanisms include inhibiting the activity of kinases upstream of STAT3 activation, inhibiting antioxidant proteins such as GSH, TrxR1 and transketolase and inducing redox modification of STAT3 that impairs its phosphorylation.

2.5. Overview Of Essential Oils

Essential oils (EOs) are distinctive plant secondary metabolites produced in specialized secretory structures called glandular trichomes that are dispersed on the surface of plant organs, mainly flowers and leaves. They are purposed to serve myriad of functions ranging from attracting pollinators to self defence against micro and macro phytophagous organisms [139]. EOs and most of the EO components are classified as Generally Recognized as Safe (GRAF) and are mostly approved as food additives [140]. They have been used in food and beverage industry, in cosmetic and personal care as well as in aromatherapy. Moreover, abundant evidence validates EOs as promising therapeutic agents with multimodal mechanisms of action including antimicrobial, anti-inflammatory and anticancer effects [141]. Chemically, EOs are highly volatile lipophilic liquids, soluble in organic solvents, limpid, and rarely coloured, with a density that is often lower than that of water [142][139].

The Latin name 'quinta essentia', which means "the fifth element," is the route from where the word "essential oil" is originated. Since "spirit" is the fifth element, an EOs is literally analogous to a spirit that has been condensed through distillation or caught from the air [139]. Several methods have been devised to extract EOs from the plant sources, like steam distillation, solvent extraction, supercritical fluid extraction, expression or cold pressing and microwave-assisted extraction [143]. After the extraction, the components in the EO are identified through gas chromatography–mass spectrometry (GC-MS) technique by comparing the obtained spectra with reference mass spectral library. On average, EOs are constituted by 20-60 various compounds belonging to various chemical groups mainly terpenes and phenylpropanoids [143]. Terpenes are chemical structures based on 5-carbon branched chains known as isoprene units. They are subclassified based on the number of isoprene units. Monoterpenes are compounds with two isoprene units, sesquiterpenes contain three isoprene units and diterpenes with four isoprene units. Diterpenes are less volatile and only rarely appear in distilled EOs. The second class of compound present in EOs is Phenylpropanoids, a group of organic compounds derived from the amino acid phenylalanine. They are characterized by a phenylpropane backbone and have various functional groups such as hydroxyl, methoxy, and/or glycosyl groups attached to them [139]. Classification of major EO components is listed in the table below (Table 1). The structures of major EO constituents are given in the **figure 7**.

Table 1: **Classification of major EO constituents**

Monoterpenes	Sesquiterpenes	Diterpenes	Phenylpropanoids
Myrcene, Linalool, Limonene, Perillyl alcohol, Thymoquinone, Carvone, α-Pinene, Geraniol, Citral	Alantolactone, β-Caryophyllene, β-Caryophyllene oxide, β-bisabolene and α-bisabolol, Costunolide, Carvacrol, Trans-nerolidol, dehydrocostuslactone, Curcumol, Zerumbone.	Sugiol, Sclareol, Oridonin Carnosol	Eugenol, Anethole, Cinnamaldehyde

Monoterpenes

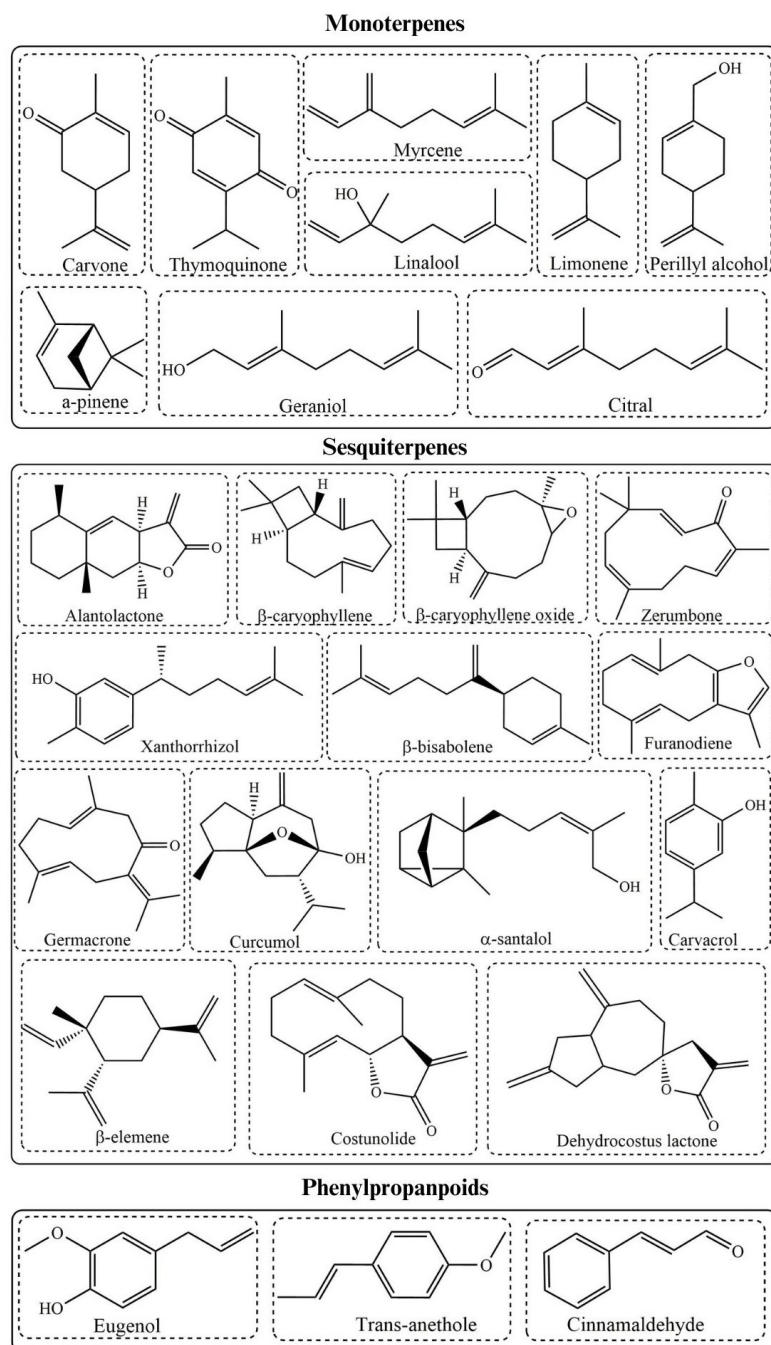**Sesquiterpenes**

Phenylpropanpoids

Figure 7: Structures of the major EO constituents.

2.6. Anticancer Activities Of Essential Oils

EOs have been used as aromatherapy to provide supportive care for cancer patients, helping to alleviate side effects such as insomnia and nausea resulting from other cancer therapies [141]. As summarized in the **figure 8**, over the last two decades accumulating evidence have shown a variety of anticancer mechanisms presented by EOs in preclinical cancer models *in vitro* in cancer cell lines and in animal models *in vivo*. A recent study has demonstrated that *Origanum majorana* EO induced apoptosis through the caspase 3/7 pathway, and reduced migration and invasion *in vitro* in lung cancer cells. Moreover, *in vivo* studies on nude mice with highly metastatic LNM35 cells showed that subcutaneous injection of OMEO led to a significant decrease in the occurrence and growth of lymph node metastasis [144]. A significant advantage of using EOs as potential anticancer drugs is their ability to selectively induce cytotoxicity in tumor cells, while sparing non-transformed cells. For instance, recent studies have shown that EOs derived from *Decatropis bicolor* and *Boswellia sacra* can induce tumor cell-specific apoptosis and suppress tumor aggressiveness in human breast cancer cells. Importantly, these effects were not observed in non-transformed breast epithelial cells (MCF-10A) [145][146]. Apart from whole EOs, several individual compounds found in EOs such as Carvacrol, α-Pinene, Geraniol, β-Myrcene, Perillyl alcohol, *β*-caryophyllene, Thymol, Thymoquinone, Cinnamaldehyde, Citral, and several others have also been reported to possess promising antitumour activities *in vitro* and *in vivo* [147].

Lipophilic nature of EOs and their constituents allow their easy penetration across the cell membrane and cause ultrastructural and morphological alterations. Moreover, their structural diversity suggests the potential for mediating multimodal mechanisms of action to exert anticancer effects. Prominent mechanisms include induction of oxidative stress, induction of Endoplasmic reticulum stress and modulation of a variety of oncogenic signaling pathways [148]. EOs from *Cymbopogon flexuosus, Pistacia lentiscus, Zataria multiflora* have all demonstrated to induced apoptosis in various human cancer cells by increasing ROS generation and oxidative stress [149][150][151]. A recent study demonstrated that the EO from the root of *Toona sinensis* can induce the generation of ROS and reduce the mitochondrial membrane potential, leading to the inhibition of phosphorylation of Akt/mTOR/NF-$\varkappa$B, as well as the expression of HSP90, HIF-α, and Bcl-2 ultimately resulting in apoptosis [152]. Moreover, it has been shown that ROS generation triggered by *Cinnamomum cassia* EO caused mitochondrial dysfunction, increased cytosolic Ca2+ levels, cytochrome c release, and ultimately caused apoptosis in human oral squamous cell carcinoma cells [108].

Of note, EOs such as *Teucrium alopecurus* EO and *Thymus hirtus* EO have been found to improve the efficacy of TNF-related apoptosis-inducing ligand (TRAIL) in inducing apoptosis in colon cancer cells by upregulating death receptors, downregulating TRAIL decoy receptors and modulating the MAPK signaling pathway [153][154]. Lastly, it is worth mentioning that the EO of *Eupatorium adenophorum* has been shown to inhibit the activation of STAT3 and AKT in hepatocellular carcinoma cells, which is relevant to the data presented in this study [155].

2.6.1. Anticancer Effects Of Essential Oils In Combination With Chemotherapy Drugs

Several lines of studies have demonstrated the promising combinatorial effects of EOs with existing chemotherapy drugs. For example, the EOs of *Zataria Multiflora* combined with doxorubicin synergically enhanced ROS generation and apoptosis induction in prostate and intestinal cancer cells respectively [156]. A recent study conducted on melanoma cells revealed the combination of *Melaleuca alternifolia* EO and its main component terpinen-4-ol with chemotherapy drugs dabrafenib and/or trametinib, synergistically reduced the viability of melanoma cells by activating apoptosis [157]. Furthermore, combination of Lemongrass EO and one of its constituents citral with cisplatin synergically enhanced cell death in chemoresistant small cell lung cancer cells [158]. EOs have been shown to overcome chemoresistance by mediating other mechanisms. For instance, Lahmar et al. showed that EOs of *Pituranthos chloranthus* and *Teucrium ramosissimum* sensitized doxorubicin-resistant human uterine sarcoma cells to chemotherapy by a decreasing the P-gp expression and its P-gp adenosine triphosphatase (ATPase) activity [159]. Furthermore, EO sesquiterpene, Curcumol enhanced the sensitivity of doxorubicin in triple-negative breast cancer via regulating the miR-181b-2-3p-ABCC3 axis [160]. Studies have also demonstrated that combination EOs with classic chemotherapy drugs can circumvent the systemic toxicities. For example, Bukhari et al. found that combining *Cinnamomum zeylanicum* EO with doxorubicin synergistically inhibited the NF-kappa B pathway and enhanced antitumour effects in rats with acute myeloid leukemia. In addition, this combination reduced cellular and hepatic toxicity and improved hematological profiles in the leukemic rats [161]. It has been reported that Geraniol, a monoterpene isolated from lemon grass EO mitigated doxorubicin-induced cardiotoxicity through Nrf2 and NF-κB signaling [161]. Similarly, Arunachalam et al showed that α-bisabolol efficiently attenuated Doxorubicin induced renal toxicity by Modulating NF-κB/MAPK signaling pathway in rats [162].

2.6.2. Essential Oils And Compounds Targeting Cancer Stem Cells

Recently studies have shown the potential of essential oils (EOs) and their compounds to inhibit the growth and self-renewal of cancer stem-like cells. For instance, *Boswellia sacra* EO was found to impede the growth of colon cancer stem cells expressing CD133 [163]. Citral, a prominent EO monoterpene, suppressed the development of MDA-MB-231 spheroids and reduced the self-renewal capacity of drug-resistant MDA-MB-231 spheroids expressing Aldehyde dehydrogenase 1 (ALDH1) through the downregulation of the Wnt/β-catenin pathway [164]. Diallyl trisulfide (DATS) found in Garlic EOs was also found to target breast cancer stem cells (BCSC) by acting on a novel target, FoxQ1 [164]. DATS administration reduced the percentage of CD44high/CD24low/ESA+ cells, suppressed mammosphere development, and ALDH1 activity *in vitro* and reduced tumour incidence and the BCSC fraction in *in vivo*[164]. Eugenol was also reported to inhibit the stemness of breast cancer in both *in vitro* and *in vivo* by degradation of β-catenin and suppression of stemness markers such as CD44, Oct4, EpCAM, and Notch1 [165].

2.6.3. Immunomodulatory Effects Of Essential Oils

EOs possess immunomodulatory activity that can boost antitumor activities. For instance, Krifa et al. reported that EO derived from *Pituranthos tortuosus* significantly increased the proliferation of splenocytes stimulated by lipopolysaccharide (LPS), implying the activation of B cells, and improved humoral immune responses in mice. Which in turn supported the EO-induced tumour growth inhibition with characteristic apoptotic changes in the cells. Recently, another study has shown that Patchouli EO can modulate immune responses and gut microbiota and exhibits potent anti-cancer effects in a mice model [166]. *Oliveria decumbens* vent EO is an essential oil that has been shown to induce selective cytotoxicity in breast cancer cells and has immunomodulatory effects *in vivo* by promoting Th1 expansion [167]. Furthermore, Jo et al. showed that α-pinene, a prominent monoterpene found in several aromatic plants, activated NK cells and increased NK cell mediated cytotoxicity in cancer cells [168].
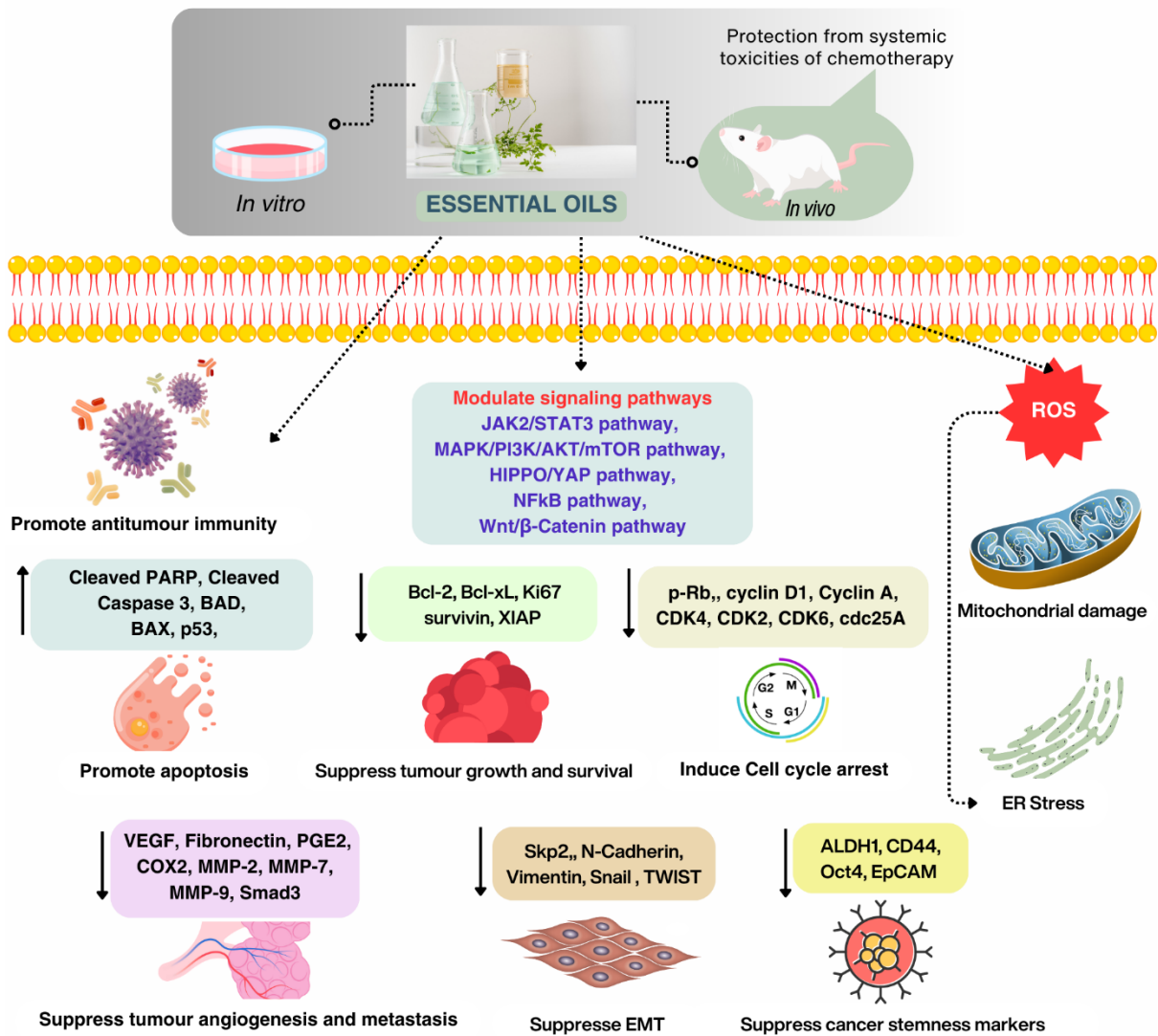
Figure 8: Anticancer activities of EOs. EOs have been reported to mediated potent anticancer activities by various mechanisms, mainly involving oxidative stress induction and modulation of various signaling pathways. As a result, EOs can suppress proliferation and survival of cancer cells, induce apoptosis, inhibit angiogenesis and metastasis, restrict cancer stem cells and promote antitumour immunity. In addition to these effects to suppress cancer growth, EOs can also reduce the systemic toxicities caused by chemotherapy.

2.7. Challenges To Therapeutic Use Of Essential Oils

Although there is growing number of preclinical evidence in support of their therapeutic effects, EOs and its components have not been translated for clinical application due to certain limitations (**figure 9**). A major issue with EOs is that different EOs from the same source plant have different chemical compositions based on the geographic region, weather, plant parts used for extraction, and the extraction techniques [169]. Developing an internationally recognised database or framework with established specifications will greatly help to overcome this difficulty. Physical and chemical properties of EOs and their constituents also have some disadvantages. High volatility and hydrophobicity are two major characteristics of EOs that confer excellent cell permeability, but at the same, in a drug development perspective hydrophobicity and volatility are major challenges [169]. EO compounds are also less stable and prone to damage by environmental factors such as light, and temperature [169]. Poor aqueous solubility and poor pharmacokinetic profile of EOs components hinders it's their clinical translation [140]. EOs and components are known for their aroma, but in some cases their aroma can have undesirable organoleptic effects on the patients. In order to facilitate a rational drug formulation based on EOs it is crucial to address and overcome these limitations [170]. Nanoformulations of EOs have been widely explored to counteract these limitations and maximize the therapeutic benefits [170].
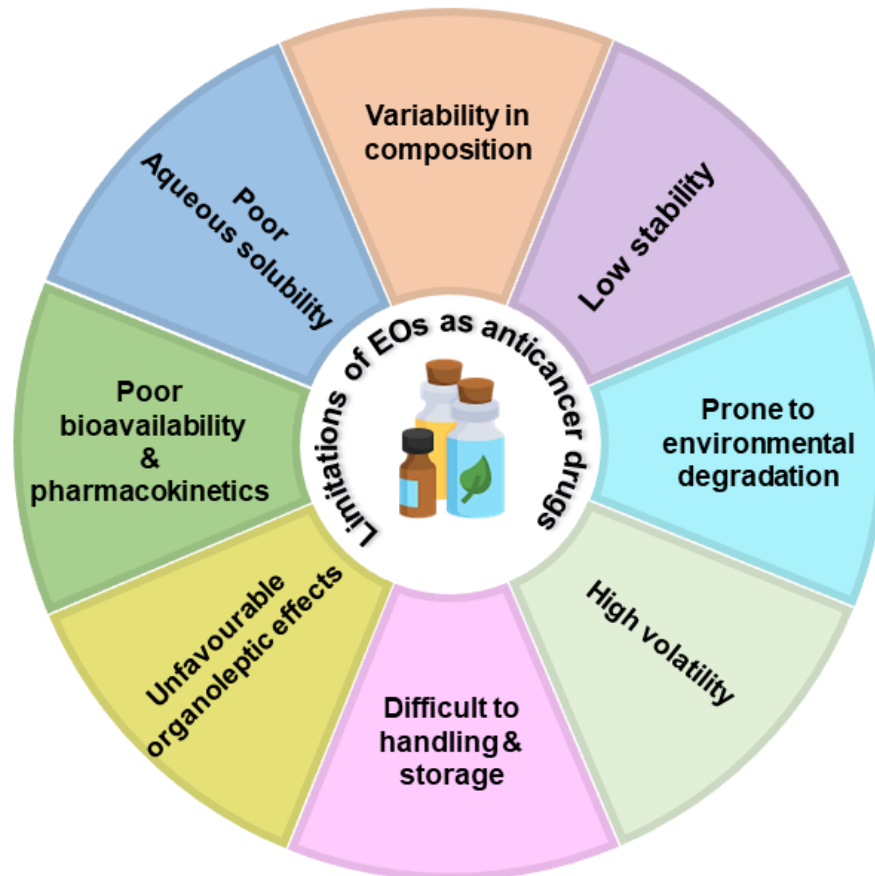

Figure 9: Limitations of EOs for their therapeutic use.

2.8. Nanoencapsulation Of Essential Oils

Nanomedicine is a highly sought and rapidly growing area wherein various innovative nanotechnology tools are incorporated into the drug delivery regime harnessed for medical application. Accumulating evidence have proven that nanoencapsulation of EOs can offer a great deal of advantages to their therapeutic use such as controlled drug release, improved physical stability of the active ingredients, shielding from the environmental interactions, reduced volatility, increased bioactivity, and lowered toxicity. These advantages also help to reduce the therapeutic dose required to elicit the desirable effects [171][172].

Over the last two decades, there has been a tremendous development in encapsulating EOs and their components in functional nano-systems for their effective and delivery to various cancer cells *in vitro* and *in vivo* [169]. EOs loaded into different types of nanocarriers such as polymer-based nanoparticles, Nanoemulsion, liposomes, solid lipid nanocarriers and molecular complexes such as cyclodextrin inclusion complexes, have demonstrated enhanced anticancer effects compared to the free EOs (**figure 10**). For example, *Morinda citrifolia* essential oils loaded chitosan nanoparticles demonstrated higher anticancer activities than the unencapsulated EO against A549 lung cancer cells [173]. Likewise, Panyajai et al. recently demonstrated that *Zingiber ottensii* essential oil (ZOEO) nanoformulations were more effective than the free EO in terms of anticancer effects against breast cancer cells. They compared the activity of four different nanoformulations, including nano- and micro-emulsions, which, when a 2% gelling agent is added, become nanogel and microgel against MCF-7 cells. Interestingly, nanoemulsion demonstrated the highest cytotoxicity, most likely because of their smaller size and low polydispersity index [174]. Liposomes have also shown promise as efficient delivery system for essential oils against cancer. For instance, *Origanum vulgare* EO-loaded Phospholipon 90H liposomes considerably increased cytotoxic activity against MCF-7 cells with respect to the free EO [175].

Poly-lactic-co-glycolic acid (PLGA) is an amorphous copolymer made up of lactic acid and glycolic acid. In the physiological environment or tumor sites, PLGA can slowly decompose into the original monomers, that are physiological metabolites of the citric acid cycle [176]. Hence PLGA has been utilized as a preferred polymer in nanoparticles development for drug delivery applications. Efficient methods such as emulsion-solvent evaporation and nanoprecipitation have been developed to incorporate EOs into PLGA nanoparticles (PLGA-NPs) [177].

Ercin et al., demonstrated successful encapsulation of *Laurus nobilis* L. into PLGA-NPs (LNEO-NPs) using emulsion solvent evaporation method. LNEO-NPs exhibited good stability and controlled release making it suitable for cancer therapy [178]. Similarly, *Cymbopogon citratus* EO has been efficiently loaded into PLGA nanoparticles. The nanoformulation displayed a hydrodynamic mean diameter of 277 nm, polydispersity index of 0.18, zeta potential of -16 mV and encapsulation efficiency of 73%. Furthermore, the release profile of the EO showed a sustained and controlled release over a week [179]. Interestingly, a recent study shows that encapsulation of *Trachyspermum Ammi* Seed EO into PLGA-NPs, improved the apoptotic effects of the EO on HT-29 colon cancer cells [180]. Moreover, *Ferula assafoetida* EO (FAEO) loaded PLGA nanoparticles reported more pronounced effect on reducing tumour growth than that of free FAEO in a nude mouse model of breast cancer [180]. Lastly, a recent study showed that co-loading of Erlotinib, an EGFR inhibitor and Alantolactone, an anti-STAT3 sesquiterpene found in EOs in PLGA nanoparticles allowed dual targeting of EGFR and STAT3 and thereby surpassed STAT3 mediated resistance to EGFR inhibitor [181].
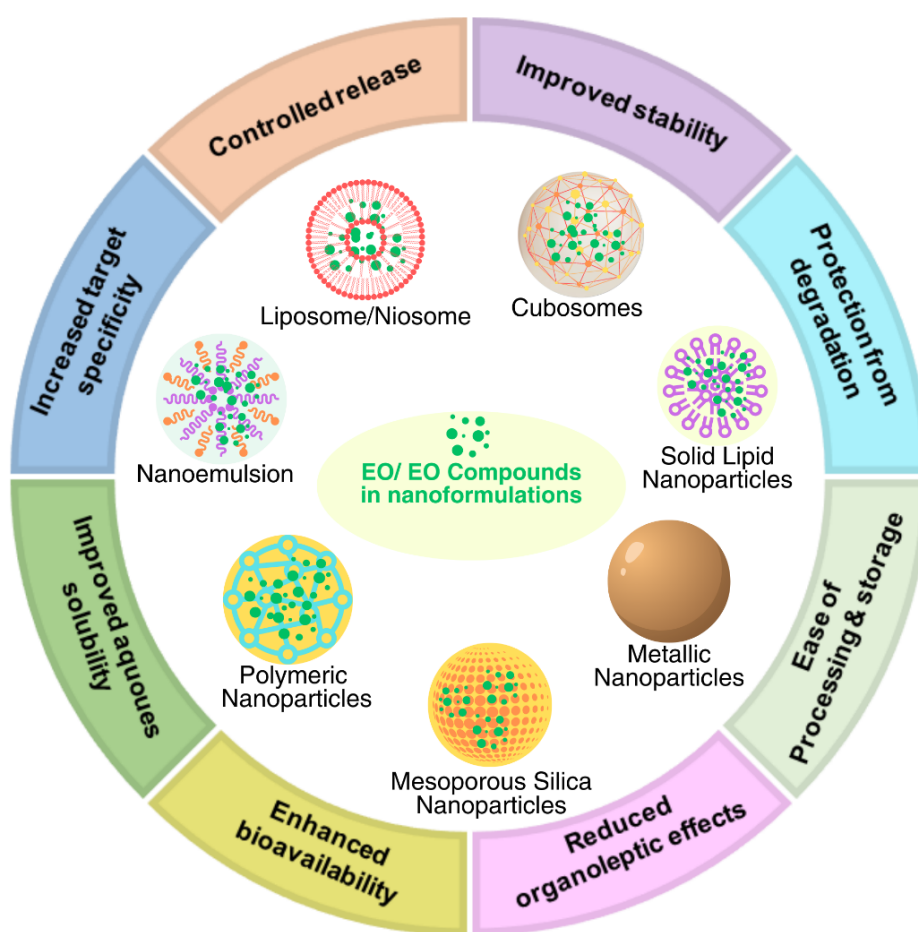

Figure 10: Different types of nanocarriers utilized for encapsulating EOs. Nanoencapsulation offers many advantages to overcome the limitations of EO in anticancer therapy.

3. OBJECTIVES AND AIMS OF THE STUDY

Constitutively active STAT3 has been demonstrated to play crucial roles in multitude of events that contribute to cancer development and progression. As a result, STAT3 has been considered as a promising target for cancer therapy. Several strategies have been explored to inhibit STAT3 signaling activation in cancer. Most of the drugs developed to target STAT3 are synthetic in nature and are failing clinically due to toxicities. While effectiveness of the existing classical chemotherapy drug is declining due to the emergence chemoresistance. To tackle these issues and effectively target STAT3 signaling activation as an anticancer strategy, researchers have been rooting to find potential candidates from phytochemicals that are shown promising and selective anticancer activities. Several studies have demonstrated the anticancer potential of essential oils (EOs) displaying growth inhibition and cytotoxicity in cancer cells. However, the molecular pathways that are targeted by EOs remain poorly validated. Pharmaceutical development of EOs have been limited by features such high volatility and poor aquoues solubility. Nanoencapsulation of EOs in attractive nanocarrier systems is suggested to overcome the limitations and boost their therapeutic applicability. By elucidating the molecular targets of EOs, this study aims to facilitate their rational application in cancer therapy that would also help to overcome the limitations of synthetic drugs and classical chemotherapy drugs.

Specifically, this study aims:

- To screen a panel of 31 essential oils (EOs) in order to identify EOs that can inhibit constitutive STAT3 activation in DU145 prostate adenocarcinoma cells. The most potent EO will be selected for further investigation into its molecular mechanism of anti-STAT3 activity and its resulting anticancer effects.

- To assess the potential combination effect of the selected EO with the standard chemotherapy drug cisplatin, with the goal of determining its efficacy as a combination therapy for cancer.

- To develop polymeric nanoparticles encapsulating the selected EO using PLGA (poly(lactic-co-glycolic acid)) and evaluate their anticancer activities in both triple negative breast cancer cells (MDA-MB-231) and breast cancer stem cells.

4. MATERIALS AND METHODS

4.1. Cell Culture

Human prostate adenocarcinoma cell lines DU145 and LnCAP and Human Triple Negative Breast Cancer cell line MDA-MB-231 were obtained from the American Type Culture Collection (ATCC, Manassas, VA, USA) and normal human primary fibroblast cell line was obtained from PromoCell (PBI, Milan, Italy). All the cell lines were maintained in Dulbecco's modified Eagle media (DMEM, Thermo Fisher Scientific, Monza, Italy) supplemented with 10% fetal bovine serum (FBS), 100 IU/mL penicillin, 100 mg/mL streptomycin, and 40 mg/mL gentamycin. All cell lines were incubated at 37 °C in a humidified incubator with an atmosphere of 5% CO2.

4.2. Dilution Of Essential Oils And Constituents

Essential oils (EOs) (Farmalabor srl, Assago, Italy) were dissolved in dimethyl-sulfoxide (DMSO) at 50 mg/mL to obtain complete solubilization and further diluted in medium for cell culture experiments, always resulting in a DMSO concentration that has no effect on cell viability.

4.3. GC-MS Analysis

Pinus mugo EO was subjected to gas chromatographic/mass spectrometric (GC/MS) analysis to characterize its composition. Briefly, the GC oven program was as follows: isothermal at 60 °C for 5 min, then ramped to 220 °C at a rate of 6 °C min−1 and finally isothermal at 220 °C for 20 min. The identification of components was performed by matching their mass spectra with those stored in the Wiley and NIST 02 mass spectra library databases. Furthermore, the linear retention indices (LRIs) (relative to C8–C30 aliphatic hydrocarbons) were calculated and compared with available retention data presented in the literature. Relative percentages of all identified components were obtained by peak area normalization from GC-FID chromatograms without the use of an internal standard or correction factors and expressed in percentages. All analyses were repeated twice.

4.4. Western Blot Analysis

Cells were washed with ice-cold PBS and homogenized at 4 °C in 20 mM HEPES (pH 7.4) buffer containing 420 mM NaCl, 1 mM EDTA, 1 mM EGTA, 1% Igepal, 20% glycerol, and protease and phosphatase inhibitor cocktails. Protein concentration was estimated by Coomassie Protein assay reagent (Thermo Fisher Scientific) or by BCA assay kit (Thermo Fisher Scientific), with reference to bovine serum albumin (BSA) standards. Total protein extracts were resolved by 7.5% or 10% SDS–polyacrylamide gel electrophoresis (SDS-PAGE) and transferred onto a polyvinylidene difluoride (PVDF) membrane (Immobilon P, Millipore, Bedford, MA, USA). Membranes were blocked with 5% BSA or 5% fat dry milk in Tris-buffered saline with 0.1% Tween 20 (TBST) at room temperature for 1 h and then incubated with primary antibodies specific for pTyr705STAT3, Cleaved Caspase-3, PARP, OCT4, SOX2, NANOG, β-actin (Cell Signalling Technology, Beverly, MA, USA), STAT3, Cyclin D1, Survivin, TWIST1 (Santa Cruz, Santa Cruz Biotechnology, Dallas, TX, USA), XIAP, Vimentin and ZEB1 (Genetex, Irvine, CA, USA) overnight at 4 °C. After washing with TBST, the membranes were hybridized with anti-rabbit or anti-mouse IgG peroxidase-conjugated secondary antibody (Cell Signalling Technology) and developed by Western Chemiluminescent HRP Substrate (Millipore) using the ChemiDoc XRS Imaging System (Bio-Rad, Hercules, CA, USA). Blotted proteins were quantified using ImageLab software (ImageLab 6.0.1, BioRAd).

4.5. RT-qPCR Analysis

Total cellular RNA was extracted using the Pure Link RNA isolation kit (ID:12183018A, Thermo Fisher Scientific) quantified at 260/280 nm and tested by 1% agarose gel electrophoresis to check the integrity of the samples. Aliquots corresponding to 1 μg of total RNA were reverse transcribed by using the SuperScriptVilo cDNA synthesis kit (ID: 11754-(50), Thermo Fisher Scientific) following the manufacturer's protocol. The cDNAs (corresponding to 50 ng of the original RNA) were subjected to real-time PCR with the QuantiTect SYBR Green PCR Kit (ID: 204143, Qiagen, Valencia, CA, USA) following the manufacturer's instructions. The mRNA levels of STAT3-regulated genes, including IL-6, Bcl-2, Cyclin D1 and Survivin, were analysed by quantitative real-time PCR. SDHA was used as the internal control. The primers used are listed in the **table 2**. Bioinformatically validated primer sets for survivin were purchased by Qiagen (QuantiTect Primer Assays: Hs_BIRC_2_SG # QT01679664). The PCR was performed with an initial pre-incubation step for 2 min at 95°C, followed by 45 cycles of 94°C for 5 s, annealing at 60°C for 30s, and extension at 72°C for 20 s. The specificity of the amplified products was monitored performing

melting curves at the end of each amplification reaction. All amplicons generated a single peak, thus reflecting the specificity of the primers.

Table 2: **List of primer sequences used for RT-qPCR analysis in this study.**

Gene	Forward	Reverse
Cyclin D1	5'-CCTCCTCAACGACCGGGTGC-3'	5'-GTTCCTCGCAGACCTCCAGCA-3'
Bcl-2	5'-GATAACGGAGGCTGGGATGCCT-3'	5'-TCCCACCAGGGCCAAACTGA-3'
IL-6	5'-AGTCCTGATCCAGTTCCTGC-3'	5'-CTACATTTGCCGAAGAGCCC-3'
SDHA	5'-GGGAACATGGAGGAGGACAA-3'	5'-TGAGGCTCTGTCCACCAAAT-3'

4.6. Cell Viability Assay

4.6.1. WST-1 Assay

2×10^4 cells were seeded in 96-well plates and left to adhere overnight. Then, cells were incubated with different concentrations of each EO, freshly prepared in Dulbecco's Modified Eagle Medium (DMEM), for 24 and 48 h. Cell viability was measured by the colorimetric assay based on the extracellular reduction of the tetrazolium salt 2-(2-methoxy-4-nitrophenyl)-3-(4-nitrophenyl)-5-(2,4-disulfophenyl)-2H-tetrazolium, monosodium salt (WST-1), into water-soluble formazan according to the manufacturer's instructions (Cayman Chemical, Ann Arbor, MI, USA). The absorbance at 450 nm was measured using a microplate reader (Infinite N Nano, Tecan Trading AG, Mannendorf, Switzerland).

4.6.2. MTT Assay

5000 cells were seeded in 96-well plates and let them adhere overnight. Cells were treated with various concentrations of either native PMEO or PMEO-NPs (0-100 μg/mL) for 24h and 48h. After the treatment media were replaced with 100μL fresh media containing the MTT reagent. After incubation of 3 h, 100 μl DMSO was added to each well to dissolve formazan crystals, and absorbance intensity was recorded at 590 nm using the microplate reader (Synergy HT, BioTek® Instruments Inc., Winooski, VT). The IC50 values were calculated using GraphPad Prism.

4.7. Measurement Of Intracellular ROS

4.7.1. Microplate ROS Measurement

ROS production was assessed with the cell-permeable probe 2'7'-dichlorodihydrofluorescein diacetate (H$_2$DCFDA; Thermo Fisher Scientific). First, 2×10^4 cells were seeded in 96-well plates, left to adhere overnight and then loaded with 10 μM H2DCFDA. After incubation of1 h, the cells were treated with 25 to 75 μg/mL PMEO for the indicated time. Fluorescence intensity was then measured with a multimode plate reader (Ex485 nm and Em535 nm) (Infinite N Nano, Tecan Trading). Fluorescence intensity was normalized against control wells for statistical analysis.

4.7.2. Flow Cytometer ROS Measurement

Briefly, 2×10^5 cells were seeded in 60 mm tissue culture dishes and let to adhere overnight. Cells are then treated with indicated concentrations of PMEO and PMEO-NPs for 1hr. After the treatment, cells were washed twice with DPBS (0.1 M. pH, 7.4) and incubated with 10 μM H$_2$DCFDA in DPBS for 30 min at 37 ∘C. After the incubation the dishes were quickly imaged using the fluorescence microscope ((Olympus DX58, JAPAN) followed by washing and analysis for ROS production in flow cytometer (BD LSR Fortessa).

4.7.3. Quantification Of Glutathione Content

The intracellular reduced glutathione (GSH) concentration was measured by endpoint spectrophotometric titration on a Jasco V/550 spectrophotometer (JASCO, Cremella, Italy) using 5,5'-dithiobis(2-nitrobenzoic acid) (DTNB, Ellman's reagent). Briefly, treated, and untreated cells were lysed by freezing and thawing in 100 mM sodium phosphate buffer, pH 7.5, containing 5 mM EDTA (KPE buffer), and after centrifugation at 16,000 rpm for 10 min, total protein concentration was determined by using the Bradford method. The supernatants were deproteinized with 5% trichloroacetic acid. For GSH measurement, acidified clear supernatants were neutralized and buffered at pH 7.4 with 200 mM K2HPO4, pH 7.5. The reaction was then started by the addition of 60 μM DTNB, and the increase in absorbance at 412 nm was measured until no variation in absorbance was evident. The amount of total GSH was determined by comparison with the GSH standard curve.

4.8. Study Of Apoptotic Hallmarks

4.8.1. Dual Staining With Annexin V–FITC And Propidium Iodide

Cells were washed with phosphate-buffered saline and stained with Annexin V–FITC (AnxV) (Miltenyi Biotec, Bergisch Gladbach, Germany) for 15 min and propidium iodide (PI) (Thermo Fisher Scientific) immediately before acquisition on a FACS Calibur cytometer (Becton–Dickinson, Franklin Lakes, NJ, USA) [42]. PI has an elevated affinity for double-strand nucleic acids but does not enter unimpaired plasma membranes, and AnxV determines the phosphatidylserine flip from the inner to the outer leaflet of the plasma membrane. Fluorescence signals were detected on FL-1 for AnxV and on FL-3 for PI.

4.8.2. Caspase-3 And PARP Cleavage

Caspase 3 and PARP1 cleavage were analysed by Western blot as described above using an anti-PARP antibody that detects endogenous levels of full-length PARP (116 kDa) as well as the large fragment (89 kDa). After stripping, membranes were rehybridized with anti-cleaved Caspase-3 (17 kDa) and anti-actin antibodies.

4.8.3. Acridine Orange/Ethidium Bromide Fluorescent Staining

Fluorescent dyes acridine orange(AO)and ethidium bromide (EtBr) was used to visualize apoptosis-associated morphological changes in the cells as previously described [182]. Briefly, after treatment, cells were washed with PBS, collected by trypsinization, and then resuspended in 200 μl PBS. After that, 25 μl cell suspension was treated in a new tube with 5μl of 1 mg/mL of AO/EB solution , spread on a cover slip and flipped onto a glass slide. The images were captured using fluorescence microscope (DM IL LED, Leica Microsystems, Filter system I3 S, blue, excitation filter BP 450-490, suppress filter LP 515).

4.8.4. Wound Healing Assay

Cells were seeded in 6-well plates. When cells were fully confluent, a wound was created using a pipette tip to make a linear scratch through the monolayer. After washing with Hanks' Balanced Salt Solution (HBSS), new medium containing the indicated concentration of EO was added to the designated wells. At 0, 16 and 24 h of treatment, cells were observed, and the degree of wound healing was evaluated using microscope imaging. The percentage of wound healing was analysed using ImageJ/Fiji software (version 1.53q), and applying the plugin as previously reported [183].

4.9. Pharmacological Synergism Studies

Cells were treated with EO and cisplatin individually or in combination. The concentration of each agent that reduced cell viability by 50% (IC50) was preliminarily determined in the cell line to derive the constant-ratio combination design. Cytotoxicity was evaluated by WST-8 assay. The effects of interaction between EO and cisplatin were analysed according to the median-effect method of Chou and Talalay using CompuSyn software 1.0 [184]. The mean combination index (CI) values were assessed, and combination data are shown as CI vs. fraction affected (Fa) plots. CI < 1 represents synergism, CI = 1 represents an additive effect and CI > 1 represents antagonism. In addition, the dose-reduction index (DRI) for each combination was calculated. The DRI is a measure of the magnitude of dose reduction allowed for each drug when administered in synergistic combination compared with the dose of a single agent that is needed to achieve the same effect. It is considered favourable when DRI > 1.

4.10. Preparation Of PMEO-NPs

PMEO loaded PLGA nanoparticles (PMEO-NPs) was prepared by single emulsion solvent evaporation method as previously described [176].Organic to aqueous phase ratio used was 1:6 and drug loading was 10%. Briefly, PLGA (50 mg) and PMEO (5 mg) were dissolved in 3 mL Dichloromethane. The above solution was emulsified in Polyvinyl alcohol (PVA, 1%) and D-α-tocopheryl polyethylene glycol succinate (TPGS, 0.1% w/v) aqueous solution by vortexing to make oil in water emulsion which was followed by sonication with a microtip probe sonicator (VC 505, Vibracell Sonics, MA) set at 37% amplitude for 2 min over an ice bath. The emulsion was kept for overnight stirring on magnetic stir plate at room temperature to evaporate organic solvent. Excess PVA was removed by ultracentrifugation at 40,0000 rpm (SW 41 Ti Swinging-Bucket Rotor, Optima XPN, Beckmann coulter) at 4 °C for 20 min. Further, it was washed thrice with double distilled water. The recovered nanoparticle (NPs)suspension was then sonicated for 2 min at 37% amplitude in an ice-bath. NPs was then lyophilized for 72 h (Labconco FreeZone 12, Labconco Corporation) at a temperature of -49 °C and pressure of 0.070 mBar. Lyophilized NPs were used for further studies. Void nanoparticles (void NPs) were prepared by the same procedure except that PMEO was not added.

4.11. Physico-Chemical Characterization Of PMEO-NPs

4.11.1. Spectrophotometric Analysis Of PMEO

PMEO was solubilized in acetonitrile and spectrum analysis was performed using UV-Vis spectrophotometer (Shimadzu® UV-2600, Japan). The spectrum analysis of PMEO revealed a maximum absorbance value at 194 nm. The unknown concentration of PMEO in different NPs preparation was calculated from standard curved obtained from increasing concentration of PMEO at 194nm. This calibration curve was used to determine the encapsulation efficiency, loading capacity, and in vitro release of PMEO in the PLGA particulate system.

4.11.2. Determination Of The Encapsulation Efficiency And Loading Capacity

The amount of PMEO incorporated into PLGA NPs was determined by a solvent extraction method as previously described [176]. Briefly, 1 mg PMEO-NPs (various batches prepared) were dissolved in 1 mL of ACN, vortexed and centrifuged at 10000 rpm at 4 °C (Sigma 1–15 K, Germany) for 1 min. Supernatants were further diluted with ACN) and analysed by UV–Vis spectrophotometry (Shimadzu® UV-2600, Japan) at 194 nm. Void NPs similarly prepared were used for baseline correction. Encapsulation efficiency (EE%), the percentage of the drug that is successfully incorporated into nanoparticle with respect to the total drug added, of various batches of PMEO-NPs was calculated by Equation 1 (*eq.1*). Moreover, the loading capacity LC% ,which refers to amount of drug loaded per unit weight of the nanoparticle, was obtained by Equation 2 (*eq.2*).

$$(\boldsymbol{eq.1})\ EE\% = 100\ \times \frac{D1}{D2}$$

$$(\boldsymbol{eq.2})\ LC\% =\ 100\ \times \frac{D1}{D3}$$

Where D1= amount of PMEO entrapped in PMEO-NPs, D2= Total amount of PMEO added, D3= Total weight of nanoparticles.

4.11.3. Particle Size, Polydispersity Index (PDI) And Zeta Potential Analyses Of PMEO-NPs

The Particle Size, Size Distribution and Zeta Potential of NPs dispersed in water was determined by Dynamic light scattering (DLS). The basic principle of DLS is that light scattered by a particle will have a different angle of scattering depending on the size of the particle. The measure of angle of scattering indicates the size of the particle whereas the intensity of the scattered light provides information about the concentration of NPs [185]. Briefly, samples of NPs were dispersed in milli-Q water and analysed in triplicates using Zetasizer (Nano ZS, ZEN3600, Malvern Instrument, UK). Polydispersity index (PDI), a unitless variable generated simultaneously, refers to the relative variance in the NP size distribution and varies from 0.0 for a sample that has uniform particle size to 1.0 for a sample that has multiple particle size populations. Values lower than 0.2 are considered acceptable for polymer-based nanoparticles [177]. The Zeta potential is estimated through the electrophoretic mobility. A high zeta potential indicates that the nanoparticles have a strong electrostatic repulsion, so they are less likely to aggregate and are more stable in solution. A low zeta potential, on the other hand, indicates that the particles are more likely to aggregate and are less stable in solution. Between -10 and +10 mV, nanoparticles are relatively neutral, while those having zeta potentials of more than +30 mV or less than -30 mV are regarded to be cationic and anionic, respectively. Since majority of the biological membranes have a net negative charge, zeta potential can influence a nanoparticle's propensity to pass through membranes, with cationic particles typically exhibiting more toxicity due to breakdown of cell walls.

4.11.4. SEM And TEM Imaging Of PMEO-NPs

The shape and surface morphology of the nanoparticles were observed by SEM and TEM. For SEM analysis, lyophilized nanoparticles were scattered and spread on a carbon tape carefully and then sputter-coated with a thin layer of gold and palladium, to make them conductive prior to image acquisition in the SEM (JEOL-JSM-1T800, JAPAN) operating at 10.00kv. For TEM analysis, samples were prepared by first creating a suspension of the nanoparticles in a milli Q water. Next to it a small droplet of 2% (w/v) Uranyl acetate was also placed. Then a small droplet of the NPs suspension is then placed onto a carbon-coated copper grid left for few seconds and then dipped onto the uranyl acetate droplet. Uranyl acetate is a negatively staining agent that is commonly used in TEM to visualize samples with low electron density, such as liposomes and nanoparticles [179]. The grid is then carefully washed by dipping in water droplets and left for drying. Once the grid is dried and the images were visualized at an accelerating voltage of 120 kV under a transmission electron microscope (JEOL).

4.11.5. In Vitro Release Kinetics Of PMEO From PMEO-NPs

In vitro release of PMEO from the PMEO -NPs was performed at physiological pH (pH 7.4) in PBS containing 0.1% (v/v Tween 80)(PBS-T)at 37 °C. Briefly, 10 mg of PMEO-NPs were dispersed in 3 ml buffer, vortexed and equally divided in three tubes, kept in a shaker at 37 °C and 150 rpm. At specified time intervals (30 minutes to 5 days), these tubes were taken out, centrifuged at 13,000 rpm at 4 °C for 10 min (Sigma 1–15 K, Germany) and collected the supernatants. The pellet was resuspended with 1 ml of fresh PBS-T for further sampling. The collected supernatants were lyophilized and then resuspended in ACN to analyse the total PMEO content using UV/Vis spectrophotometer as described above.

4.12. Cellular Uptake Study

The fluorescent dye 6-coumarin is easily incorporated into the PLGA NPs, to visualize the NPs [176]. 6-coumarin loaded PLGA-NPs were prepared as described above adding 100 μg of 6-coumarin to the organic phase. For the cellular uptake study, cells were treated with 100 ng/mL of 6-coumarin or 6-coumarin loaded PLGA- NPs for 1h. After that cells were washed twice with ice cold PBS to remove uninternalized 6-coumarin or 6-coumarin-NPs and then imaged with fluorescent microscope (Olympus DX58, JAPAN).

4.13. Aldefluor Assay

Aldefluor assay was performed using ALDEFLUOR™ kit (Stem Cell Technologies) as per manufacturer's instructions to identify the aldehyde dehydrogenase-positive (ALDH +) cell population. Briefly, after 48h of treatment with either 75μg/mL of PMEO or equivalent concentration of PMEO-NPs for 48h, mammospheres were made single cells, and then suspended at a concentration of $6x10^4$ cells/ml The cells were then washed with PBS and stained with ALDH substrate for 45 min at 37 °C. For each sample, a fraction of cells was incubated under identical condition with ALDH inhibitor diethylaminobenzaldehyde (DEAB) which serves as a negative control. The fluorescent signals were measured in flow cytometer (BD LSR Fortessa).

4.14. Mammosphere Formation Assay

Mammosphere formation assay was performed as previously reported [176]. For primary mammospheres, MDA-MB-231 cells were plated at a density of $2x10^4$ cells per well in an ultra-low attachment 6 well plate (Corning) in stem cell specific media (DMEM/F12 supplemented with various growth factors viz 20 ng/ml EGF, 20 ng/ml FGF, 5 µg/ml insulin, 1X B27 supplement, 0.4% BSA and 100 U/ml Pencillin-Streptomycin) for a week to form mammospheres, and then treated with varying concentration of PMEO or PMEO-NPs for 48h. Thereafter, number of primary mammospheres formed were manually counted and representative images were acquired using inverted microscope (DM IL LED, Leica Microsystems) at 10X magnification. For secondary mammospheres, the above primary mammospheres were made single cells and 5000 dissociated cells were plated and cultured as before in absence of either PMEO or PMEO-NPs. After a week secondary mammospheres were counted and representative images were taken as before.

4.15. Statistical Analysis

The results are expressed as the mean ± SEM of at least four independent experiments and were statistically analysed with GraphPad Prism 8.4.2 (GraphPad Software, San Diego, CA, USA) by one-way ANOVA followed by Tukey's multiple comparison test with the control group or within the groups. When only two groups were compared, Student's t-test was used to determine significance, and $p < 0.05$ was considered statistically significant.

5. RESULTS

5.1. Essential Oils Inhibit STAT3 Activation In DU145 Prostate Cancer Cells

To study the effect of Essential Oils (EOs) on STAT3 signaling, we chose DU145 cell line as the experimental model as it presents high levels of constitutively Tyr705 phosphorylated STAT3. Cells were treated with EOs at concentrations of 25, 50, and 100 μg/mL for 1 hour, and the effect on STAT3 activation was analysed by Western blot. A panel of 33 various EOs were screened and classified as "active" or "not active" for inhibition of STAT3 activation, as summarized in the **table 3**. Densitometric analysis of Western blot membranes revealed that 12 EOs reduced the levels of pTyr705 STAT3 without altering expression levels of total STAT3. The potency of each of these oils was determined by measuring its inhibitory concentration (IC50). As summarised in the **table 4**, the potencies of the EOs were clustered into three categories: strong inhibition (IC50 < 50 μg/mL), medium inhibition (IC50 50-100 μg/mL), and weak inhibition (IC50 > 100 μg/mL).

The results show that these EOs have the potential to specifically target the activation of STAT3, while leaving normal levels of STAT3 unaffected. Given the key role played by STAT3 in various cellular processes, further study of these EOs may reveal their efficacy in selectively suppressing the activity of STAT3 in cancer cells, providing a safer adjuvant therapies for cancer treatment. Specifically, four EOs - *Pinus mugo* EO (PMEO), *Lavandula angustifolia* EO (LAEO), *Pinus sylvestris* (PSEO), and *Cupressus sempervirens* (CSEO) displayed strong inhibitory effects on STAT3 activation (**figure 11 A**). Additionally, *Melissa officinalis* EO (MOEO), *Hyssopus officinalis* EO (HOEO), *Juniperus oxycedrus* EO (JOEO), *Eucalyptus globulus* EO (EGEO), *Chamaemelum nobile* EO (CNEO), and *Myrtus communis* EO (MCEO) exhibited medium inhibitory effects (**figure 11B**).
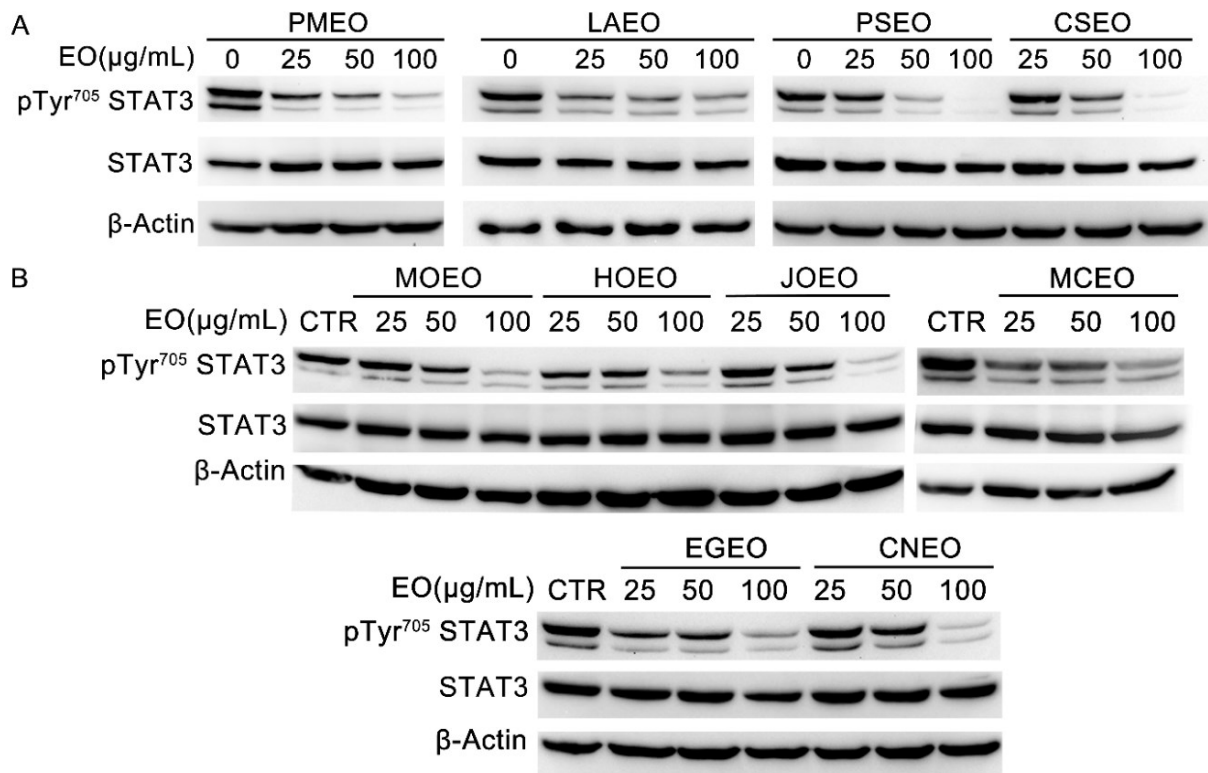
Figure 11: EOs Inhibit STAT3 Tyrosine Phosphorylation in DU145 Cancer Cells. DU145 cells were treated with the indicated concentrations of EOs for 1 h, and total protein extracts were analysed by Western blot with pTyr705STAT3 antibody and with anti-STAT3 antibody after membrane stripping. β-Actin is shown as the internal loading control. The data shown are representative of three independent experiments. **(A)** EOs showed strong inhibition of STAT3 activation **B.)** EOs showed medium inhibition of STAT3 activation.

Table 3: EOs analysed for their anti-STAT3 activity.

No.	EO Plant Name	Anti-STAT3
1	*Pinus mugo*	active
2	*Lavandula angustifoglia*	active
3	*Pinus sylvestris*	active
4	*Cupressus sempervirens*	active
5	Hyssopus officinalis	active
6	*Juniperus oxycedrus*	active
7	*Myrtus communis*	active
8	*Chamaemelum Nobile*	active
9	*Melissa officinalis*	active
10	*Eucalyptus globulus*	active
11	*Pimpinella anisum*	active
12	*Cananga odorata*	active
13	*Salvia sclarea*	Not active
14	*Salvia officinalis*	Not active
15	*Thymus Zygis*	Not active
16	*Melaleuca alternifolia*	Not active
17	*Pelargonium graveolens*	Not active
18	*Origanum vulgaris*	Not active
19	*Elettaria cardamomum*	Not active
20	*Citrus grandis*	Not active
21	*Abies sibirica*	Not active
22	*Cinnamomum camphora*	Not active
23	*Citrus aurantium amara*	Not active
24	*Citrus bergamia*	Not active
25	*Juniperus communis*	Not active
26	*Thuja occidentalis*	Not active
27	*Citrus limon*	Not active
28	*Satureja hortensis*	Not active
29	*Citrus sinensis*	Not active
30	*Melaleuca leucadendra*	Not active
31	*Mentha piperita*	Not active
32	*Origanum majorana*	Not active
33	*Ocimum basilicum*	Not active

Table 4: Essential oils classified based on EC50 values of pTyr705STAT3 inhibition.

EO Plant name	Notation	pTyr^{705}STAT3 inhibition IC50 (mg/mL)	anti-STAT3 Potency
Pinus mugo	PMEO	<50	Strong
Lavandula angustifoglia	LAEO	<50	Strong
Pinus sylvestris	PSEO	<50	Strong
Cupressus sempervirens	CSEO	<50	Strong
Hyssopus officinalis	HOEO	50-100	Medium
Juniperus oxycedrus	JOEO	50-100	Medium
Myrtus communis	MCEO	50-100	Medium
Chamaemelum Nobile	CNEO	50-100	Medium
Melissa officinalis	MOEO	50-100	Medium
Eucalyptus globulus	EGEO	50-100	Medium
Pimpinella anisum	PAEO	>100	Weak
Cananga odorata	COEO	>100	Weak

5.2.   Essentials Oils Induce Cytotoxicity In DU145 Cells

Inhibition of STAT3 activation can have direct effects on the cell proliferation and viability. The cytotoxic effect of anti-STAT3 EOs cells was evaluated by treating for 24 and 48 h DU145 cells with increasing concentrations of EOs from the strong and medium cluster. The cell viability was measured by a WST-1 assay. As shown in **figure 12A**, all four EOs in the strong cluster of anti-STAT3 activity dose-dependently affected the viability of cells in 24 h and 48 h treatments. PMEO appeared to be the most active, with IC50 less than 70 μg/mL at 24 h. Moreover, after 48 h treatment, three EOs, PMEO, PSEO and CSEO, exhibited high cytotoxicity, with an IC50 value less than 50 μg/mL. Among the EOs in the medium cluster of anti-STAT3 activity, MOEO and JOEO demonstrated high cytotoxicity within 24h of treatment and CNEO was cytotoxic in 48h treatment. MCEO, HOEO and EGEO shown only minimal cytotoxicity (**figure 12C**). The IC50 values of cytotoxic EOs are summarized in **figure 12B**.

Selective cytotoxicity is a critical aspect of cancer therapy as it enables the specific targeting of cancer cells, minimizing the damage to normal cells and increasing the chances of successful treatment outcome. Pharmacological research of the last 20 years focuses its attention on natural compounds and phytochemicals in drug discovery especially for cancer and infectious disease [186]. Among them, several EOs have been previously described to be selectively cytotoxic towards cancer cells while sparing normal cells unaffected [147]. Moreover, EOs have also been reported to have synergic or additional cytotoxic effect with conventional therapy reducing the toxicity of chemotherapy drugs [148]. WST-1 Cell viability assay was conducted to evaluate their effect on non-transformed human fibroblasts to assess if the cytotoxicity of EOs is selective towards cancer cells. The analysis of cells viability after 24 h treatment with the increasing concentrations of the five cytotoxic EOs reveals that , LAEO and PSEO highly reduced the

viability of fibroblasts, while PMEO, CSEO and MOEO had only minimal cytotoxicity in not transformed cells (**figure 12D**).

5.3. Chemical Composition Of PMEO

PMEO was selected for further investigation due to its potent anti-STAT3 activity, as well as its ability to exhibit high cytotoxicity specifically towards cancer cells while causing minimal effects on normal human fibroblast cells. GC-MS is a widely used technique for identifying the composition of essential oils. This method involves separating and identifying the different compounds present in the essential oil, which can provide valuable information about its purity, authenticity, and therapeutic properties. Moreover, GC-MS can be applied throughout the production process to monitor the quality of essential oils. From a drug development perspective, it can also be used to identify lead compounds and assess their potential as drug candidates by examining their interactions. PMEO was subjected to GC-MS analysis to reveal the composition. In total, 22 different compounds have been identified to be present in the PMEO and constitute 99.99% composition. The compounds belonged to monoterpenes, oxygenated monoterpenes and Sesquiterpenes. The major components were found to be β-caryophyllene (21.4%), bornyl acetate (13.5%), α-pinene (12.5%), limonene (10.9%), δ-3-carene (10.8%), β-pinene (7.6%), and β-phellandrene (7.0%). The structures of these major components are illustrated in the **figure 13**. The detailed composition of PMEO provided in the **table 5**. (Analysis was performed in collaboration with the group of Prof. Rino Ragno).
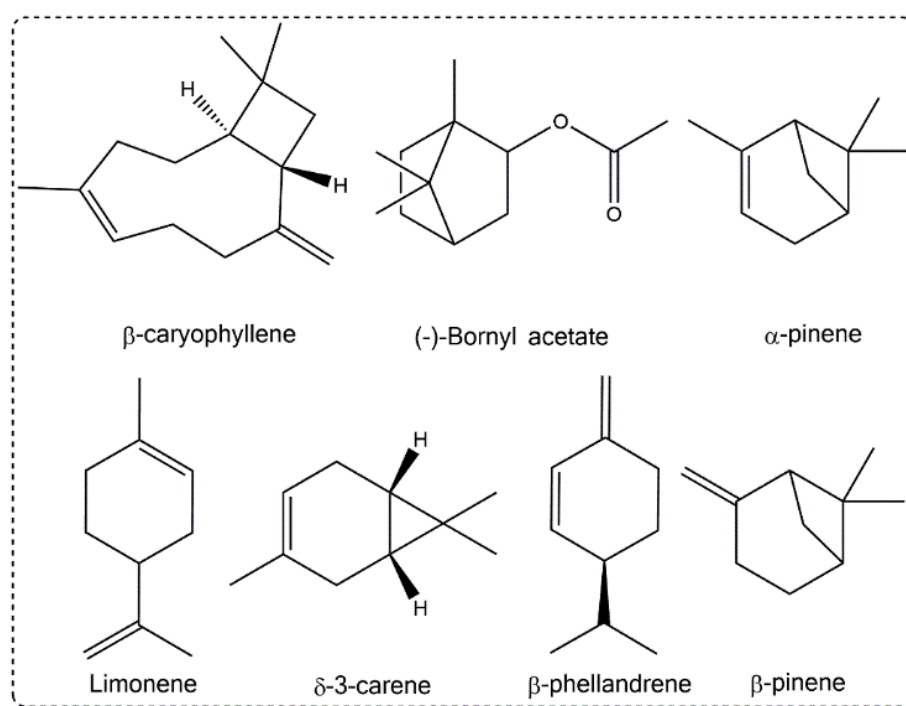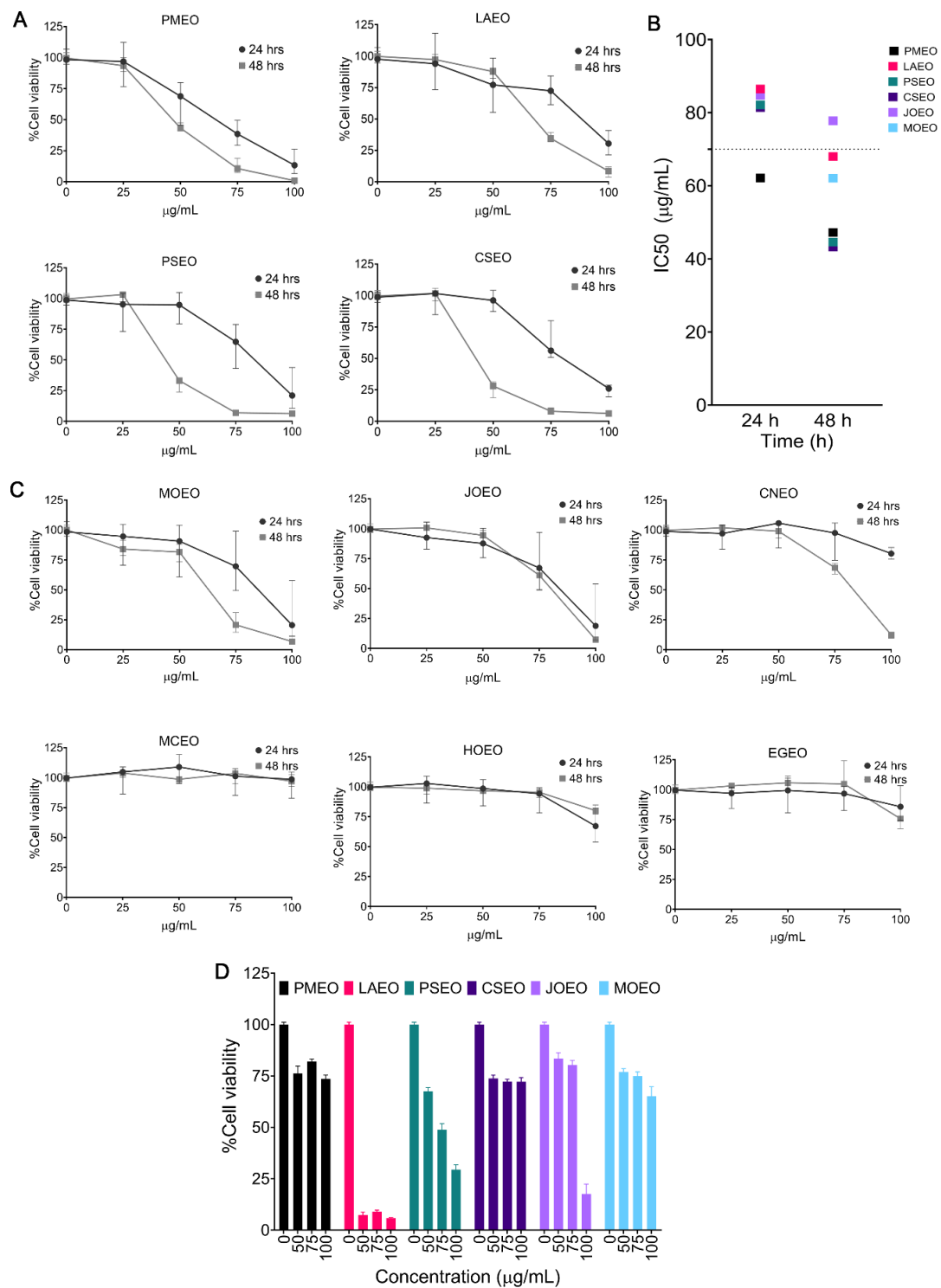

Figure 13: Chemical structure of main PMEO components

56

Figure 12: **Cytotoxicity of in DU145 cancer cell line and normal human fibroblast cells**. DU145 cells were treated with increasing concentrations of EOs belonging to the strong and medium cluster for 24 and 48 h, and cell viability was analysed by WST-8 assay. **(A)** Graph report the cytotoxicity of EOs in strong cluster **(B)** EO doses required to affect 50% cell viability (IC50) are reported in the graph **(C)** Graph report the cytotoxicity of EOs in medium cluster. **(D)** The graph reports the % viability of human fibroblast cells after EO treatment (Data represent the mean ±SEM, n=3).

Table 5: Pinus mugo EO chemical composition.

No.	Components[1]	Class of the compound[2]	LRI[3]	LRI[4]	%[5]
1	α-Pinene	Monoterpene	1018	1021	12.52
2	β-Pinene	Monoterpene	1090	1099	7.63
3	δ-3-Carene	Monoterpene	1142	1146	10.75
4	Limonene	Monoterpene	1190	1198	10.95
5	β-Phellandrene	Monoterpene	1201	1204	6.98
6	o-Cymene	Monoterpene	1279	1287	2.14
7	α-Copaene	Sesquiterpene	1492	1489	0.92
8	β-Cubebene	Sesquiterpene	1528	1532	1.17
9	Linalool	Monoterpene	1545	1547	0.18
10	Bornyl acetate	Monoterpene	1466	1567	13.44
11	Crypton	Monoterpene	1672	1675	3.70
12	β-Caryophyllene	Sesquiterpene	1612	1619	21.41
13	Isopinocarveol	Monoterpene	1642	1646	0.47
14	α-Terpineol	Monoterpene	1650	1655	0.44
15	cis-Verbenol	Monoterpene	1665	1663	0.46
16	α-Humulene	Sesquiterpene	1669	1667	1.20
17	α-Muurolene	Sesquiterpene	1733	1729	1.08
18	δ-Cadinene	Sesquiterpene	1762	1758	1.61
19	Calamenene	Sesquiterpene	1835	1832	0.67
20	p-Cymen-8-ol	Monoterpene	1836	1838	0.85
21	trans-2-Caren-4-ol	Monoterpene	1844	*	0.59
22	Cumaldehyde	Monoterpene	1782	1781	0.55
	SUM				99.99

[1] The components are reported according to their elution order on a polar column; [2]Class of chemical group the compound belongs to [3] linear retention indices measured on a polar column; [4] linear retention indices from the literature; * LRI not available; [4] percentage mean values of Pinus mugo EO components (%).

5.4. PMEO Suppresses Constitutive STAT3 Signaling

During the initial screening, it was identified that PMEO showed a dose-dependent inhibition of constitutive STAT3 activation. To further understand the kinetics of PMEO's modulation of STAT3 signaling, DU145 cells were treated with 50 μg/mL of PMEO for different time intervals ranging from 1 to 24 hours. The results, as demonstrated in figure 14A, indicated that PMEO treatment resulted in a gradual decrease in STAT3 Tyr705 phosphorylation over time.

Maximum reduction in pTyr705-STAT3 levels was observed after 2 hours of PMEO treatment and the signal was slightly restored after 24 hours. This implies that there may be another compensatory pathway activated which needs to be investigated further. As the results clearly indicated that PMEO was able to inhibit constitutive activation of STAT3, the downstream effects of PMEO on STAT3 targets at gene and protein levels were subsequently evaluated. To this end, DU145 cells were treated with 50 μg/mL of PMEO for 24 hours and performed an mRNA expression analysis and western blotting. PMEO treatment significantly decreased the mRNA expression of genes such as Cyclin D1, Bcl-2, Survivin, and IL-6 (**figure 14B**). Furthermore, results of the western blotting revealed decrease in the protein levels of Bcl-2, MCL1, Cyclin D1, XIAP, COX2, and Survivin (**figure 14C**). These results suggest that PMEO's ability to downmodulate STAT3 activation also led to the downregulation of genes and proteins that are targeted by STAT3.
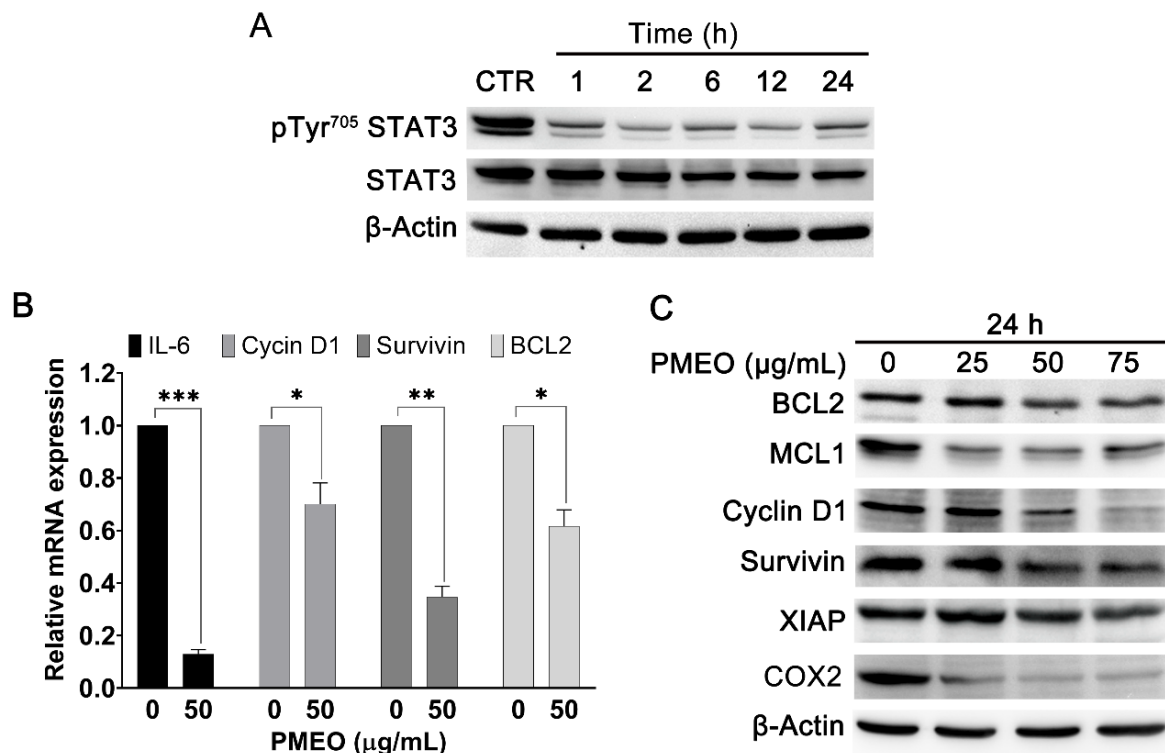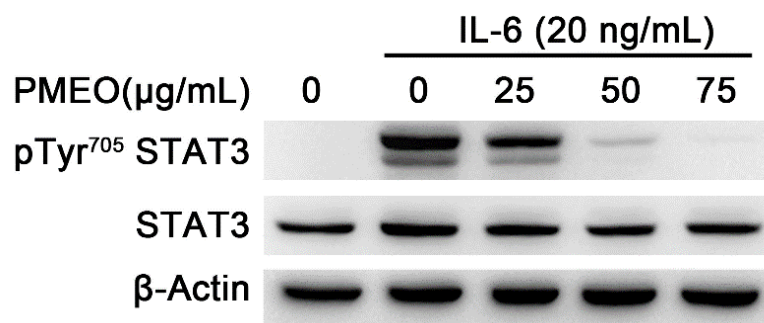

(Figure legend in the next page)

Figure 14: **PMEO suppresses constitutive STAT3 signaling activation and the expression of downstream STAT3 targets at mRNA and protein levels (A)** DU145 cells were treated with 50 µg/mL PMEO for the indicated time points. Total protein extracts were analysed by Western blot using anti-pTyr705STAT3 antibody and anti-STAT3 antibody after membrane stripping. β-Actin is shown as the internal loading control **(B)** DU145 cells were exposed to 50 µg/mL PMEO for 24 h, and total RNA was analysed by real-time PCR assay. The data were normalized against SDHA RNA, and the levels of mRNA are expressed as the value relative to untreated cells. Each bar represents the mean±SD of four independent experiments performed in triplicate and Two-way ANOVA test with Tukey's multiple comparison was performed to determine statistical significance, $p < 0.0001$ (***); $p < 0.001$ (**); $p < 0.01$(*). **(C)** DU145 cells were treated with the indicated concentrations of PMEO for 24 h, untreated cells represented as 0 µg/mL is negative control. Total protein extracts were analysed by Western blot using antibodies specific for Bcl2, MCL1, Cyclin D1, Survivin, XIAP and COX2 proteins. β-Actin is shown as the internal loading control. The data shown are representative of four independent experiments.

5.5. PMEO Suppresses IL-6-Induced STAT3 Activation

IL-6 plays a crucial role in maintaining normal cell growth through STAT3 activation but its aberrant activation results in the proliferation of cancer cells. Interestingly, in the TME surrounding the tumor cells, IL-6 is also produced by other types of cells, such as tumor-infiltrating immune cells and stromal cells, resulting in the hyperactivation of STAT3 signaling. STAT3 in turn also promotes IL6 expression, resulting in a feedback loop that further contributes to malignancies [83]. Therefore, the inhibitory effect PMEO on IL-6-induced activation of STAT3 was evaluated. For this experiment, LnCAP cell line another human prostate adenocarcinoma cell line was chosen as the model wherein STAT3 is not constitutively active but can be induced by treating with IL-6. Western blot analysis showed that 20 ng/mL IL-6 rapidly induced STAT3 Try705 phosphorylation in 15 min treatment. Further, pre-treatment of cells for 45 min with PMEO decreased IL-6-induced Tyr705 phosphorylation of STAT3 in a dose-dependent manner, without affecting the total amount of STAT3 protein (**figure 15**).

(Figure legend in the next page)

Figure 15: PMEO inhibit STAT3 activation induced by IL-6. LnCAP cells were treated with the indicated concentrations of PMEO for 45 min and then with 20 ng/mL IL-6, untreated cells represented as 0 μg/mL is negative control. Total protein extracts were analysed by Western blot using anti-pTyr705STAT3 antibody and anti-STAT3 antibody after membrane stripping. β-Actin is shown as the internal loading control. The data shown are representative of four independent experiments.

5.6. Inhibition Of STAT3 Activation By PMEO Is Mediated Through Oxidative Stress

Interestingly, several EOs and their constituents have been reported to mediate pro-oxidant mechanisms. We hypothesized that a similar mechanism might be mediated by PMEO as well. To analyse whether PMEO affects the intracellular redox state, DU145 cells were loaded with the cell-permeable ROS-specific fluorescent probe H2DCFDA and then treated with 50 and 75 μg/mL PMEO for 30 min and 1 h. The fluorescence intensity of cells rapidly increased in a dose- and time-dependent manner, suggesting an enhancement of intracellular ROS levels. We observed the maximum fold change in fluorescence intensity at 30 min compared to 1 h treatment (**figure 16A**). Then the levels of intracellular GSH was evaluated after PMEO treatment. Spectrophotometric analysis showed that 50 μg/mL PMEO induced a rapid and significant drop in GSH concentration (**figure 16B**). Finally, to evaluate if the inhibition of STAT3 activation by PMEO is correlated with induced oxidative stress, DU145 cells were pre-treated with 10 mM N-Acetyl-L-Cysteine (NAC), a well-known ROS scavenger, for 1 h and then treated with the indicated concentrations of PMEO for 1 h. Western blot analysis showed that NAC pre-treatment partially reversed the effects of PMEO on the inhibition of STAT3 phosphorylation (**figure 16C**).

Collectively the results show that PMEO induce ROS generation and a rapid decline in the GSH levels. Further inhibition of STAT3 phosphorylation by PMEO treatment is dictated through a ROS dependant mechanism.
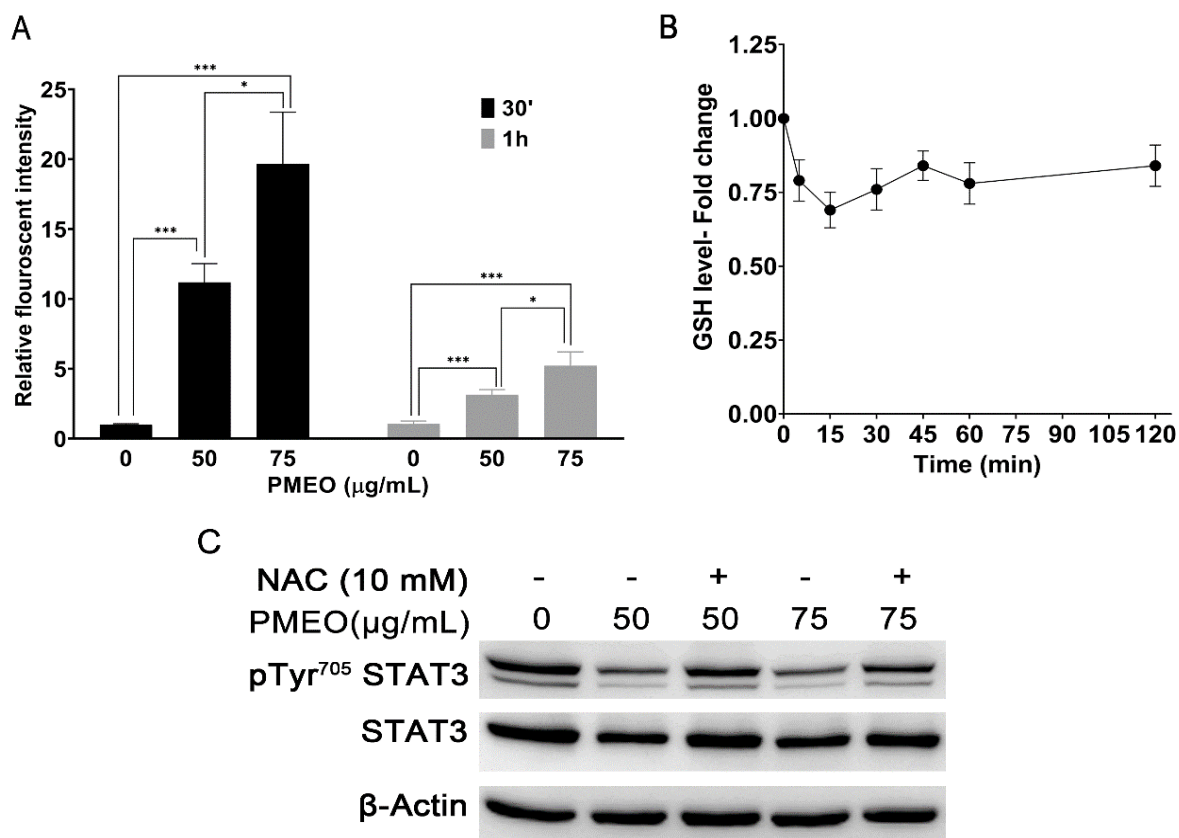
Figure 16. STAT3 inactivation by PMEO is mediated through increased ROS generation. (A) DU145 cells loaded with H2DCF-DA were treated with 50 and 75 μg/mL PMEO for 30 min or 1 h, untreated cells represented as 0 μg/mL is negative control. The fluorescence was analysed for ROS production. ROS levels are expressed as the value relative to untreated cells. The data are presented as means ±SEM of three independent experiments and Two-way ANOVA test with Tukey's multiple comparison was performed to determine statistical significance, $p < 0.0001$ (***); $p < 0.001$ (**); $p < 0.01$(*). **(B)** DU145 cells were treated with 50 μg/mL PMEO for the indicated time points, and GSH levels were spectrophotometrically analysed by DTNB. GSH levels are expressed as the value relative to untreated cells. Data are presented as means ±SEM of five independent experiments. **(C)** DU145 cells were pre-treated with 10 mM NAC for 1 h and then treated with the indicated concentrations of PMEO for 1 h more. Untreated cells represented as 0 μg/mL is negative control. Total protein extracts were analysed by Western blot with pTyr705STAT3 antibody and with anti-STAT3 antibody after membrane stripping. β-Actin is shown as the internal loading control. The data shown are representative of three independent experiments.

5.7. PMEO Inhibits Activation Of STAT3 Upstream Kinase, Src

Increasing oxidative stress using small molecules and phytochemicals has been shown to inhibit the activity of upstream kinases that activate STAT3 [92]. The upstream kinases that activate STAT3, include JAKs and Src family kinases. Among the JAKs, JAK2 has been shown to be more frequently activated in cancer cells and may play a more important role in cancer development and progression [187]. Src kinase is also particularly important in cancer development, progression and chemoresistance. Src is overexpressed and activated in many types of cancer, including breast, ovarian, colon, lung, and prostate cancer [188]. These kinases are reported to phosphorylate STAT3 and sustain its constitutive activation [189].

Therefore, the effect PMEO treatment on the activation of JAK2 and Src kinases were evaluated. For this, DU145 cells were treated with various concentrations of PMEO for one hour and analysed the protein expression by western blotting. The results obtained indicate that PMEO treatment had no effects on the levels of phosphorylated JAK2 or JAK2 (**figure 17A)** but there was a dose dependant decrease in the levels of phosphorylated Src without changing the total Src expression (**figure 17B)**. This result suggests that one possible route through which PMEO inhibit STAT3 activation is by the inhibition of Src activation.
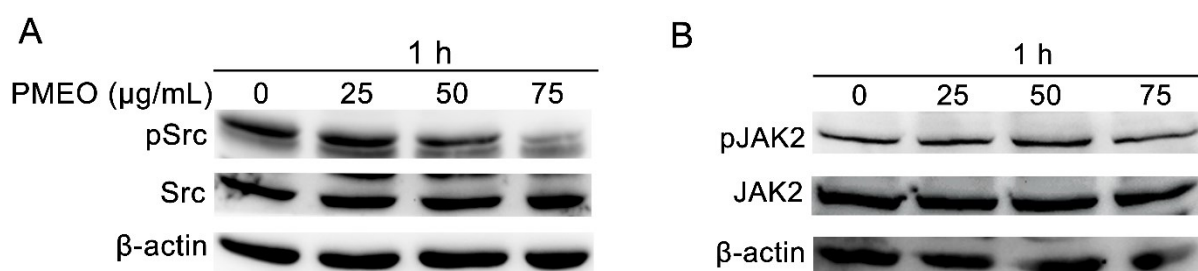

Figure 17. PMEO inhibit activation of STAT3 upstream kinase Src. DU145 cells were treated with the indicated concentrations of PMEO for 1 h, Untreated cells represented as 0 μg/mL is negative control. Total protein extracts were analysed by Western blot with antibodies specific for pJAK2, pSrc and with JAK2, and Src antibodies after membrane stripping. β-Actin is shown as the internal loading control. The data shown are representative of three independent experiments.

5.8. PMEO Induces Apoptotic Death In DU145 Cells

To assess if the mechanism by which PMEO cause cytotoxicity is apoptosis, PMEO-treated DU145 cells were subjected to Annexin V/PI double staining and flow cytometry analysis. An Annexin V/PI plot uses 4 quadrants to analyse cell apoptosis. The % of cells in each quadrant indicates their stage of apoptosis/necrosis: Q1 (Annexin V-/PI-): live cells, Q2 (Annexin V+/PI): early apoptosis, Q3 (Annexin V+/PI+): late apoptosis, Q4 (Annexin V-/PI+): dead/necrosis.

A dose-dependent increase in Annexin V+/PI- and Annexin V+/PI+ cells was observed, suggesting the irreversible onset of the apoptotic cascade. Altogether, 38% and 50% of cells were Annexin V+/PI- and Annexin V+/PI+, respectively, after treatment with 50 μg/mL and 75 μg/mL PMEO for 24 h (**Figure 18A**). Caspase 3, a member of the caspase family of cysteine proteases is activated during intrinsic apoptosis, triggers cell death by cleaving downstream caspases and proteins such as PARP and their levels are important markers of apoptosis induction [190].

Results from flow cytometry through was further confirmed through western blotting analysis of Cleaved caspase-3 and Cleaved PARP expression in the DU145 cells treated with 25, 50 and 75 μg/mL PMEO for 24 h. As shown in **figure 18B**, PMEO dose-dependently increased the levels of Cleaved caspase-3 and Cleaved PARP. To evaluate the time kinetics, cells were treated with 50 μg/mL PMEO for different time points and as demonstrated in the **figure 18C**, expression of cleaved caspase-3 was observed starting from 2 hours of treatment, corresponding increase in cleaved PARP and decrease in full length PARP, confirming that PMEO mediated cell death through apoptotic pathway.
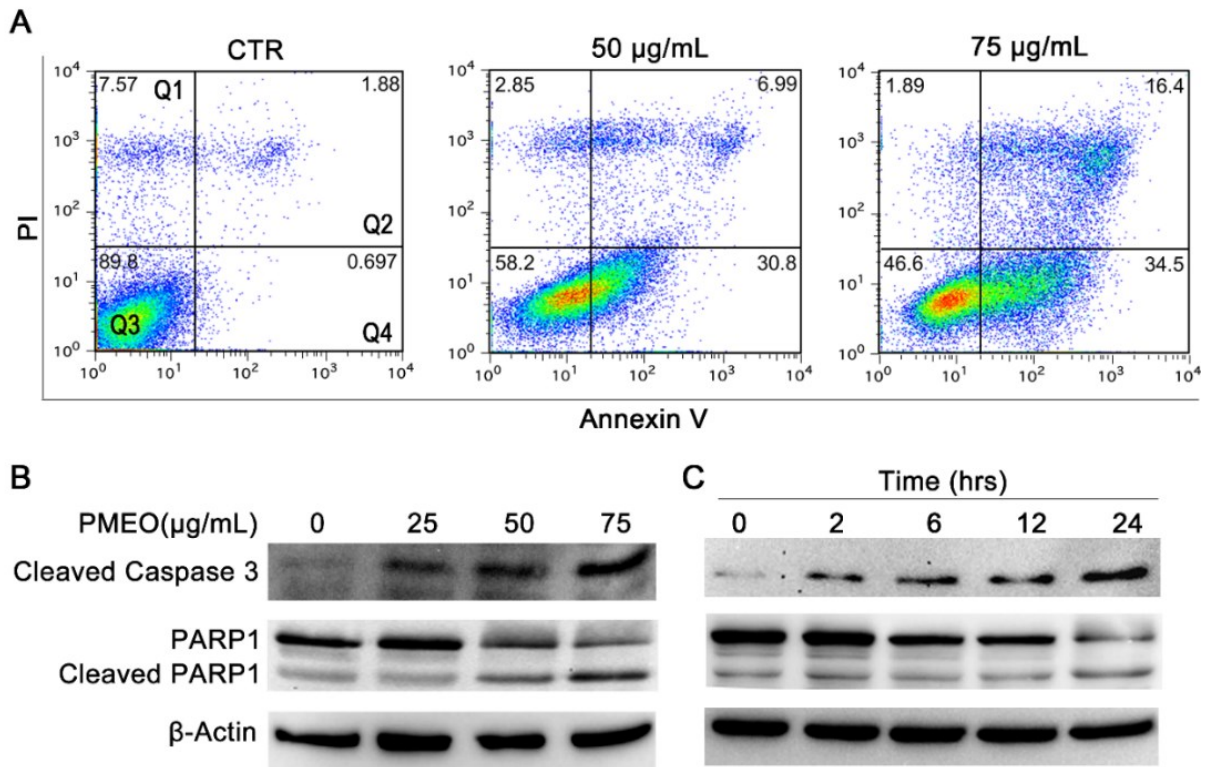
Figure 18. PMEO induces apoptosis in DU145 cells. **(A)** DU145 cells were treated with 50 and 75 μg/mL PMEO for 24 h, CTRL represent untreated cells as negative control, stained with Annexin V/PI, and analysed by flow cytometry for apoptosis detection. The plots represent population of cells in different quadrants (Q1- Dead/Necrotic cells, Q2- Late apoptosis, Q3- healthy live cells, Q4- Early apoptotic cells). **(B)** DU145 cells were treated with indicated doses of PMEO for 24 h **(C)** and for the indicated time points with 50 μg/mL PMEO, Untreated cells represented as 0 μg/mL is negative control, total protein extracts were analysed by Western blot for the expression of cleaved caspase-3 and PARP1. PARP1 antibody recognizes both intact PARP (116 kDa) and the cleaved fragment (89 kDa). β-Actin was used as the internal loading control. The data shown are representative of three independent experiments.

5.9. PMEO Impairs Migration Of DU145 Cells

STAT3 has been reported to regulate several genes responsible for the cell migration and is regarded as a crucial transcription factor that mediate cancer metastasis. Furthermore, Inhibition of STAT3 activation has been demonstrated to reduce cancer cell migration cell migration and suppress metastatic factors [191]. Therefore, the effects of PMEO on cell migration was evaluated by using a wound healing assay (scratch assay). It was observed that PMEO treatment dose-dependently inhibited the migration of DU145 cells and prevented wound closure (**figure 19A&B)**. Consistent with this result, western blot analysis revealed that, 24 h PMEO treatment dose-dependently inhibited the expression of genes implicated in the migration and epithelial-to-mesenchymal transition such as ZEB1, TWIST1 and Vimentin, as well as the angiogenic factor

VEGFC (**figure 19C)**. Taken together, these results suggest that PMEO can effectively suppress cancer metastasis by impairing the activation of STAT3 signaling.
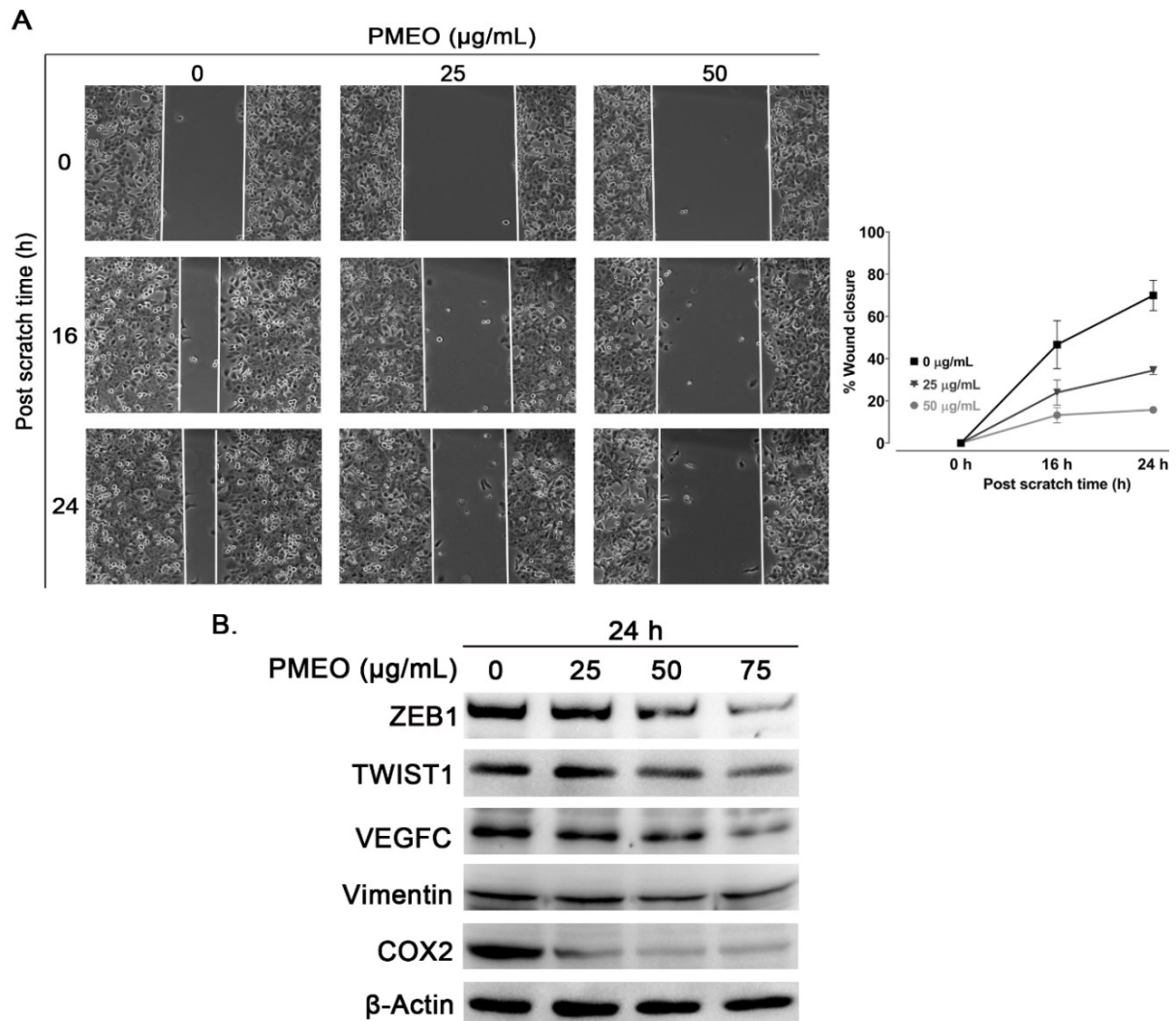

Figure 19: Pinus mugo EO inhibits cell migration in DU145 cells. **(A)** DU145 cells were treated with 25 and 50 µg/mL PMEO for the indicated time points. Untreated cells represented as 0 µg/mL is negative control. % Wound closure was calculated using ImageJ/Fiji software (https://imagej.net/Fiji) is also represented **(D)** DU145 cells were treated with 25, 50 and 75 µg/mL PMEO for 24 h, and total protein extracts were analysed by western blot using anti-ZEB1, anti-TWIST-1 and anti-Vimentin antibodies. β-Actin was used as the internal loading control. The data shown are representative of three independent experiments.

5.10. PMEO Is Synergistic With Cisplatin And Enhances Chemosensitivity Of DU145 Cells.

Combining existing chemotherapy drugs with phytochemicals like essential oils has been proposed to enhance efficacy, overcome chemoresistance, and mitigate severe side effects [148]. Several studies link STAT3 activation in chemoresistance to major drugs such as Doxorubicin and Cisplatin [192]. As PMEO efficiently inhibited STAT3 activation and induced cytotoxicity, we sought to evaluate the combinatorial effect of PMEO with cisplatin in DU145 cells. To this end, PMEO was combined with cisplatin at a constant ratio of 2:1 and analysed the combinatorial effect on cytotoxicity after 24 h treatment employing the median-effect method described by Chou and Talalay [184].

The Chou-Talalay method is widely used to determine the effects of drug combinations, by using a metric called combination index (CI) and factor affected (FA) for a given dose of two or more drugs. A CI value of 1 indicates additive effects, less than 1 indicates synergistic effects, and greater than 1 indicates antagonistic effects [184]. As depicted in the **figure 20**, the results show that the combination of PMEO with cisplatin enhanced the cytotoxicity and the FA-CI plot (Factor Affected-Combination index plot) proved a synergistic mechanism of action. The CIs (Combination index) and DRIs (Dose reduction index) of drug combinations for concentrations that inhibited 50, 75, 90 and 95% of cell viability (IC50, IC75, IC90 and IC95, respectively) are represented in **table 6**. The combination of PMEO and cisplatin allowed a dose reduction of cisplatin of up to 113.88 -fold (IC95). A favourable DRI > 1 allows a dose reduction that leads to toxicity reduction in the therapeutic applications.
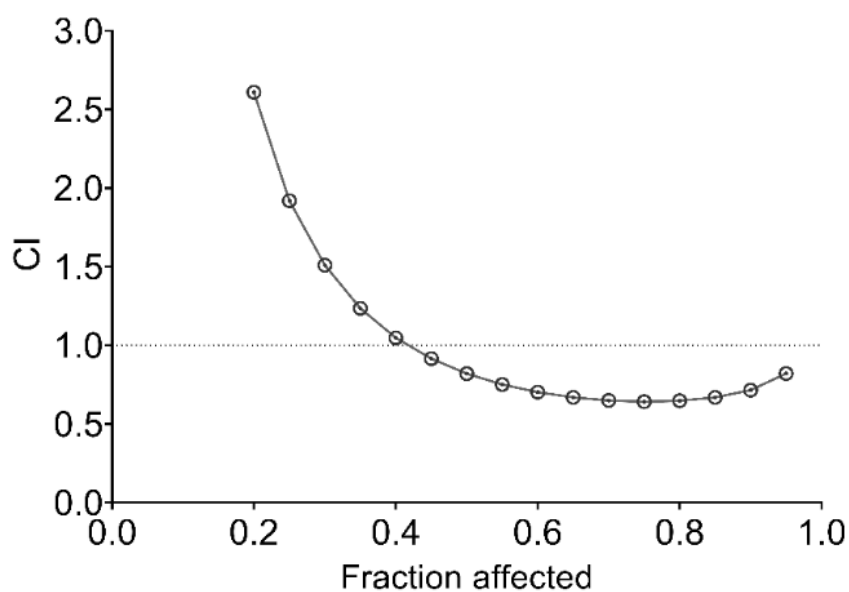

Figure 20: Fa–CI plot of interaction between Pinus mugo EO and cisplatin.

Table 6. Combination index (CI) and dose-reduction index (DRI) when PMEO and cisplatin   at combined a constant ratio of 2:1.

	CI	DRI	
		Cisplatin	PMEO
IC50	0.82	2.59	2.31
IC 75	0.64	10.62	1.82
IC 90	0.72	43.59	1.44
IC 95	0.82	113.88	1.23

5.11. Preparation Of PMEO Loaded PLGA Nanoparticles (PMEO-NPs)

Emulsion solvent evaporation method have been established as an efficient method for the encapsulation hydrophobic phytochemicals such as EOs in polymeric nanocarriers. For example, Ercin et al. recently reported preparation of the *Laurus Nobilis* EO loaded PLGA-PVA nanoparticles using the single-emulsion method [178]. In a similar manner, PMEO loaded PLGA-nanoparticles (PMEO-NPs) was prepared using PVA and TPGS as emulsifying agent by single emulsion solvent evaporation method, as schematically depicted (**figure 21).**
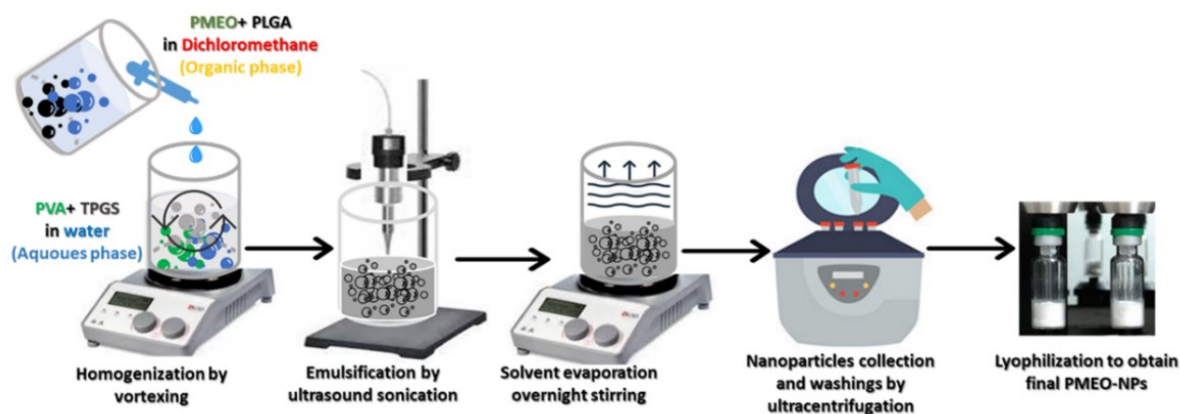

Figure 21: Preparation and encapsulation efficiency of PMEO-NPs. Schematic diagram of PMEO-NPs preparation using single emulsion solvent evaporation method

5.12. Physicochemical Characterization Of PMEO-NPs

Firstly, the UV/visible spectra of different concentration of PMEO prepared in acetonitrile was acquired (**figure 22A**). Maximum absorbance values (λmax) at 194 nm were used to draw standard calibration curve of PMEO (**figure 22B**). Then, the UV spectra of NPs solutions, prepared by dissolving 1 mg of three different baches of PMEO-NPs in 1 mL acetonitrile, and further diluted by 10 times were obtained. The amount of PMEO encapsulated in the nanoparticles were estimated using the standard calibration curve. Accordingly, average encapsulation efficiency (EE%) and loading capacity (LC%) of PMEO into the NPs were estimated to be approximately 55% and 5.5%, respectively (**figure 22C)**.

TEM and SEM images of PMEO-NPs revealed that the nanoparticles had a uniform size distribution, characterized by smooth and spherical surfaces (**figure 22D&E**). Further DLS analysis was performed to measure the average particle size, the polydispersity index and Zeta potential. The results showed that PMEO-NPs had an average particle diameter of 253.3 nm and a polydispersity index of 0.158, (**figure 22F**). These results revealed that PMEO NPs were slightly larger and more dispersed than the void PLGA nanoparticles, having an average size of 223.9 nm and a PDI of 0.130. This size and PDI difference may be attributed to the PMEO encapsulation in the NPs. The zeta potential of PMEO-NPs was around -19.1 mV, lower than that of void nanoparticles (-15 mV) (Figure 12G), consistent with previously reported values for PLGA nanoparticles. Finally, *in vitro* kinetics of PMEO release from NPs in PBS buffer was assessed from samples collected at various time points starting from 30 minutes and up to 5 days. The results demonstrated that PMEO-NPs followed a biphasic trend in the PMEO release as a burst release in the initial hours till 24h followed by a sustained release for 5 days (**figure 22H**).
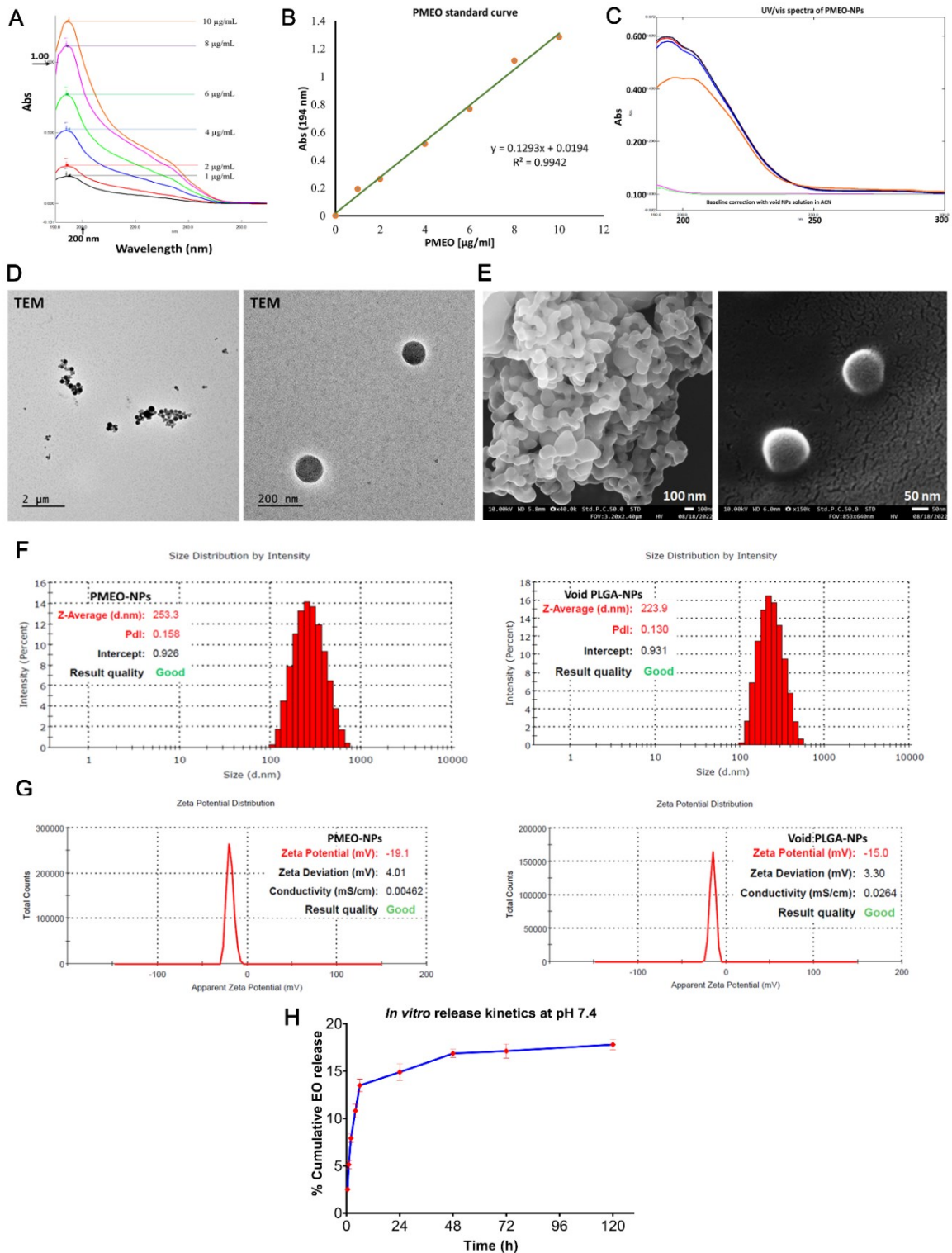
Figure 22: Physicochemical characterization of PMEO-NPs. (A) UV/Vis spectra of PMEO. (**B)** Standard curve of PMEO drawn with the obtained absorbance values. **(C)** The UV/vis spectra of PMEO-NPs used for determining the encapsulation efficiency and loading capacity of PMEO-NPs. **(D)** TEM images and SEM images of PMEO-NPs. **(F)** Size distribution and **(G)** Zeta potential of PMEO-NPs and Void PLGA-NPs. **(H)** *In vitro* drug release profile at physiological pH (The data are presented as means ±SD of three independent experiments).

5.13. MDA-MB-231 Cells Efficiently Take Up 6-Coumarin-Loaded PLGA-NPs

The understanding of cellular uptake is vital for the successful application of nanoparticle-based products in therapy. Cellular uptake of fluorescent dye, 6-coumarin (6C) has been previously used as a model to analyse the cellular uptake of PLGA-NPs [193]. Similarly, to evaluate the cellular uptake of the nanoformulation, 6-C dye was loaded in the PLGA-NPs instead of PMEO and synthesized the 6C-PLGA-NPs following the same scheme. The encapsulation efficiency of 6-Coumarin in PLGA-NPs was calculated using standard curve method based on UV/Vis spectroscopy (λmax at 466nm). Then MDA-MB-231 cells were treated with equivalent concentrations (100 ng/ml) of native 6-coumarin or 6C-PLGA-NPs for 1h and observed the fluorescent intensity using fluorescence microscope. The fluorescent intensity of 6-coumarin was observed to be higher in cells treated with 6C-PLGA-NPs compared to native 6-coumarin, (**Figure 23A&B**), suggesting the efficient cellular uptake of the nanoparticles.
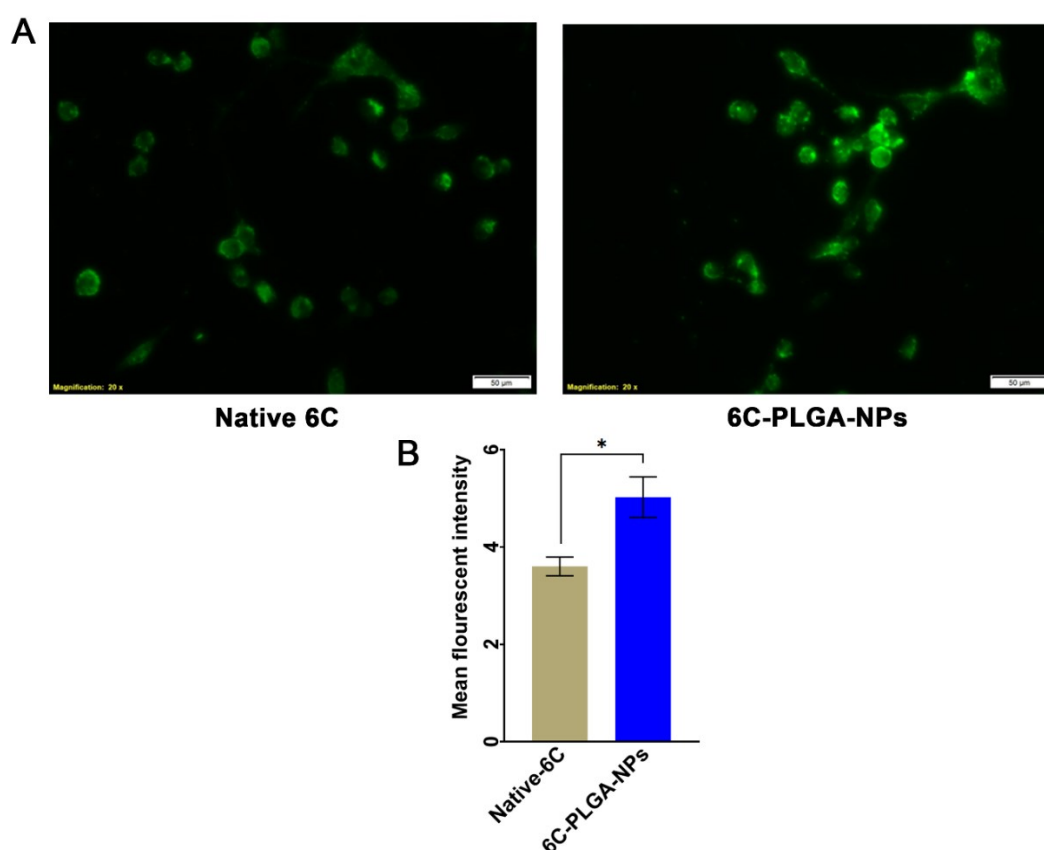

Figure 23. In vitro cellular uptake of PLGA-NP in MDA-MB-231 cells. In vitro cellular uptake study of native 6-coumarin or 6-coumarin NPs (100 ng/ml) at 1 h by fluorescence microscopy **(A)** Representative images **(B)** Graph report the quantification of fluorescent intensity using ImageJ software (data represented as mean $\pm$ SD of three independent experiments and $P < 0.01$ (*) statistical significance in two-tailed student's t-test).

5.14. PMEO-NPs Show higher Cytotoxicity In MDA-MB-231 Cells.

Biological effects of PMEO-NPs in comparison to the free PMEO was evaluated. Cytotoxicity of PMEO and PMEO-NPs, containing equivalent PMEO amount of PMEO on MDA-MB-231 cells for 24 and 48 h was analysed by MTT assay. The results demonstrated that the nanoformulation significantly increased the cytotoxicity of PMEO. IC50 values were reduced from ≈105 to ≈70 and from ≈90 to ≈50 (µg/mL) in 24 and 48 h, respectively (**figures 24A and 24B**). Notably, Void PLGA-NPs that were prepared using the same method but without incorporating drugs were previously proven to be safe and non-cytotoxic [176].These findings indicate that encapsulating PMEO encapsulated in PLGA nanoparticles improved anticancer cytotoxic efficacy and can be further investigated as alternative or complementary option for cancer therapy.
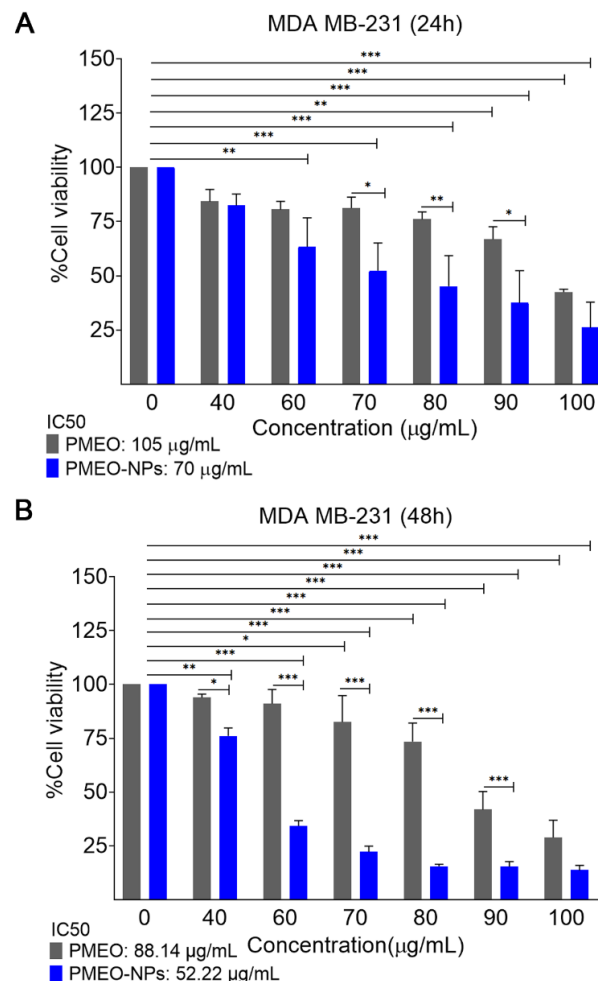

Figure 24: PMEO-NPs enhanced the cytotoxicity towards cancer cells. (A) Graph report cytotoxicity of Void PLGA-NPs on MDA-MB-231 cells in 48h treatment, CTRL represent untreated cells as negative control, Graphs report comparative analysis of cytotoxicity of PMEO and PMEO-NPs on MDA-MB-231 cells in **(B)** 24h and **(C)** 48h (Each bar represents the mean ±SD of three independent experiments performed in technical triplicate and Two-way ANOVA test with Tukey's multiple comparison was performed to determine statistical significance, $p < 0.0001$ (***); $p < 0.001$ (**); $p < 0.01$(*).

5.15. PMEO-NPs Enhances ROS levels In MDA-MB-231 Cells.

The impact of PMEO nanoformulation on ROS generation was assessed in MDA-MB-231 cells treated with PMEO, and PMEO-NPs containing equivalent amount of PMEO for 1h (1 hour was chosen due to significant cellular uptake of nanoparticles), incubated with H2DCFDA dye, and then analysed by flow cytometry. The results demonstrate that PMEO and PMEO-NPs significantly enhanced ROS levels in MDA-MB-231 cells with respect to untreated control cells. Moreover, PMEO-NPs significantly enhanced ROS generation compared to compared to free PMEO (**figure 25**). The findings imply that utilizing a nanoformulation can enhance the effectiveness of PMEO by promoting ROS generation, potentially due to the increased cellular retention. This approach may also be useful for enhancing the therapeutic properties of other volatile and unstable compounds, such as EOs.
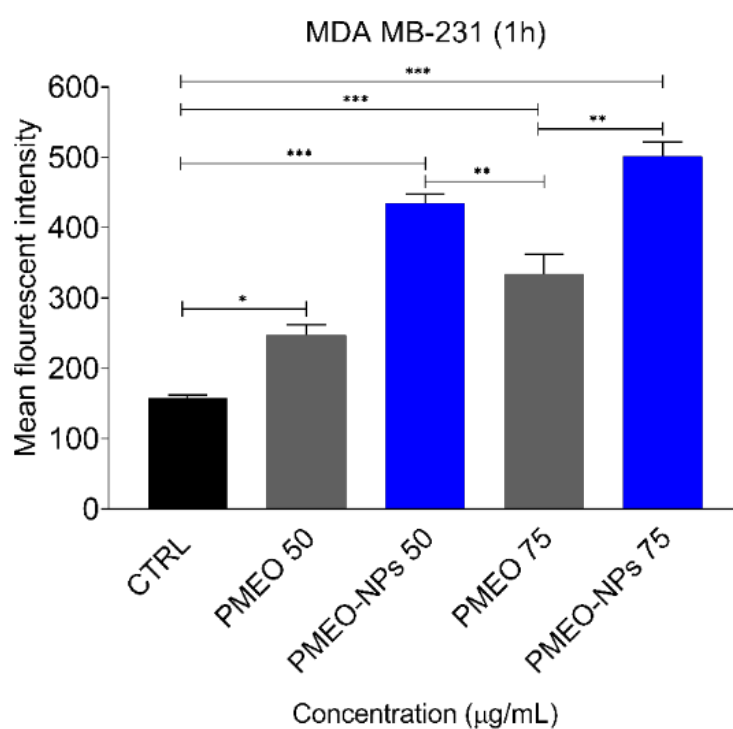

Figure 25: PMEO NPs enhanced ROS generation in MDA-MB-231 cells. MDA-MB-231 cells were treated with PMEO and PMEO-NPs containing an equivalent amount of PMEO at concentrations of 50 and 75 μg/mL for 1 h, untreated cells are represented as CTRL (negative control). After the treatment cells were washed and incubated with H2DCFDA dye and fluorescence intensity was analysed for ROS production. ROS levels are expressed as the value relative to untreated cells. The data are presented as means ±SD of three independent experiments. Two-way ANOVA test with Tukey's multiple comparison was performed to determine statistical significance, $p < 0.0001$ (***); $p < 0.001$ (**); $p < 0.01$(*).

5.16. PMEO-NPs Increased Apoptotic Cells In MDA-MB-231 Cells

Our previous finding has shown that PMEO induces cytotoxicity through apoptosis pathway. Therefore, we wanted to determine if nanoencapsulation enhances the apoptotic effects of PMEO. For this, Acridine Orange and Ethidium Bromide (AO/EtBr) dual staining in the cells treated with PMEO and PMEO-NPs was performed. AO/EtBr dual staining is a method used to determine apoptotic cells based on the principle that healthy cells emit green fluorescence, early and late apoptotic cells emit yellow-green fluorescence, and dead or necrotic cells emit red fluorescence. This is based on the principle that AO and EtBr bind to DNA in different ways depending on the integrity of the cell membrane and the level of DNA fragmentation. AO intercalates into DNA and emits green fluorescence, while EtBr only enters cells with damaged membranes and emits red fluorescence when intercalated into fragmented DNA. This staining method allows for a qualitative analysis of apoptosis [182]. The results showed that cells treated with PMEO and PMEO-NPs showed a higher incidence of apoptotic morphology. Particularly in the PMEO-NPs group, we observed that majority of the cells displayed early and late apoptotic morphology (**figure 26**). These results suggest that the nanoformulation of PMEO may enhance its apoptotic effect, which merits further investigation to elucidate the underlying mechanisms.
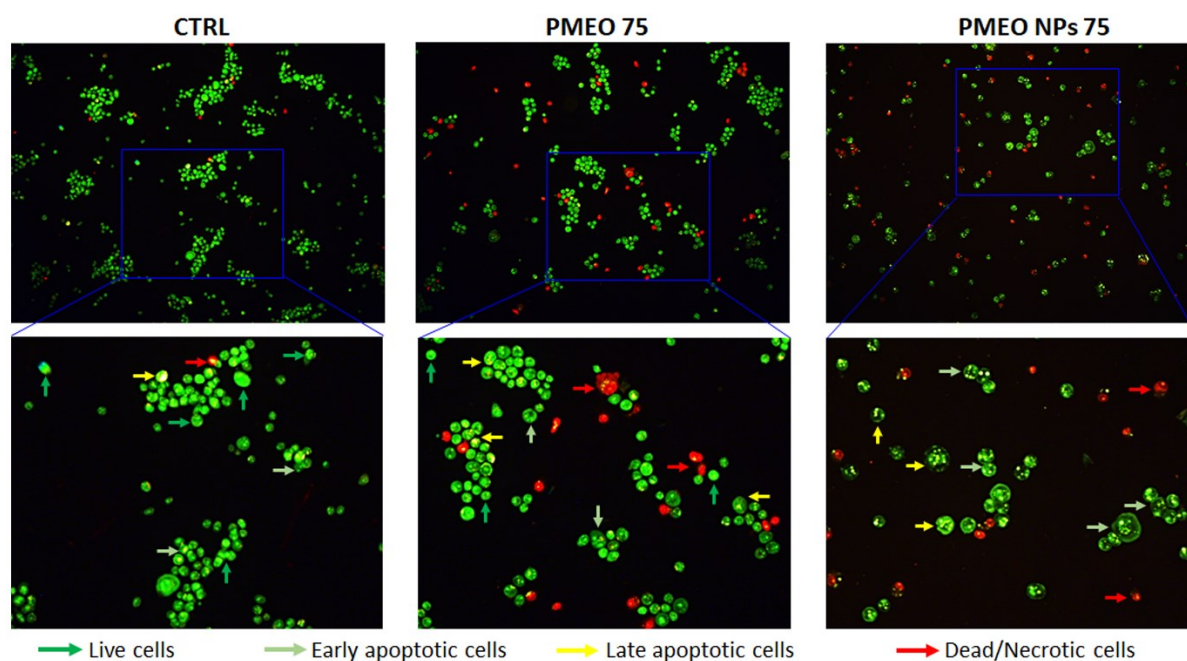

Figure 26: PMEO-NPs enhanced apoptosis apoptotic cells in MDA-MB-231 cells. Microscope images of the Acridine Orange and Ethidium Bromide (AO/EtBr) staining of MDA-MB-231 cells treated with PMEO and PMEO-NPs containing an equivalent amount of PMEO at concentrations of 50 and 75 µg/mL for 48h. Arrows with different colours represent cells in different stages as indicated.
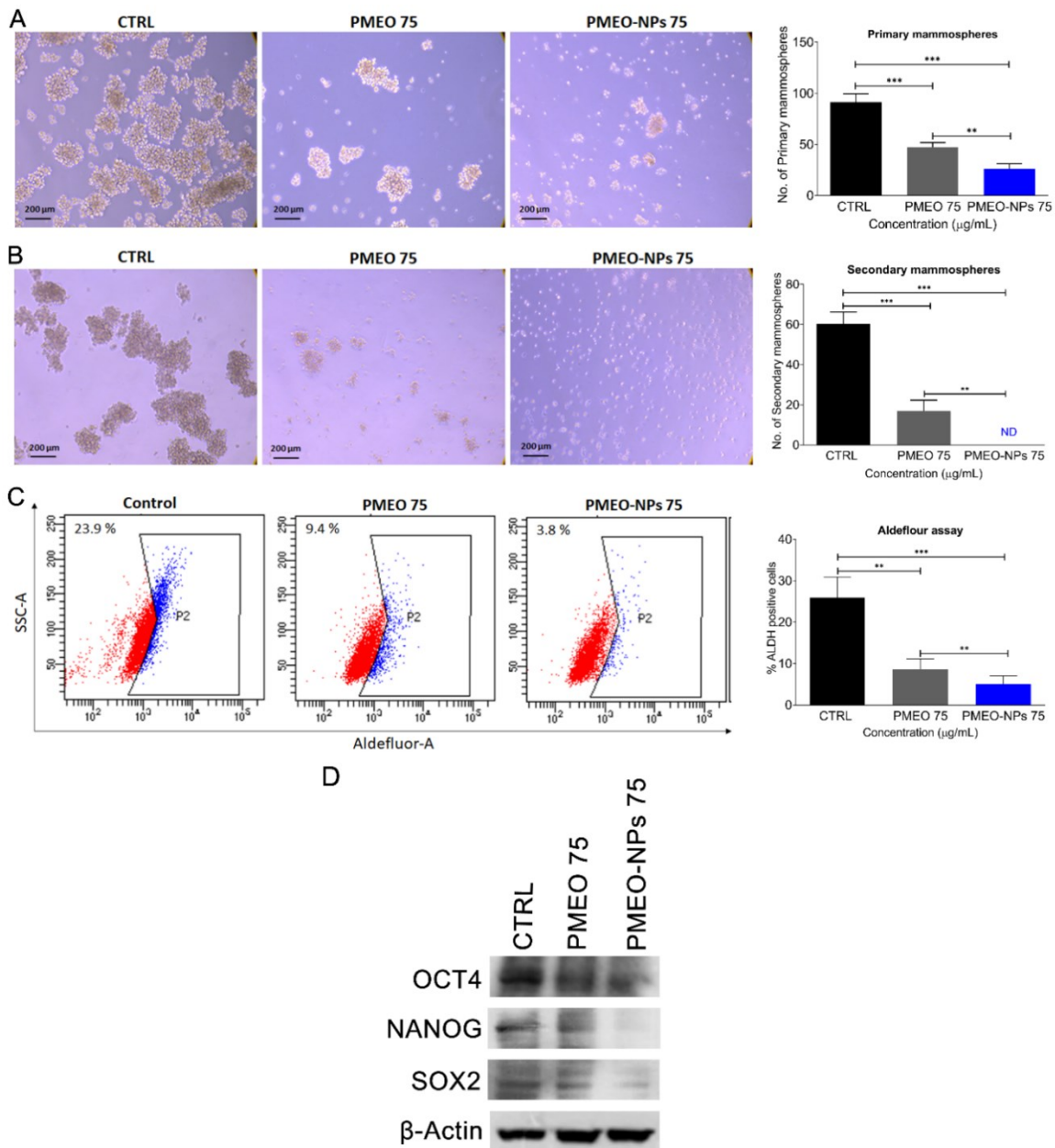
5.17. PMEO-NPs Enhanced Inhibition Of Stemness And Self-Renewal Properties Of Mammospheres

Recently phytochemicals have garnered significant interest as potential agents for suppressing the stemness and self-renewal properties of cancer stem cells, particularly in breast cancer. EO constituents such as Citral, Eugenol and Diallyl Disulfide have been reported to reduce the stemness characteristics in breast cancer [165][164][194]. It has been reported Citral encapsulated in polyethylene glycol-block-polycaprolactone (PEG-b-PCL) polymeric nanoparticles (Citral-NPs), showed strong inhibition of ALDHA13 activity, which is an important breast cancer stemness marker and suppressed the growth of MDA-MB-231 cells [195]. These findings inspired us to evaluate the effect of PMEO and PMEO-NPs on the stemness and self-renewal properties of breast cancer.

Mammospheres were generated from MDA-MB-231 cells as described in the methods and the effect of PMEO and PMEO-NPs on primary sphere formation was assessed by treating them with a concentration of 75 μg/mL for 48h. The results as shown in the **figure 27A&B** demonstrate that both PMEO and PMEO-NPs significantly reduced the formation of primary mammospheres compared to the control. A significant difference was observed between the PMEO and PMEO-NPs groups, suggesting that the nanoformulation has enhanced efficacy. Further, the self-renewal capacity of mammospheres was evaluated using the secondary sphere formation assay. This assay is designed to measure the ability of mammospheres to self-renew and proliferate into secondary mammospheres by dissociating existing mammospheres into individual cells and plating them at low density. The treatments used in the primary sphere formation assay were repeated, and as shown in **figure 27C&D** and it was noted that PMEO treatment led to a significant decrease in the formation of secondary spheres, while in the case of PMEO-NPs, the formation of secondary spheres was not detected, suggesting the loss of self-renewal capacity of the mammospheres.

Subsequently, the impact of PMEO and its nanoformulation on cancer stemness was evaluated from a molecular perspective by Aldefluor assay. This assay measures the population of ALDH (aldehyde dehydrogenase) positive cells, which is an enzyme linked to the regulation of stem cell properties and cancer stemness. Mammospheres were treated with PMEO and PMEO-NPs at a concentration of 75 μg/mL for 48 hours, then dissociated into individual cells. The cells were then stained with an ALDH substrate and analyzed using a flow cytometer.

The results showed that in comparison to the control, PMEO and PMEO-NPs markedly reduced the percentage of ALDH-positive cells **(figure 27E&F).** Consistent with these results, western blotting analysis of MDA-MB-231 cells treated with 75 µg/mL PMEO and PMEO-NPs for 48h showed decline in the expression of key proteins that drive stemness properties including OCT4, NANOG and SOX2 **(figure 27G)**. Overall results provide evidence for the potential of PMEO in suppressing the stem cell and self-renewal properties of breast cancer, with the nanoformulation exhibiting enhanced effectiveness. Therefore, EOs and their nanoformulations merit further investigation for the development as complementary or alternative therapies to conventional chemotherapy in the treatment of highly metastatic cancers.

(Figure legend in the next page)

Figure 27. PMEO-NPs show enhanced inhibition of stemness and self-renewal properties of mammospheres. (A) Mammosphere formation assay-mammospheres were treated with 75 µg/mL of either PMEO or PMEO-NPs, representative images of primary mammospheres taken at 10X objective in phase contrast microscope, scale bar 200 µm, **(B)** Graph report the number of primary mammospheres, **(C)** Representative images of secondary mammospheres **(D)** Graph report the number of secondary mammospheres **(E)** ALDH assay was performed with 75 µg/mL of either PMEO or PMEO-NPs and analysed through flow cytometry using ALDEFLUORTM kit, representative flow cytometry images and **(F)** Graph report the % population ALDH positive cells in each group. **(G)** MDA-MB-231 cells were treated with 75 µg/mL PMEO and PMEO-NPs for 48 h, and total protein extracts were analysed by western blot using antibodies specific against OCT4, NANOG and SOX2. β-Actin was used as the internal loading control. All the images are representative of three independent experiments. Data represented in the graphs are mean ± SD of three independent experiments and two-tailed student's t-test was performed to determine statistical significance between the groups, $p < 0.0001$ (***); $p < 0.001$ (**); $p < 0.01$(*).

6. DISCUSSION AND CONCLUSIONS

The transcription factor STAT3 is extensively involved in various oncogenic events and abundant evidence support the critical role of constitutively active STAT3 signaling underlying the hallmarks of cancer and other major challenges such as promoting cancer stem cells and chemoresistance [196][1]. In this regard, pharmacological strategies counteracting the STAT3 hyperactivation has been considered a potential anticancer strategy [123].

Due to major clinical roadblocks, such as toxicity towards non-transformed healthy cells, ineffectiveness due to chemoresistance, and other side effects, the use of synthetically derived anticancer drugs is being is under concern. As an alternative, bioactive natural compounds such as phytochemicals have been revived as potential anticancer agents and as adjuvant therapy. The advantages of phytochemicals include low systemic toxicity, high chemical diversity, and multimodal mechanisms of action which make them attractive candidates for developing novel anticancer agents.

Essential oils (EOs) are phyto-complexes comprised of several low molecular-weight, volatile, and hydrophobic compounds that exhibit diverse biological activities [142]. Some EOs and their constituents have been shown to have significant anticancer effects, including inhibiting cell growth, promoting cell death, and boosting immune response[141][147]. Furthermore, research has demonstrated that combining certain EOs and their constituents with standard chemotherapy drugs can enhance their effectiveness, sensitize cancer cells that are resistant to certain drugs, as well as reduce systemic toxicities *in vivo* [148].

In this study we report the anti-STAT3 activity and associated cytotoxic effects of a panel of essential oils (EOs) in human prostate cancer cells which shows constitutive STAT3 activation. Through an initial screening of 33 EOs, the EOs of *Pinus mugo* (PMEO), *Lavandula angustifolia* (LAEO), *Pinus sylvestris* (PSEO), and *Cupressus sempervirens* (CSEO) were identified as the most potent agents in inhibiting constitutive STAT3 phosphorylation (IC50 < 50 μg/mL) and inducing cytotoxicity at 24 hours (IC50 < 80 μg/mL). Moreover, only couple of EOs, *Lemongrass EO* and *Eupatorium adenophorum* are previously reported to have anti-STAT3 activity. Our results demonstrating the anti-STAT3 activity of 10 EOs is valuable addition to this. Successively, we found that, PMEO, MOEO, and CSEO showed only very low cytotoxicity in non-transformed human fibroblasts, suggesting their potential as safe adjuvants to conventional chemotherapeutic agents. These findings will pave the way to delineate the underlying mechanisms of action of these EOs and to assess their rational utilization in cancer therapy. Notably, the antiproliferative and

apoptosis inducing effects of MOEO and CSEO have been previously described. Queiroz et al. reported that MOEO induced apoptosis in glioblastoma multiforme cells through ROS dependant caspase-3 activation and DNA-fragmentation [197]. Another study has showed that CSEO induced cytotoxicity in amelanotic melanoma and renal adenocarcinoma cells [198]. Our finding that these EOs can downregulate STAT3 activation is a valuable addition to the mechanistic validation of their anticancer activity. Accordingly, we chose to further evaluate the mechanisms of anti-STAT3 and its consequent anticancer activities of PMEO.

Pinus mugo (synonyms: *P. pumilio* Haenke), commonly known as 'the dwarf pine' or the 'mountain pine' is a shrub-like conifer that thrives at high altitudes in the mountainous regions of southern and central Europe. Essential oil from *Pinus mugo* has been utilized in traditional medicine for its antiseptic, anti-inflammatory, antitussive, expectorant, and fluidizing properties to treat rheumatic and pulmonary diseases [199].

Previously, studies have reported the anticancer properties of essential oils (EOs) from different pine species, such as *Pinus sylvestris*, *Pinus roxburghii* and *Pinus koraiensis*. For instance, Hoai et al. showed that *Pinus sylvestris* EO exhibited cytoxicity against breast cancer cells, especially the triple negative breast cancer cells MDA-MB-231, without reporting the underlying mechanism [200]. It is likely that Pinus sylvestris EO acted via inhibition of STAT3, as it was identified as one of the potent anti-STAT3 EOs in our screening. Moreover, *Pinus roxburghii* EO has been found to induce cytotoxicity in several human cancer cells and to trigger apoptosis in myelogenous leukemia cell line KBM-5 by suppressing NF-$\varkappa$B and NF-$\varkappa$B-regulated genes linked to cell survival, proliferation, and metastasis [201]. Couple of studies have reported anticancer activities of *Pinus densiflora* EO. Ren et al. reported that *Pinus densiflora* needles EO along with two other EOs, suppressed tumor growth in an MCF-7 xenograft mouse model by modulating the AMPK/mTOR signaling pathway [202]. Whereas Jo et al. reported that *Pinus densiflora* leaf EO induced apoptosis via ROS generation, phosphorylation of ERK and activation of caspases in YD-8 human oral cancer cells [203]. Additionally, EO from *Pinus koraiensis* pinecones has been reported to induce apoptosis in gastric cancer cells by regulating the HIPPO-YAP signaling pathway and in in HCT116 colorectal cancer cells through the inhibition of p21 activated kinase 1 pathway [204]. Interestingly, Zhang et al. have recently demonstrated that a nanoemulsion containing *Pinus koraiensis* EO demonstrated *in vivo* antitumour effects in MGC-803 tumor-bearing mice by suppressing tumor proliferation, inducing apoptosis, and alleviating spleen damage [205]. Our results stand in line with these previous findings and validate PMEO as a potential anticancer agent that exhibit cytotoxicity selectively on cancer cells with minimal effect on the viability of non-transformed fibroblasts. Moreover, to the best of our knowledge, this is the first report providing

evidence that a pine EO exerts anti-proliferative and pro-apoptotic effects down-regulation of STAT3 signaling. This study highlights another important finding that PMEO not only inhibits the constitutive activation of STAT3 but also effectively blocks its inducible activation through IL-6 in LnCAP cells that lack constitutively active STAT3. This finding is significant because IL-6 is frequently overexpressed in various cancers, and several chemotherapy drugs induce chemoresistance by activating a feedback mechanism that involves IL-6/STAT3 activation [192]. It has also been reported that the activation of STAT3 by IL-6 in the TME can suppress the functional maturation of dendritic cells (DCs), thereby preventing the activation of effector T cells and hindering the initiation of an antitumor immune response in cancers [83]. Therefore, PMEO could enhance antitumour immunity and opens avenue to its potential utilization as complementary therapy with immunotherapy.

According to the results obtained by GC-MS analysis the major constituents in the chemical composition PMEO are, bicyclic sesquiterpene β-caryophyllene, oxygenated monoterpene bornyl acetate, and monoterpenes such as limonene, α-pinene and 3-carene are the most abundant compounds of PMEO. The major compounds identified is in line with a previously reported composition of PMEO and the anti-STAT3 activity of PMEO may be mediated by one or more of these compounds [206][199]. Of note, β-Caryophyllene has been previously reported to down-modulate STAT3 signaling and as a result chemosensitizes cancer cells to doxorubicin or sorafenib treatments [207]. However, there are no report existing on the anti-STAT3 activity of bornyl acetate, limonene, α-pinene and 3-carene. Nonetheless, the involvement of other minor PMEO constituents also can't be ruled out. Although further analysis aimed at identifying the precise compounds responsible for the anti-STAT3 activity of PMEO is underway in our laboratory, it is possible that the anti-STAT3 activity could potentially be attributed to the activity of multiple compounds. In fact, it has been observed that, when used alone, the same purified single molecules do not usually possess the same effect as the whole EO. This can be ascribed to the presence of several other molecules with similar structures that can synergistically influence the biological activity [208].

Previously, our research group and others have demonstrated that cellular redox balance plays a crucial role in the activation of STAT3, with intracellular GSH levels and ROS concentrations mainly dictate the regulation of STAT3 activity [208][209][133]. While some studies have suggested that moderate levels of ROS triggers tyrosine phosphorylation and increases DNA binding activity[210], other reports indicate that excessive ROS may lead to oxidation of conserved cysteine residues in specific STAT3 domains and induced modifications on STAT3 such as S-nitrosylation and S-glutathionylation, which in turn block its phosphorylation and ultimately leading to a

decrease in its transcriptional activity [211][133]. In this context, our research group identified three oxidative-stress inducing sesquiterpene lactones (dehydrocostuslactone, costunolide, and cynaropicrin) induced STAT3 S-glutathionylation and as a result inhibited the STAT3 signaling pathway in cancer cells [134].

In this study, we observed that PMEO treatment caused an elevation in intracellular ROS generation, accompanied by a rapid reduction in intracellular GSH levels, thereby resulting in an overall prooxidant effect on cells. This finding is consistent with several other studies that have reported a decrease in intracellular antioxidants such as GSH and an increase in ROS production as the most common response of cancer cells to prooxidant natural compounds [136][135][212]. The temporal sequence of these events corresponds with the swift suppression of STAT3 phosphorylation caused by PMEO treatment, which was noticeable within the first hour of treatment. Furthermore, we observed that pre-treatment of cells with NAC, an antioxidant known to scavenge ROS, blocked the effect of PMEO on STAT3 and preserved the phosphorylated STAT3 levels, confirmed that oxidative stress plays critical role in mediating the anti-STAT3 activity of PMEO. Additionally, we observed that Phosphorylation of Src, an upstream kinase was also inhibited by PMEO treatment, which could have an inhibitory effect downstream on the STAT3 phosphorylation. However, whether PMEO induced oxidative stress cause any direct modification on STAT3 such as the S-glutathionylation is yet to be clarified. Subsequently, we assessed the biological impact of PMEO-induced inhibition of STAT3 activation and observed a decrease in the expression of genes it regulates, which are critical for tumor survival, angiogenesis, and metastasis. The results demonstrated that PMEO induced apoptosis and impaired cellular migration in DU145 cancer cells.

Chemoresistance is a major challenge that limit the efficiency of chemotherapy drugs. Combining natural compounds that will synergistically act with chemotherapy drugs and potentiate their effects has been propounded to chemosensitize the chemoresistant cancer cells and effectively overcome chemoresistance. Our analysis in this study demonstrates that PMEO synergises with Cisplatin within a dose range that affected more than 50% of cell viability. This suggests that PMEO could be rationally formulated to an adjuvant that can be further studied in cisplatin resistant cancers.

Nanoencapsulation of EOs is currently being extensively investigated to overcome their inherent limitations, including high volatility, low stability, and poor aqueous solubility [172][170]. Promising results have been obtained by previous studies in encapsulating EOs in different types of nanocarriers and enhancing their anticancer effects. Recently, biodegradable PLGA based

nanoformulations have been successfully utilized for the encapsulation of EOs and their constituents [177]. In this work, we report the preparation of a polymeric nanoformulation of PMEO using PLGA-PVA-TPGS nanoparticles (PMEO-NPs). The resulting PMEO-NPs exhibited good morphological characteristics and physicochemical properties that were similar to other PLGA nanoformulations that have been previously reported. The hydrodynamic size, polydispersity index, and zeta potential of the PMEO-NPs were within the expected range for PLGA nanoparticles. The best formulation demonstrated an encapsulation efficiency and loading capacity of approximately 55% and 5.5% respectively. Further research is needed to enhance the encapsulation efficiency and loading capacity. One of the main sought out advantages of nanomedicine is that they allow controlled and sustained release of the encapsulated drug over an extended period [170]. Consistent with this, our data shows that PMEO-NPs exhibited a sustained release of PMEO over an observation period of 5 days. Controlled release of PMEO would help to maintaining sufficient levels of drugs for longer periods while minimizing toxic effects associated with high concentrations.

In vitro studies in MDA-MB-231 breast cancer cells demonstrate that PLGA-NPs were efficiently taken up by the cells within one hour. PMEO-NPs containing the same amount of EO produced more pronounced increase in ROS generation and cytotoxic effects by markedly reducing the IC50 values than that of the free EO. Our data also show that the apoptosis induction was also more pronounced in the case of nanoformulation compared to the free PMEO. Our findings are in concert with similar studies reported enhancement of anticancer activity of EOs by encapsulating in polymeric nanoparticles. An instance of this is the loading of *Boswellia sacra* EO into PLGA-Polycaprolactone (PCL) nanoparticles, which also resulted in increased cytotoxic and apoptotic effects against breast cancer cells [213]. In short, the efficient cellular uptake and the enhanced anticancer effects observed with PMEO-NPs indicate the potential for improved efficacy and reduced toxicity of anticancer drugs when administered in nanoformulations. Further studies are needed to better understand the comprehensive molecular mechanisms and investigate the efficacy of these nanoformulations *in vivo* and to evaluate their safety profile. Nonetheless, these findings present a promising opportunity to develop more effective alternative or complementary therapeutic strategies combining EOs and nanoparticle-based drug delivery systems to combat cancer. Moreover, as we observed these effects, in a highly aggressive breast cancer cells, it adds up to our previous findings in prostate cancer cells and imply that rationally formulated PMEO could be an effective alternative approach to combat highly aggressive cancers.

This notion is even more strongly supported by the data we obtained in breast cancer stem cells. Cancer stem cell population are usually difficult to manage with traditional chemotherapy

approaches and alternative approached are being explored to efficiently tackle them. Few studies have recently investigated the potential of EOs and few EO compounds to mitigate the growth and self-renewability of cancer stem cells [163][165]. In this study we provide with the clear evidence of reduction in the molecular markers of breast cancer stemness, that PMEO and its nanoformulation efficiently suppressed the growth and self-renewability of breast cancer stem cells. Therefore, PMEO may be well utilized alone or in combination with existing therapies as adjuvant to eliminate cancer stem cells and effectively combat highly aggressive and resistant cancers.

Taken together, the data presented in this thesis highlight that EOs can exert promising anticancer activities by suppressing the activation of STAT3 signaling in highly aggressive cancer cells. Furthermore, incorporating PMEO into nanoparticle-based drug delivery systems may offer a promising and innovative approach to combatting cancer in the future. However, additional research is necessary to thoroughly assess the efficacy and safety of this approach in animal models and optimize its potential for clinical use.

7. ANNEXXES

A part of this thesis work has been contributed to a publication:

Thalappil MA, Butturini E, Carcereri de Prati A, et al. Pinus mugo Essential Oil Impairs STAT3 Activation through Oxidative Stress and Induces Apoptosis in Prostate Cancer Cells. Molecules. 2022;27(15):4834. Published 2022 Jul 28. doi:10.3390/molecules27154834 [214].

8. REFERENCES

[1]   H.Q. Wang, Q.W. Man, F.Y. Huo, X. Gao, H. Lin, S.R. Li, J. Wang, F.C. Su, L. Cai, Y. Shi, B. Liu, L.L. Bu, STAT3 pathway in cancers: Past, present, and future, MedComm. 3 (2022) 1–29. https://doi.org/10.1002/mco2.124.

[2]   G.R. Stark, J.E. Darnell, The JAK-STAT Pathway at Twenty, Immunity. 36 (2012) 503–514. https://doi.org/10.1016/j.immuni.2012.03.013.

[3]   J. LINDENMANN, D.C. BURKE, A. ISAACS, Studies on the production, mode of action and properties of interferon., Br. J. Exp. Pathol. 38 (1957) 551–562.

[4]   M.Z. Kamran, P. Patil, R.P. Gude, Role of STAT3 in cancer metastasis and translational advances, Biomed Res. Int. 2013 (2013). https://doi.org/10.1155/2013/421821.

[5]   T. Bowman, R. Garcia, J. Turkson, R. Jove, STATs in oncogenesis, Oncogene. 19 (2000) 2474–2488. https://doi.org/10.1038/sj.onc.1203527.

[6]   R. Morris, N.J. Kershaw, J.J. Babon, The molecular details of cytokine signaling via the JAK/STAT pathway, Protein Sci. 27 (2018) 1984–2009. https://doi.org/10.1002/pro.3519.

[7]   H. Yu, H. Lee, A. Herrmann, R. Buettner, R. Jove, Revisiting STAT3 signalling in cancer: New and unexpected biological functions, Nat. Rev. Cancer. 14 (2014) 736–746. https://doi.org/10.1038/nrc3818.

[8]   M. Wu, D. Song, H. Li, Y. Yang, X. Ma, S. Deng, C. Ren, X. Shu, Negative regulators of STAT3 signaling pathway in cancers, Cancer Manag. Res. 11 (2019) 4957–4969. https://doi.org/10.2147/CMAR.S206175.

[9]   E.C. Brantley, L.B. Nabors, G.Y. Gillespie, Y.H. Choi, C.A. Palmer, K. Harrison, K. Roarty, E.N. Benveniste, Loss of protein inhibitors of activated STAT-3 expression in glioblastoma multiforme tumors: Implications for STAT-3 activation and gene expression, Clin. Cancer Res. 14 (2008) 4694–4704. https://doi.org/10.1158/1078-0432.CCR-08-0618.

[10]   H. Isomoto, Epigenetic alterations in cholangiocarcinoma-sustained IL-6/STAT3 signaling in Cholangio- carcinoma due to SOCS3 epigenetic silencing, Digestion. 79 (2009) 2–8. https://doi.org/10.1159/000167859.

[11]   Y. Niwa, H. Kanda, Y. Shikauchi, A. Saiura, K. Matsubara, T. Kitagawa, J. Yamamoto, T. Kubo, H. Yoshikawa, Methylation silencing of SOCS-3 promotes cell growth and migration by enhancing JAK/STAT and FAK signalings in human hepatocellular carcinoma, Oncogene. 24 (2005) 6406–6417. https://doi.org/10.1038/sj.onc.1208788.

[12]   B. He, L. You, K. Uematsu, K. Zang, Z. Xu, A.Y. Lee, J.F. Costello, F. McCormick, D.M. Jablons, SOCS-3 is frequently silenced by hypermethylation and suppresses cell growth in human lung cancer, Proc. Natl. Acad. Sci. U. S. A. 100 (2003) 14133–14138. https://doi.org/10.1073/pnas.2232790100.

[13]   A. Weber, U.R. Hengge, W. Bardenheuer, I. Tischoff, F. Sommerer, A. Markwarth, A. Dietz, C. Wittekind, A. Tannapfel, SOCS-3 is frequently methylated in head and neck squamous cell carcinoma and its precursor lesions and causes growth inhibition, Oncogene. 24 (2005) 6699–6708. https://doi.org/10.1038/sj.onc.1208818.

[14]   V.W.Y. Lui, N.D. Peyser, P.K.S. Ng, J. Hritz, Y. Zeng, Y. Lu, H. Li, L. Wang, B.R. Gilbert, I.J. General, I. Bahar, Z. Ju, Z. Wang, K.P. Pendleton, X. Xiao, Y. Du, J.K. Vries, P.S.

Hammerman, L.A. Garraway, G.B. Mills, D.E. Johnson, J.R. Grandis, Frequent mutation of receptor protein tyrosine phosphatases provides a mechanism for STAT3 hyperactivation in head and neck cancer, Proc. Natl. Acad. Sci. U. S. A. 111 (2014) 1114–1119. https://doi.org/10.1073/pnas.1319551111.

[15] C. Pilati, M. Amessou, M.P. Bihl, C. Balabaud, J.T. Van Nhieu, V. Paradis, J.C. Nault, T. Izard, P. Bioulac-Sage, G. Couchy, K. Poussin, J. Zucman-Rossi, Somatic mutations activating STAT3 in human inflammatory hepatocellular adenomas, J. Exp. Med. 208 (2011) 1359–1366. https://doi.org/10.1084/jem.20110283.

[16] G. Hu, T.E. Witzig, M. Gupta, A Novel Missense (M206K) STAT3 Mutation in Diffuse Large B Cell Lymphoma Deregulates STAT3 Signaling, PLoS One. 8 (2013). https://doi.org/10.1371/journal.pone.0067851.

[17] S.P. Gao, K.G. Mark, K. Leslie, W. Pao, N. Motoi, W.L. Gerald, W.D. Travis, W. Bornmann, D. Veach, B. Clarkson, J.F. Bromberg, Mutations in the EGFR kinase domain mediate STAT3 activation via IL-6 production in human lung adenocarcinomas, J. Clin. Invest. 117 (2007) 3846–3856. https://doi.org/10.1172/JCI31871.

[18] S. Dimri, Sukanya, A. De, Approaching non-canonical STAT3 signaling to redefine cancer therapeutic strategy, Integr. Mol. Med. 4 (2017) 1–10. https://doi.org/10.15761/imm.1000268.

[19] S. Dimri, R. Malhotra, T. Shet, S. Mokal, S. Gupta, A. De, Noncanonical pS727 post translational modification dictates major STAT3 activation and downstream functions in breast cancer, Exp. Cell Res. 396 (2020) 112313. https://doi.org/10.1016/j.yexcr.2020.112313.

[20] Q. Zhang, V. Raje, V.A. Yakovlev, A. Yacoub, K. Szczepanek, J. Meier, M. Derecka, Q. Chen, Y. Hu, J. Sisler, H. Hamed, E.J. Lesnefsky, K. Valerie, P. Dent, A.C. Larner, Mitochondrial localized Stat3 promotes breast cancer growth via phosphorylation of serine 727, J. Biol. Chem. 288 (2013) 31280–31288. https://doi.org/10.1074/jbc.M113.505057.

[21] J. Srivastava, J. DiGiovanni, Non-canonical Stat3 signaling in cancer, Mol. Carcinog. 55 (2016) 1889–1898. https://doi.org/10.1002/mc.22438.

[22] J. Sgrignani, S. Olsson, D. Ekonomiuk, D. Genini, R. Krause, C. V. Catapano, A. Cavalli, Molecular Determinants for Unphosphorylated STAT3 Dimerization Determined by Integrative Modeling, Biochemistry. 54 (2015) 5489–5501. https://doi.org/10.1021/bi501529x.

[23] D. Hanahan, Hallmarks of Cancer: New Dimensions, Cancer Discov. 12 (2022) 31–46. https://doi.org/10.1158/2159-8290.CD-21-1059.

[24] R.L. Carpenter, H.W. Lo, STAT3 target genes relevant to human cancers, Cancers (Basel). 6 (2014) 897–925. https://doi.org/10.3390/cancers6020897.

[25] J. Luo, R. Yan, X. He, J. He, Constitutive activation of STAT3 and cyclin D1 overexpression contribute to proliferation, migration and invasion in gastric cancer cells, Am. J. Transl. Res. 9 (2017) 5671–5677.

[26] J. Bollrath, T.J. Phesse, V.A. von Burstin, T. Putoczki, M. Bennecke, T. Bateman, T. Nebelsiek, T. Lundgren-May, Ö. Canli, S. Schwitalla, V. Matthews, R.M. Schmid, T. Kirchner, M.C. Arkan, M. Ernst, F.R. Greten, gp130-Mediated Stat3 Activation in Enterocytes Regulates Cell Survival and Cell-Cycle Progression during Colitis-Associated Tumorigenesis, Cancer Cell. 15 (2009) 91–102. https://doi.org/10.1016/j.ccr.2009.01.002.

[27] W. Béguelin, M.C. Díaz Flaqué, C.J. Proietti, F. Cayrol, M.A. Rivas, M. Tkach, C. Rosemblit, J.M. Tocci, E.H. Charreau, R. Schillaci, P. V. Elizalde, Progesterone Receptor Induces ErbB-2 Nuclear Translocation To Promote Breast Cancer Growth via a Novel Transcriptional Effect: ErbB-2 Function as a Coactivator of Stat3, Mol. Cell. Biol. 30 (2010) 5456–5472. https://doi.org/10.1128/mcb.00012-10.

[28] L. Konnikova, M.C. Simeone, M.M. Kruger, M. Kotecki, B.H. Cochran, Signal transducer and activator of transcription 3 (STAT3) regulates human telomerase reverse transcriptase (hTERT) expression in human cancer and primary cells, Cancer Res. 65 (2005) 6516–6520. https://doi.org/10.1158/0008-5472.CAN-05-0924.

[29] S. Koganti, J. Hui-Yuen, S. McAllister, B. Gardner, F. Grasser, U. Palendira, S.G. Tangye, A.F. Freeman, S. Bhaduri-McIntosh, STAT3 interrupts ATR-Chk1 signaling to allow oncovirus-mediated cell proliferation, Proc. Natl. Acad. Sci. U. S. A. 111 (2014) 4946–4951. https://doi.org/10.1073/pnas.1400683111.

[30] G. Niu, K.L. Wright, Y. Ma, G.M. Wright, M. Huang, R. Irby, J. Briggs, J. Karras, W.D. Cress, D. Pardoll, R. Jove, J. Chen, H. Yu, Role of Stat3 in Regulating p53 Expression and Function, Mol. Cell. Biol. 25 (2005) 7432–7440. https://doi.org/10.1128/mcb.25.17.7432-7440.2005.

[31] J.R. Grandis, S.D. Drenning, Q. Zeng, S.C. Watkins, M.F. Melhem, S. Endo, D.E. Johnson, L. Huang, Y. He, J.D. Kim, Constitutive activation of stat3 signaling abrogates apoptosis in squamous cell carcinogenesis in vivo, Proc. Natl. Acad. Sci. U. S. A. 97 (2000) 4227–4232. https://doi.org/10.1073/pnas.97.8.4227.

[32] S.O. Rahaman, P.C. Harbor, O. Chernova, G.H. Barnett, M.A. Vogelbaum, S.J. Haque, Inhibition of constitutively active Stat3 suppresses proliferation and induces apoptosis in glioblastoma multiforme cells, Oncogene. 21 (2002) 8404–8413. https://doi.org/10.1038/sj.onc.1206047.

[33] T. Gritsko, A. Williams, J. Turkson, S. Kaneko, T. Bowman, M. Huang, S. Nam, I. Eweis, N. Diaz, D. Sullivan, S. Yoder, S. Enkemann, S. Eschrich, J.H. Lee, C.A. Beam, J. Cheng, S. Minton, C.A. Muro-Cacho, R. Jove, Persistent activation of Stat3 signaling induces survivin gene expression and confers resistance to apoptosis in human breast cancer cells, Clin. Cancer Res. 12 (2006) 11–19. https://doi.org/10.1158/1078-0432.CCR-04-1752.

[34] B. Bauvois, E. Pramil, L. Jondreville, C. Quiney, F. Nguyen-Khac, S.A. Susin, Activation of interferon signaling in chronic lymphocytic leukemia cells contributes to apoptosis resistance via a jak-src/stat3/mcl-1 signaling pathway, Biomedicines. 9 (2021) 1–15. https://doi.org/10.3390/biomedicines9020188.

[35] P. Gao, N. Niu, T. Wei, H. Tozawa, X. Chen, C. Zhang, J. Zhang, Y. Wada, C.M. Kapron, J. Liu, The roles of signal transducer and activator of transcription factor 3 in tumor angiogenesis, Oncotarget. 8 (2017) 69139–69161. https://doi.org/10.18632/oncotarget.19932.

[36] D. Wei, X. Le, L. Zheng, L. Wang, J.A. Frey, A.C. Gao, Z. Peng, S. Huang, H.Q. Xiong, J.L. Abbruzzese, K. Xie, Stat3 activation regulates the expression of vascular endothelial growth factor and human pancreatic cancer angiogenesis and metastasis, Oncogene. 22 (2003) 319–329. https://doi.org/10.1038/sj.onc.1206122.

[37] M. Kujawski, M. Kortylewski, H. Lee, A. Herrmann, H. Kay, H. Yu, Stat3 mediates myeloid cell-dependent tumor angiogenesis in mice, J. Clin. Invest. 118 (2008) 3367–3377. https://doi.org/10.1172/JCI35213.

[38] Y. Shen, X. Wang, Y. Liu, M. Singhal, C. Gürkaşlar, A.F. Valls, Y. Lei, W. Hu, G. Schermann, H. Adler, F.X. Yu, T. Fischer, Y. Zhu, H.G. Augustin, T. Schmidt, C.R. De Almodóvar, STAT3-YAP/TAZ signaling in endothelial cells promotes tumor angiogenesis, Sci. Signal. 14 (2021) 1–16. https://doi.org/10.1126/scisignal.abj8393.

[39] L. He, A. Feng, H. Guo, H. Huang, Q. Deng, E. Zhao, M. Yang, LRG1 mediated by ATF3 promotes growth and angiogenesis of gastric cancer by regulating the SRC/STAT3/VEGFA pathway, Gastric Cancer. 25 (2022) 527–541. https://doi.org/10.1007/s10120-022-01279-9.

[40] H.F. Zhang, R. Lai, STAT3 in cancer-friend or foe?, Cancers (Basel). 6 (2014) 1408–1440. https://doi.org/10.3390/cancers6031408.

[41] T.X. Xie, D. Wei, M. Liu, A.C. Gao, F. Ali-Osman, R. Sawaya, S. Huang, Stat3 activation regulates the expression of matrix metalloproteinase-2 and tumor invasion and metastasis, Oncogene. 23 (2004) 3550–3560. https://doi.org/10.1038/sj.onc.1207383.

[42] G. Yuan, L. Qian, M. Shi, F. Lu, D. Li, M. Hu, M. Yu, B. Shen, N. Guo, HER2-dependent MMP-7 expression is mediated by activated STAT3, Cell. Signal. 20 (2008) 1284–1291. https://doi.org/10.1016/j.cellsig.2008.02.017.

[43] T.N. Dechow, L. Pedranzini, A. Leitch, K. Leslie, W.L. Gerald, I. Linkov, J.F. Bromberg, Requirement of matrix metalloproteinase-9 for the transformation of human mammary epithelial cells by Stat3-C, Proc. Natl. Acad. Sci. U. S. A. 101 (2004) 10602–10607. https://doi.org/10.1073/pnas.0404100101.

[44] M. Snyder, X.Y. Huang, J.J. Zhang, Signal Transducers and Activators of Transcription 3 (STAT3) directly regulates cytokine-induced fascin expression and is required for breast cancer cell migration, J. Biol. Chem. 286 (2011) 38886–38893. https://doi.org/10.1074/jbc.M111.286245.

[45] H. Xiong, J. Hong, W. Du, Y.W. Lin, L.L. Ren, Y.C. Wang, W.Y. Su, J.L. Wang, Y. Cui, Z.H. Wang, J.Y. Fang, Roles of STAT3 and ZEB1 proteins in E-cadherin down-regulation and human colorectal cancer epithelial-mesenchymal transition, J. Biol. Chem. 287 (2012) 5819–5832. https://doi.org/10.1074/jbc.M111.295964.

[46] J.H. Ma, J. Qi, S.Q. Lin, C.Y. Zhang, F.Y. Liu, W.D. Xie, X. Li, STAT3 targets ERR-α to promote epithelial-mesenchymal transition, migration, and invasion in triple-negative breast cancer cells, Mol. Cancer Res. 17 (2019) 2184–2195. https://doi.org/10.1158/1541-7786.MCR-18-1194.

[47] D. Schiavone, S. Dewilde, F. Vallania, J. Turkson, F. Di Cunto, V. Poli, The RhoU/Wrch1 Rho GTPase gene is a common transcriptional target of both the gp130/STAT3 and Wnt-1 pathways, Biochem. J. 421 (2009) 283–292. https://doi.org/10.1042/BJ20090061.

[48] J. Corry, H.R. Mott, D. Owen, Activation of STAT transcription factors by the Rho-family GTPases, Biochem. Soc. Trans. 48 (2020) 2213–2227. https://doi.org/10.1042/BST20200468.

[49] E.J. Lim, J.H. Kang, Y.J. Kim, S. Kim, S.J. Lee, ICAM-1 promotes cancer progression by regulating SRC activity as an adapter protein in colorectal cancer, Cell Death Dis. 13 (2022) 1–11. https://doi.org/10.1038/s41419-022-04862-1.

[50] L. Zhang, K. Kuca, L. You, Y. Zhao, K. Musilek, E. Nepovimova, Q. Wu, W. Wu, V. Adam, Signal transducer and activator of transcription 3 signaling in tumor immune evasion, Pharmacol. Ther. 230 (2022) 107969.

https://doi.org/10.1016/j.pharmthera.2021.107969.

[51] S. Zou, Q. Tong, B. Liu, W. Huang, Y. Tian, X. Fu, Targeting stat3 in cancer immunotherapy, Mol. Cancer. 19 (2020) 1–19. https://doi.org/10.1186/s12943-020-01258-7.

[52] J. Wu, F.X. Gao, C. Wang, M. Qin, F. Han, T. Xu, Z. Hu, Y. Long, X.M. He, X. Deng, D.L. Ren, T.Y. Dai, IL-6 and IL-8 secreted by tumour cells impair the function of NK cells via the STAT3 pathway in oesophageal squamous cell carcinoma, J. Exp. Clin. Cancer Res. 38 (2019) 1–15. https://doi.org/10.1186/s13046-019-1310-0.

[53] X. Mu, W. Shi, Y. Xu, C. Xu, T. Zhao, B. Geng, J. Yang, J. Pan, S. Hu, C. Zhang, J. Zhang, C. Wang, J. Shen, Y. Che, Z. Liu, Y. Lv, H. Wen, Q. You, Tumor-derived lactate induces M2 macrophage polarization via the activation of the ERK/STAT3 signaling pathway in breast cancer, Cell Cycle. 17 (2018) 428–438. https://doi.org/10.1080/15384101.2018.1444305.

[54] L. Xu, M. Shen, X. Chen, D.R. Yang, Y. Tsai, P.C. Keng, S.O. Lee, Y. Chen, In vitro-induced M2 type macrophages induces the resistance of prostate cancer cells to cytotoxic action of NK cells, Exp. Cell Res. 364 (2018) 113–123. https://doi.org/10.1016/j.yexcr.2018.01.041.

[55] X.L. Fu, W. Duan, C.Y. Su, F.Y. Mao, Y.P. Lv, Y.S. Teng, P.W. Yu, Y. Zhuang, Y.L. Zhao, Interleukin 6 induces M2 macrophage differentiation by STAT3 activation that correlates with gastric cancer progression, Cancer Immunol. Immunother. 66 (2017) 1597–1608. https://doi.org/10.1007/s00262-017-2052-5.

[56] K. Gabrusiewicz, X. Li, J. Wei, Y. Hashimoto, A.L. Marisetty, M. Ott, F. Wang, D. Hawke, J. Yu, L.M. Healy, A. Hossain, J.C. Akers, S.N. Maiti, S. Yamashita, Y. Shimizu, K. Dunner, M.A. Zal, J.K. Burks, J. Gumin, F. Nwajei, A. Rezavanian, S. Zhou, G. Rao, R. Sawaya, G.N. Fuller, J.T. Huse, J.P. Antel, S. Li, L. Cooper, E.P. Sulman, C. Chen, C. Geula, R. Kalluri, T. Zal, A.B. Heimberger, Glioblastoma stem cell-derived exosomes induce M2 macrophages and PD-L1 expression on human monocytes, Oncoimmunology. 7 (2018). https://doi.org/10.1080/2162402X.2017.1412909.

[57] C. Heichler, K. Scheibe, A. Schmied, C.I. Geppert, B. Schmid, S. Wirtz, O.M. Thoma, V. Kramer, M.J. Waldner, C. Büttner, H.F. Farin, M. Pešić, F. Knieling, S. Merkel, A. Grüneboom, M. Gunzer, R. Grützmann, S. Rose-John, S.B. Koralov, G. Kollias, M. Vieth, A. Hartmann, F.R. Greten, M.F. Neurath, C. Neufert, STAT3 activation through IL-6/IL-11 in cancer-associated fibroblasts promotes colorectal tumour development and correlates with poor prognosis, Gut. 69 (2020) 1269–1282. https://doi.org/10.1136/gutjnl-2019-319200.

[58] Y. Cheng, H. Li, Y. Deng, Y. Tai, K. Zeng, Y. Zhang, W. Liu, Q. Zhang, Y. Yang, Cancer-associated fibroblasts induce PDL1+ neutrophils through the IL6-STAT3 pathway that foster immune suppression in hepatocellular carcinoma, Cell Death Dis. 9 (2018). https://doi.org/10.1038/s41419-018-0458-4.

[59] A. Li, P. Chen, Y. Leng, J. Kang, Histone deacetylase 6 regulates the immunosuppressive properties of cancer-associated fibroblasts in breast cancer through the STAT3–COX2-dependent pathway, Oncogene. 37 (2018) 5952–5966. https://doi.org/10.1038/s41388-018-0379-9.

[60] M. Demaria, V. Poli, PKM2, STAT3 and HIF-1α, Jak-Stat. 1 (2012) 194–196. https://doi.org/10.4161/jkst.20662.

[61]   M. Demaria, C. Giorgi, M. Lebiedzinska, G. Esposito, L. D'angeli, A. Bartoli, D.J. Gough, J. Turkson, D.E. Levy, C.J. Watson, M.R. Wieckowski, P. Provero, P. Pinton, V. Poli, A STAT3-mediated metabolic switch is involved in tumour transformation and STAT3 addiction, Aging (Albany. NY). 2 (2010) 823–842. https://doi.org/10.18632/aging.100232.

[62]   X. Gao, H. Wang, J.J. Yang, X. Liu, Z.R. Liu, Pyruvate Kinase M2 Regulates Gene Transcription by Acting as a Protein Kinase, Mol. Cell. 45 (2012) 598–609. https://doi.org/10.1016/j.molcel.2012.01.001.

[63]   Y.H. Bi, W.Q. Han, R.F. Li, Y.J. Wang, Z.S. Du, X.J. Wang, Y. Jiang, Signal transducer and activator of transcription 3 promotes the Warburg effect possibly by inducing pyruvate kinase M2 phosphorylation in liver precancerous lesions, World J. Gastroenterol. 25 (2019) 1936–1949. https://doi.org/10.3748/wjg.v25.i16.1936.

[64]   20140612 A novel miR-155 miR-143 cascade controls glycolysis by regulating hexokinase 2 in breast cancer cells 2012 emboj.pdf, (n.d.).

[65]   X. Qin, L. Lin, L. Cao, X. Zhang, X. Song, J. Hao, Y. Zhang, R. Wei, X. Huang, J. Lu, Q. Ge, Extracellular matrix protein Reelin promotes myeloma progression by facilitating tumor cell proliferation and glycolysis, Sci. Rep. 7 (2017) 1–12. https://doi.org/10.1038/srep45305.

[66]   Z. Yu, T.G. Pestell, M.P. Lisanti, R.G. Pestell, Cancer stem cells, Int. J. Biochem. Cell Biol. 44 (2012) 2144–2151. https://doi.org/10.1016/j.biocel.2012.08.022.

[67]   C. Cheng, P. Liao, A. Ho, K. Lim, J. Chang, Y. Su, STAT3 exacerbates survival of cancer stem-like tumorspheres in EGFR-positive colorectal cancers : RNAseq analysis and therapeutic screening, (2018) 1–12.

[68]   S.Y. Kim, J.W. Kang, X. Song, B.K. Kim, Y.D. Yoo, Y.T. Kwon, Y.J. Lee, Role of the IL-6-JAK1-STAT3-Oct-4 pathway in the conversion of non-stem cancer cells into cancer stem-like cells, Cell. Signal. 25 (2013) 961–969. https://doi.org/10.1016/j.cellsig.2013.01.007.

[69]   A. Hermann, C. Suess, M. Fauser, S. Kanzler, M. Witt, K. Fabel, J. Schwarz, G.U. Höglinger, A. Storch, Rostro-caudal gradual loss of cellular diversity within the periventricular regions of the ventricular system, Stem Cells. 27 (2009) 928–941. https://doi.org/10.1002/stem.21.

[70]   I. Tošić, D.A. Frank, STAT3 as a mediator of oncogenic cellular metabolism: Pathogenic and therapeutic implications, Neoplasia (United States). 23 (2021) 1167–1178. https://doi.org/10.1016/j.neo.2021.10.003.

[71]   J. Xiong, X. Zhang, Y. Zhang, B. Wu, L. Fang, N. Wang, H. Yi, N. Chang, L. Chen, J. Zhang, Aryl hydrocarbon receptor mediates Jak2/STAT3 signaling for non-small cell lung cancer stem cell maintenance, Exp. Cell Res. 396 (2020) 112288. https://doi.org/10.1016/j.yexcr.2020.112288.

[72]   C. Won, B.H. Kim, E.H. Yi, K.J. Choi, E.K. Kim, J.M. Jeong, J.H. Lee, J.J. Jang, J.H. Yoon, W. Il Jeong, I.C. Park, T.W. Kim, S.S. Bae, V.M. Factor, S. Ma, S.S. Thorgeirsson, Y.H. Lee, S.K. Ye, Signal transducer and activator of transcription 3-mediated CD133 up-regulation contributes to promotion of hepatocellular carcinoma, Hepatology. 62 (2015) 1160–1173. https://doi.org/10.1002/hep.27968.

[73]   Y. Liu, X. Gao, S. Wang, X. Yuan, Y. Pang, J. Chen, J. Wang, Cancer stem cells are regulated by STAT3 signalling in Wilms Tumour, J. Cancer. 9 (2018) 1486–1499.

https://doi.org/10.7150/jca.23277.

[74] P.J. Real, A. Sierra, A. De Juan, J.C. Segovia, J.M. Lopez-Vega, J.L. Fernandez-Luna, Resistance to chemotherapy via Stat3-dependent overexpression of Bcl-2 in metastatic breast cancer cells, Oncogene. 21 (2002) 7611–7618. https://doi.org/10.1038/sj.onc.1206004.

[75] C. Yang, L. He, P. He, Y. Liu, W. Wang, Y. He, Y. Du, F. Gao, Increased drug resistance in breast cancer by tumor-associated macrophages through IL-10/STAT3/bcl-2 signaling pathway, Med. Oncol. 32 (2015). https://doi.org/10.1007/s12032-014-0352-6.

[76] STAT3- and GSK3β-mediated Mcl-1 regulation modulates TPF resistance in oral squamous cell carcinoma.pdf, (n.d.).

[77] Z. Fang, W. Chen, Z. Yuan, X. Liu, H. Jiang, LncRNA-MALAT1 contributes to the cisplatin-resistance of lung cancer by upregulating MRP1 and MDR1 via STAT3 activation, Biomed. Pharmacother. 101 (2018) 536–542. https://doi.org/10.1016/j.biopha.2018.02.130.

[78] Q. Zhang, R.X. Liu, K.W. Chan, J. Hu, J. Zhang, L. Wei, H. Tan, X. Yang, H. Liu, Exosomal transfer of p-STAT3 promotes acquired 5-FU resistance in colorectal cancer cells, J. Exp. Clin. Cancer Res. 38 (2019) 1–14. https://doi.org/10.1186/s13046-019-1314-9.

[79] G. Li, L. Zhao, W. Li, K. Fan, W. Qian, S. Hou, H. Wang, J. Dai, H. Wei, Y. Guo, Feedback activation of STAT3 mediates trastuzumab resistance via upregulation of MUC1 and MUC4 expression, Oncotarget. 5 (2014) 8317–8329. https://doi.org/10.18632/oncotarget.2135.

[80] A. Vultur, J. Villanueva, C. Krepler, G. Rajan, Q. Chen, M. Xiao, L. Li, P.A. Gimotty, M. Wilson, J. Hayden, F. Keeney, K.L. Nathanson, M. Herlyn, MEK inhibition affects STAT3 signaling and invasion in human melanoma cell lines, Oncogene. 33 (2014) 1850–1861. https://doi.org/10.1038/onc.2013.131.

[81] R.S. Kenchappa, A. Dovas, M.G. Argenziano, C.T. Meyer, L.E. Stopfer, M.A. Banu, B. Pereira, J. Griffith, A. Mohammad, S. Talele, A. Haddock, N. Zarco, W. Elmquist, F. White, V. Quaranta, P. Sims, P. Canoll, S.S. Rosenfeld, Activation of STAT3 through combined SRC and EGFR signaling drives resistance to a mitotic kinesin inhibitor in glioblastoma, Cell Rep. 39 (2022) 110991. https://doi.org/10.1016/j.celrep.2022.110991.

[82] W. Wen, J. Wu, L. Liu, Y. Tian, R. Buettner, M. Hsieh, D. Horne, T.H. Dellinger, E.S. Han, R. Jove, J.H. Yim, Synergistic anti-tumor effect of combined inhibition of EGFR and JAK / STAT3 pathways in human ovarian cancer, ??? (2015) 1–11. https://doi.org/10.1186/s12943-015-0366-5.

[83] H. Kitamura, Y. Ohno, Y. Toyoshima, J. Ohtake, S. Homma, H. Kawamura, N. Takahashi, A. Taketomi, Interleukin-6/STAT3 signaling as a promising target to improve the efficacy of cancer immunotherapy, Cancer Sci. 108 (2017) 1947–1952. https://doi.org/10.1111/cas.13332.

[84] A. Méndez-Clemente, A. Bravo-Cuellar, S. González-Ochoa, M. Santiago-Mercado, L. Palafox-Mariscal, L. Jave-Suárez, F. Solorzano-Ibarra, M. Villaseñor-García, P. Ortiz-Lazareno, G. Hernández-Flores, Dual STAT-3 and IL-6R inhibition with stattic and tocilizumab decreases migration, invasion and proliferation of prostate cancer cells by targeting the IL-6/IL-6R/STAT-3 axis, Oncol. Rep. 48 (2022). https://doi.org/10.3892/or.2022.8349.

[85] H. Tsoi, E.P.S. Man, K.M. Chau, U.S. Khoo, Targeting the IL-6/STAT3 signalling cascade to reverse tamoxifen resistance in estrogen receptor positive breast cancer, Cancers (Basel). 13 (2021). https://doi.org/10.3390/cancers13071511.

[86] M. Sen, N.I. Pollock, J. Black, K.A. DeGrave, S. Wheeler, M.L. Freilino, S. Joyce, V.W.Y. Lui, Y. Zeng, S.I. Chiosea, J.R. Grandis, JAK Kinase Inhibition Abrogates STAT3 Activation and Head and Neck Squamous Cell Carcinoma Tumor Growth, Neoplasia (United States). 17 (2015) 256–264. https://doi.org/10.1016/j.neo.2015.01.003.

[87] A. Scuto, P. Krejci, L. Popplewell, J. Wu, Y. Wang, M. Kujawski, C. Kowolik, H. Xin, L. Chen, Y. Wang, L. Kretzner, H. Yu, W.R. Wilcox, Y. Yen, S. Forman, R. Jove, The novel JAK inhibitor AZD1480 blocks STAT3 and FGFR3 signaling, resulting in suppression of human myeloma cell growth and survival, Leukemia. 25 (2011) 538–550. https://doi.org/10.1038/leu.2010.289.

[88] C.E. Dos Santos, L. Li, T. McDonald, L. Li, A. Lin, Y.-H. Kuo, R. Bhatia, Src Kinase Inhibition by Dasatinib Enhances Targeting of Human AML Stem/Progenitor Cells by Chemotherapeutic Agents, Blood. 118 (2011) 4270–4270. https://doi.org/10.1182/blood.v118.21.4270.4270.

[89] A. Rebbaa, P.M. Chou, B.L. Mirkin, Factors Secreted by Human Neuroblastoma Mediate Doxorubicin Resistance by Activating STAT3 and Inhibiting Apoptosis, Mol. Med. 7 (2001) 393–400. https://doi.org/10.1007/bf03402185.

[90] X. Liu, Q. Xiao, X. Bai, Z. Yu, M. Sun, H. Zhao, X. Mi, E. Wang, W. Yao, F. Jin, L. Zhao, J. Ren, M. Wei, Activation of STAT3 is involved in malignancy mediated by CXCL12-CXCR4 signaling in human breast cancer, Oncol. Rep. 32 (2014) 2760–2768. https://doi.org/10.3892/or.2014.3536.

[91] A. Zamo, R. Chiarle, R. Piva, J. Howes, Y. Fan, M. Chilosi, D.E. Levy, G. Inghirami, Anaplastic lymphoma kinase (ALK) activates Stat3 and protects hematopoietic cells from cell death, Oncogene. 21 (2002) 1038–1047. https://doi.org/10.1038/sj.onc.1205152.

[92] Y.Y. Liu, Q. Zheng, B. Fang, W. Wang, F.Y. Ma, S. Roshan, A. Banafa, M.J. Chen, J.L. Chang, X.M. Deng, K.X. Li, G.X. Yang, G.Y. He, Germacrone induces apoptosis in human hepatoma HepG2 cells through inhibition of the JAK2/STAT3 signalling pathway, J. Huazhong Univ. Sci. Technol. - Med. Sci. 33 (2013) 339–345. https://doi.org/10.1007/s11596-013-1121-z.

[93] H. Chen, W. Zhou, A. Bian, Q. Zhang, Y. Miao, X. Yin, J. Ye, S. Xu, C. Ti, Z. Sun, J. Zheng, Y. Chen, M. Liu, Z. Yi, Selectively Targeting STAT3 Using a Small Molecule Inhibitor is a Potential Therapeutic Strategy for Pancreatic Cancer, Clin. Cancer Res. (2022) OF1–OF16. https://doi.org/10.1158/1078-0432.ccr-22-0997.

[94] G.H. Liu, T. Chen, X. Zhang, X.L. Ma, H.S. Shi, Small molecule inhibitors targeting the cancers, MedComm. 3 (2022) 1–74. https://doi.org/10.1002/mco2.181.

[95] R. Fagard, V. Metelev, I. Souissi, F. Baran-Marszak, STAT3 inhibitors for cancer therapy: Have all roads been explored?, Jak-Stat. 2 (2013) e22882. https://doi.org/10.4161/jkst.22882.

[96] J. Turkson, S. Zhang, J. Palmer, H. Kay, J. Stanko, L.B. Mora, S. Sebti, H. Yu, R. Jove, Inhibition of constitutive signal transducer and activator of transcription 3 activation by novel platinum complexes with potent antitumor activity, Mol. Cancer Ther. 3 (2004) 1533–1542. https://doi.org/10.1158/1535-7163.1533.3.12.

[97] D. Zuo, K.L. Shogren, J. Zang, D.E. Jewison, B.E. Waletzki, A.L. Miller, S.H. Okuno, Z. Cai, M.J. Yaszemski, A. Maran, Inhibition of STAT3 blocks protein synthesis and tumor metastasis in osteosarcoma cells 06 Biological Sciences 0601 Biochemistry and Cell Biology, J. Exp. Clin. Cancer Res. 37 (2018) 1–11. https://doi.org/10.1186/s13046-018-0914-0.

[98] D.J. Son, J. Zheng, Y.Y. Jung, C.J. Hwang, H.P. Lee, J.R. Woo, S.Y. Baek, Y.W. Ham, M.W. Kang, M. Shong, G.R. Kweon, M.J. Song, J.K. Jung, S.B. Han, B.Y. Kim, D.Y. Yoon, B.Y. Choi, J.T. Hong, MMPP attenuates non-small cell lung cancer growth by inhibiting the STAT3 DNA-binding activity via direct binding to the STAT3 DNA-binding domain, Theranostics. 7 (2017) 4632–4642. https://doi.org/10.7150/thno.18630.

[99] J.D. Beebe, J.Y. Liu, J.T. Zhang, Two decades of research in discovery of anticancer drugs targeting STAT3, how close are we?, Pharmacol. Ther. 191 (2018) 74–91. https://doi.org/10.1016/j.pharmthera.2018.06.006.

[100] X. Zhang, J. Zhang, H. Wei, Z. Tian, STAT3-decoy oligodeoxynucleotide inhibits the growth of human lung cancer via down-regulating its target genes, Oncol. Rep. 17 (2007) 1377–1382. https://doi.org/10.3892/or.17.6.1377.

[101] N. Jing, Q. Zhu, P. Yuan, Y. Li, L. Mao, D.J. Tweardy, Targetting signal transducer and activator of transcriptor 3 with G-quartet oligonucleotides: A potential novel therapy for head and neck cancer, Mol. Cancer Ther. 5 (2006) 279–286. https://doi.org/10.1158/1535-7163.MCT-05-0302.

[102] N. Jing, Y. Li, W. Xiong, W. Sha, L. Jing, D.J. Tweardy, G-quartet oligonucleotides: A new class of signal transducer and activator of transcription 3 inhibitors that suppresses growth of prostate and breast tumors through induction of apoptosis, Cancer Res. 64 (2004) 6603–6609. https://doi.org/10.1158/0008-5472.CAN-03-4041.

[103] L. Yang, S. Lin, X. Huang, J. Lin, C. Zhao, Cytokine and Growth Factor Reviews Novel activators and small-molecule inhibitors of STAT3 in cancer, Cytokine Growth Factor Rev. 49 (2019) 10–22. https://doi.org/10.1016/j.cytogfr.2019.10.005.

[104] C.L. Esposito, S. Nuzzo, S. Catuogno, S. Romano, F. de Nigris, V. de Franciscis, STAT3 Gene Silencing by Aptamer-siRNA Chimera as Selective Therapeutic for Glioblastoma, Mol. Ther. - Nucleic Acids. 10 (2018) 398–411. https://doi.org/10.1016/j.omtn.2017.12.021.

[105] K. Tian, W. Liu, J. Zhang, X. Fan, J. Liu, N. Zhao, C. Yao, G. Miao, MicroRNA-125b exerts antitumor functions in cutaneous squamous cell carcinoma by targeting the STAT3 pathway, Cell. Mol. Biol. Lett. 25 (2020). https://doi.org/10.1186/s11658-020-00207-y.

[106] S. Xu, N. Zhao, L. Hui, M. Song, Z.W. Miao, X.J. Jiang, MicroRNA-124-3p inhibits the growth and metastasis of nasopharyngeal carcinoma cells by targeting STAT3, Oncol. Rep. 35 (2016) 1385–1394. https://doi.org/10.3892/or.2015.4524.

[107] H. Zhou, L. Bai, R. Xu, Y. Zhao, J. Chen, D. McEachern, K. Chinnaswamy, B. Wen, L. Dai, P. Kumar, C.Y. Yang, Z. Liu, M. Wang, L. Liu, J.L. Meagher, H. Yi, D. Sun, J.A. Stuckey, S. Wang, Structure-Based Discovery of SD-36 as a Potent, Selective, and Efficacious PROTAC Degrader of STAT3 Protein, J. Med. Chem. 62 (2019) 11280–11300. https://doi.org/10.1021/acs.jmedchem.9b01530.

[108] H. Zhou, L. Bai, R. Xu, D. Mceachern, K. Chinnaswamy, R. Li, B. Wen, M. Wang, C. Yang, J.L. Meagher, D. Sun, J.A. Stuckey, S. Wang, SD-91 as A Potent and Selective STAT3 Degrader Capable of Achieving Complete and Long-Lasting Tumor Regression, (2021). https://doi.org/10.1021/acsmedchemlett.1c00155.

[109] J. Kim, A. Park, J. Hwang, Article KS10076 , a chelator for redox-active metal ions , induces ROS-mediated STAT3 degradation in auto- phagic cell death and eliminates ALDH1 + stem cells ll ll KS10076 , a chelator for redox-active metal ions , induces ROS-mediated STAT3 degradation , CellReports. 40 (2022) 111077. https://doi.org/10.1016/j.celrep.2022.111077.

[110] M. Huang, J.J. Lu, J. Ding, Natural Products in Cancer Therapy: Past, Present and Future, Nat. Products Bioprospect. 11 (2021) 5–13. https://doi.org/10.1007/s13659-020-00293-7.

[111] M. Wink, Evolutionary Advantage and Molecular Modes of Action of Multi-Component Mixtures Used in Phytomedicine, Curr. Drug Metab. 9 (2008) 996–1009. https://doi.org/10.2174/138920008786927794.

[112] K. Eljounaidi, B.R. Lichman, Nature's Chemists: The Discovery and Engineering of Phytochemical Biosynthesis, Front. Chem. 8 (2020) 1–10. https://doi.org/10.3389/fchem.2020.596479.

[113] C. Wawrosch, S.B. Zotchev, Production of bioactive plant secondary metabolites through in vitro technologies—status and outlook, Appl. Microbiol. Biotechnol. 105 (2021) 6649–6668. https://doi.org/10.1007/s00253-021-11539-w.

[114] S. Verdura, E. Cuyàs, L. Llorach-Parés, A. Pérez-Sánchez, V. Micol, A. Nonell-Canals, J. Joven, M. Valiente, M. Sánchez-Martínez, J. Bosch-Barrera, J.A. Menendez, Silibinin is a direct inhibitor of STAT3, Food Chem. Toxicol. 116 (2018) 161–172. https://doi.org/10.1016/j.fct.2018.04.028.

[115] Y. Ge, B. Yang, Z. Chen, R. Cheng, Cryptotanshinone suppresses the proliferation and induces the apoptosis of pancreatic cancer cells via the STAT3 signaling pathway, Mol. Med. Rep. 12 (2015) 7782–7788. https://doi.org/10.3892/mmr.2015.4379.

[116] D.S. Shin, H.N. Kim, K.D. Shin, Y.J. Yoon, S.J. Kim, D.C. Han, B.M. Kwon, Cryptotanshinone inhibits constitutive signal transducer and activator of transcription 3 function through blocking the dimerization in DU145 prostate cancer cells, Cancer Res. 69 (2009) 193–202. https://doi.org/10.1158/0008-5472.CAN-08-2575.

[117] G. Sethi, S. Chatterjee, P. Rajendran, F. Li, M.K. Shanmugam, K.F. Wong, A.P. Kumar, P. Senapati, A.K. Behera, K.M. Hui, J. Basha, N. Natesh, J.M. Luk, T.K. Kundu, Inhibition of STAT3 dimerization and acetylation by garcinol suppresses the growth of human hepatocellular carcinoma in vitro and in vivo, Mol. Cancer. 13 (2014) 1–14. https://doi.org/10.1186/1476-4598-13-66.

[118] G.D. Susmitha, K. Miyazato, K. Ogura, S. Yokoyama, Y. Hayakawa, Anti-metastatic effects of baicalein by targeting STAT3 activity in breast cancer cells, Biol. Pharm. Bull. 43 (2020) 1899–1905. https://doi.org/10.1248/bpb.b20-00571.

[119] B. Bin Hafeez, M.S. Jamal, J.W. Fischer, A. Mustafa, A.K. Verma, Plumbagin, a plant derived natural agent inhibits the growth of pancreatic cancer cells in in vitro and in vivo via targeting EGFR, Stat3 and NF-$\varkappa$B signaling pathways, Int. J. Cancer. 131 (2012) 2175–2186. https://doi.org/10.1002/ijc.27478.

[120] X. Zhang, M.A. Blaskovich, K.D. Forinash, S.M. Sebti, Withacnistin inhibits recruitment of STAT3 and STAT5 to growth factor and cytokine receptors and induces regression of breast tumours, Br. J. Cancer. 111 (2014) 894–902. https://doi.org/10.1038/bjc.2014.349.

[121] T.A.E.R.I.N. Min, H.J.I. Park, K.I.T.A.E. Ha, G.Y. Chi, Y.H. Choi, S.H. Park, Suppression of EGFR / STAT3 activity by lupeol contributes to the induction of the apoptosis of

human non - small cell lung cancer cells, (2019) 320–330. https://doi.org/10.3892/ijo.2019.4799.

[122] P. Deng, C. Wang, L. Chen, C. Wang, Y. Du, X. Yan, M. Chen, G. Yang, G. He, Sesamin induces cell cycle arrest and apoptosis through the inhibition of signal transducer and activator of transcription 3 signalling in human hepatocellular carcinoma cell line HepG2, Biol. Pharm. Bull. 36 (2013) 1540–1548. https://doi.org/10.1248/bpb.b13-00235.

[123] S. Sikka, R. Surana, X. Dai, J. Zhang, A.P. Kumar, B.K.H. Tan, G. Sethi, A. Bishayee, Targeting the STAT3 signaling pathway in cancer: Role of synthetic and natural inhibitors, Biochim. Biophys. Acta - Rev. Cancer. 1845 (2014) 136–154. https://doi.org/10.1016/j.bbcan.2013.12.005.

[124] A. Saha, J. Blando, E. Silver, L. Beltran, J. Sessler, J. DiGiovanni, 6-Shogaol from dried ginger inhibits growth of prostate cancer cells both in vitro and in vivo through inhibition of STAT3 and NF-ϰB signaling, Cancer Prev. Res. 7 (2014) 627–638. https://doi.org/10.1158/1940-6207.CAPR-13-0420.

[125] Y.X. Liu, B.W. Xu, Y.J. Chen, X.Q. Fu, P.L. Zhu, J.X. Bai, J.Y. Chou, C. Le Yin, J.K. Li, Y.P. Wang, J.Y. Wu, Y. Wu, K.K. Chan, C. Liang, Z.L. Yu, Inhibiting the Src/STAT3 signaling pathway contributes to the anti-melanoma mechanisms of dioscin, Oncol. Lett. 19 (2020) 2508–2514. https://doi.org/10.3892/ol.2020.11315.

[126] C. Kim, S.H. Baek, J.Y. Um, B.S. Shim, K.S. Ahn, Resveratrol attenuates constitutive STAT3 and STAT5 activation through induction of PTPε and SHP-2 tyrosine phosphatases and potentiates sorafenib-induced apoptosis in renal cell carcinoma, BMC Nephrol. 17 (2016). https://doi.org/10.1186/s12882-016-0233-7.

[127] M.K. Shanmugam, P. Rajendran, F. Li, C. Kim, S. Sikka, K.S. Siveen, A.P. Kumar, K.S. Ahn, G. Sethi, Abrogation of STAT3 signaling cascade by zerumbone inhibits proliferation and induces apoptosis in renal cell carcinoma xenograft mouse model, Mol. Carcinog. 54 (2015) 971–985. https://doi.org/10.1002/mc.22166.

[128] S. Saraswati, A. Alhaider, A.M. Abdelgadir, P. Tanwer, H.M. Korashy, Phloretin attenuates STAT-3 activity and overcomes sorafenib resistance targeting SHP-1-mediated inhibition of STAT3 and Akt/VEGFR2 pathway in hepatocellular carcinoma, Cell Commun. Signal. 17 (2019) 1–18. https://doi.org/10.1186/s12964-019-0430-7.

[129] Y. Jin, Y.J. Yoon, Y.J. Jeon, J. Choi, Y.J. Lee, J. Lee, S. Choi, O. Nash, D.C. Han, B.M. Kwon, Geranylnaringenin (CG902) inhibits constitutive and inducible STAT3 activation through the activation of SHP-2 tyrosine phosphatase, Biochem. Pharmacol. 142 (2017) 46–57. https://doi.org/10.1016/j.bcp.2017.06.131.

[130] M. Azmanova, A. Pitto-Barry, Oxidative Stress in Cancer Therapy: Friend or Enemy?, ChemBioChem. 23 (2022). https://doi.org/10.1002/cbic.202100641.

[131] J.E. Park, B. Park, I.G. Chae, D. Kim, J. Kundu, J.K. Kundu, K. Chun, Carnosic acid induces apoptosis through inactivation of Src / STAT3 signaling pathway in human renal carcinoma Caki cells, (2016) 2723–2732. https://doi.org/10.3892/or.2016.4642.

[132] K.S. Prabhu, A.A. Bhat, K.S. Siveen, S. Kuttikrishnan, S. Shadab, T. Raheed, A. Jochebeth, A.Q. Khan, M.Z. Chawdhery, M. Haris, M. Kulinski, S. Dermime, M. Steinhoff, Biomedicine & Pharmacotherapy Sanguinarine mediated apoptosis in Non-Small Cell Lung Cancer via generation of reactive oxygen species and suppression of JAK / STAT pathway, Biomed. Pharmacother. 144 (2021) 112358. https://doi.org/10.1016/j.biopha.2021.112358.

[133] Y. Xie, S. Kole, P. Precht, M.J. Pazin, M. Bernier, S-Glutathionylation impairs signal transducer and activator of transcription 3 activation and signaling, Endocrinology. 150 (2009) 1122–1131. https://doi.org/10.1210/en.2008-1241.

[134] E. Butturini, A. Carcereri De Prati, G. Chiavegato, A. Rigo, E. Cavalieri, E. Darra, S. Mariotto, Mild oxidative stress induces S-glutathionylation of STAT3 and enhances chemosensitivity of tumoural cells to chemotherapeutic drugs, Free Radic. Biol. Med. 65 (2013) 1322–1330. https://doi.org/10.1016/j.freeradbiomed.2013.09.015.

[135] E. Butturini, E. Cavalieri, A.C. de Prati, E. Darra, A. Rigo, K. Shoji, N. Murayama, H. Yamazaki, Y. Watanabe, H. Suzuki, S. Mariotto, Two naturally occurring terpenes, dehydrocostuslactone and costunolide, decrease intracellular GSH content and inhibit STAT3 activation, PLoS One. 6 (2011) 1–9. https://doi.org/10.1371/journal.pone.0020174.

[136] A. Maryam, T. Mehmood, H. Zhang, Y. Li, M. Khan, T. Ma, Alantolactone induces apoptosis, promotes STAT3 glutathionylation and enhances chemosensitivity of A549 lung adenocarcinoma cells to doxorubicin via oxidative stress, Sci. Rep. 7 (2017) 1–18. https://doi.org/10.1038/s41598-017-06535-y.

[137] Y. Zhu, P. Yue, C.F. Dickinson, J.K. Yang, K. Datanagan, N. Zhai, Y. Zhang, G. Miklossy, F. Lopez-Tapia, M.A. Tius, J. Turkson, Natural product preferentially targets redox and metabolic adaptations and aberrantly active STAT3 to inhibit breast tumor growth in vivo, Cell Death Dis. 13 (2022). https://doi.org/10.1038/s41419-022-05477-2.

[138] S.N. Jung, D.S. Shin, H.N. Kim, Y.J. Jeon, J. Yun, Y.J. Lee, J.S. Kang, D.C. Han, B.M. Kwon, Sugiol inhibits STAT3 activity via regulation of transketolase and ROS-mediated ERK activation in DU145 prostate carcinoma cells, Biochem. Pharmacol. 97 (2015) 38–50. https://doi.org/10.1016/j.bcp.2015.06.033.

[139] N. Sadgrove, G.F. Padilla-González, M. Phumthum, Compounds , Methods of Analysis and Authentication, Compd. , Methods Anal. Authentication. 11 (2022) 34.

[140] C. Cimino, O.M. Maurel, T. Musumeci, A. Bonaccorso, F. Drago, E.M.B. Souto, R. Pignatello, C. Carbone, Essential Oils: Pharmaceutical Applications and Encapsulation Strategies into Lipid-Based Delivery Systems, Pharmaceutics. 13 (2021) 327. https://doi.org/10.3390/pharmaceutics13030327.

[141] M. Bunse, R. Daniels, C. Gründemann, J. Heilmann, D.R. Kammerer, M. Keusgen, U. Lindequist, M.F. Melzig, G.E. Morlock, H. Schulz, R. Schweiggert, M. Simon, F.C. Stintzing, M. Wink, Essential Oils as Multicomponent Mixtures and Their Potential for Human Health and Well-Being, Front. Pharmacol. 13 (2022) 1–25. https://doi.org/10.3389/fphar.2022.956541.

[142] J. Sharifi-Rad, A. Sureda, G.C. Tenore, M. Daglia, M. Sharifi-Rad, M. Valussi, R. Tundis, M. Sharifi-Rad, M.R. Loizzo, A. Oluwaseun Ademiluyi, R. Sharifi-Rad, S.A. Ayatollahi, M. Iriti, Biological activities of essential oils: From plant chemoecology to traditional healing systems, 2017. https://doi.org/10.3390/molecules22010070.

[143] A. El Asbahani, K. Miladi, W. Badri, M. Sala, E.H.A. Addi, H. Casabianca, A. El Mousadik, D. Hartmann, A. Jilale, F.N.R. Renaud, A. Elaissari, Essential oils: From extraction to encapsulation, Int. J. Pharm. 483 (2015) 220–243. https://doi.org/10.1016/j.ijpharm.2014.12.069.

[144] K. Arafat, S. Sulaiman, A.M. Al-Azawi, J. Yasin, S. Sugathan, A. Nemmar, S. Karam, S. Attoub, Origanum majorana essential oil decreases lung tumor growth and metastasis in

vitro and in vivo, Biomed. Pharmacother. 155 (2022) 113762. https://doi.org/10.1016/j.biopha.2022.113762.

[145] C.C. Estanislao Gómez, A. Aquino Carreño, D.G. Pérez Ishiwara, E. San Martín Martínez, J. Morales López, N. Pérez Hernández, M.C. Gómez García, Decatropis bicolor (Zucc.) Radlk essential oil induces apoptosis of the MDA-MB-231 breast cancer cell line, BMC Complement. Altern. Med. 16 (2016) 1–11. https://doi.org/10.1186/s12906-016-1136-7.

[146] M.M. Suhail, W. Wu, A. Cao, F.G. Mondalek, K.M. Fung, P.T. Shih, Y.T. Fang, C. Woolley, G. Young, H.K. Lin, Boswellia sacra essential oil induces tumor cell-specific apoptosis and suppresses tumor aggressiveness in cultured human breast cancer cells, BMC Complement. Altern. Med. 11 (2011). https://doi.org/10.1186/1472-6882-11-129.

[147] B. Bayala, I.H.N. Bassole, R. Scifo, C. Gnoula, L. Morel, J.M.A. Lobaccaro, J. Simpore, Anticancer activity of essential oils and their chemical components - A review, Am. J. Cancer Res. 4 (2014) 591–607.

[148] J.F. Lesgards, N. Baldovini, N. Vidal, S. Pietri, Anticancer activities of essential oils constituents and synergy with conventional therapies: A review, Phyther. Res. 28 (2014) 1423–1446. https://doi.org/10.1002/ptr.5165.

[149] A. Kumar, F. Malik, S. Bhushan, V.K. Sethi, A.K. Shahi, J. kaur, S.C. Taneja, G.N. Qazi, J. Singh, An essential oil and its major constituent isointermedeol induce apoptosis by increased expression of mitochondrial cytochrome c and apical death receptors in human leukaemia HL-60 cells, Chem. Biol. Interact. 171 (2008) 332–347. https://doi.org/10.1016/j.cbi.2007.10.003.

[150] S. Catalani, F. Palma, S. Battistelli, S. Benedetti, Oxidative stress and apoptosis induction in human thyroid carcinoma cells exposed to the essential oil from Pistacia lentiscus aerial parts, PLoS One. 12 (2017) 1–15. https://doi.org/10.1371/journal.pone.0172138.

[151] N. Ahani, M.H. Sangtarash, M. Alipour Eskanda-Ni, M. Houshmand, Zataria multiflora boiss. Essential oil induce apoptosis in two human colon cancer cell lines (HCT116 & SW48), Iran. J. Public Health. 49 (2020) 753–762. https://doi.org/10.18502/ijph.v49i4.3183.

[152] Y.C. Chen, C.L. Hsieh, B.M. Huang, Y.C. Chen, Induction of mitochondrial-dependent apoptosis by essential oil of toona sinensis root through akt, mtor and nf-kb signalling pathways in human renal cell carcinoma cells, J. Food Drug Anal. 29 (2021) 433–447. https://doi.org/10.38212/2224-6614.3367.

[153] F. Guesmi, S. Prasad, W. Tahri, I. Dridi, M. Ben Ali, A. Hedfi, I.A. Ismail, A. Landoulsi, Volatile oil of Teucrium alopecurus sensitizes colon cancer cells to TRAIL-induced cell death, Front. Biosci. - Sch. 13 (2021) 1–13. https://doi.org/10.52586/S548.

[154] F. Guesmi, S. Prasad, M. Ben Ali, I.A. Ismail, A. Landoulsi, TRAIL / Apo2L induced apoptosis and inhibits colon carcinogenesis through upregulation of death receptor pathway, 13 (2021).

[155] H. Chen, B. Zhou, J. Yang, X. Ma, S. Deng, Y. Huang, Y. Wen, J. Yuan, X. Yang, Essential oil derived from Eupatorium adenophorum Spreng. mediates anticancer effect by inhibiting STAT3 and AKT activation to induce apoptosis in hepatocellular carcinoma, Front. Pharmacol. 9 (2018) 1–17. https://doi.org/10.3389/fphar.2018.00483.

[156] E. Zare, T. Jamali, S.K. Ardestani, G. Kavoosi, Synergistic effect of Zataria Multiflora essential oil on doxorubicin-induced growth inhibition of PC3 cancer cells and apoptosis,

Complement. Ther. Clin. Pract. 42 (2021) 101286. https://doi.org/10.1016/j.ctcp.2020.101286.

[157] M. Di Martile, S. Garzoli, M. Sabatino, E. Valentini, S. D'Aguanno, R. Ragno, D. Del Bufalo, Antitumor effect of Melaleuca alternifolia essential oil and its main component terpinen-4-ol in combination with target therapy in melanoma models, Cell Death Discov. 7 (2021) 127. https://doi.org/10.1038/s41420-021-00510-3.

[158] T. Maruoka, A. Kitanaka, Y. Kubota, G. Yamaoka, T. Kameda, O. Imataki, H. Dobashi, S. Bandoh, N. Kadowaki, T. Tanaka, Lemongrass essential oil and citral inhibit Src/Stat3 activity and suppress the proliferation/survival of small-cell lung cancer cells, alone or in combination with chemotherapeutic agents, Int. J. Oncol. 52 (2018) 1738–1748. https://doi.org/10.3892/ijo.2018.4314.

[159] A. Lahmar, A. Mathey, V. Aires, D. Elgueder, A. Vejux, R. Khlifi, F. Sioud, L. Chekir-Ghedira, D. Delmas, Essential oils, pituranthos chloranthus and teucrium ramosissimum, chemosensitize resistant human uterine sarcoma mes-sa/dx5 cells to doxorubicin by inducing apoptosis and targeting p-glycoprotein, Nutrients. 13 (2021). https://doi.org/10.3390/nu13051719.

[160] C. Zeng, D. Fan, Y. Xu, X. Li, J. Yuan, Q. Yang, X. Zhou, Curcumol enhances the sensitivity of doxorubicin in triple-negative breast cancer via regulating the miR-181b-2-3p-ABCC3 axis, Biochem. Pharmacol. 174 (2020) 113795. https://doi.org/10.1016/j.bcp.2020.113795.

[161] S. Bukhari, M.H. Siddique, A. Naeem, I.U. Khan, Z. Ali, A. Essa, F. Fazal, R.A. Anis, L. Moran, A. Sultan, I. Murtaza, P. Vanhara, M. Anees, Combined efficacy of Cinnamomum zeylanicum and doxorubicin against leukemia through regulation of TRAIL and NF-kappa B pathways in rat model, Mol. Biol. Rep. 49 (2022) 6495–6507. https://doi.org/10.1007/s11033-022-07478-y.

[162] S. Arunachalam, M.F. Nagoor Meeran, S. Azimullah, N.K. Jha, D. Saraswathiamma, S. Subramanya, A. Albawardi, S. Ojha, α-Bisabolol Attenuates Doxorubicin Induced Renal Toxicity by Modulating NF-ϰB/MAPK Signaling and Caspase-Dependent Apoptosis in Rats, Int. J. Mol. Sci. 23 (2022). https://doi.org/10.3390/ijms231810528.

[163] E. Becer, H. Kabadayı, K.H.C. Başer, H.S. Vatansever, Boswellia sacra essential oil manages colon cancer stem cells proliferation and apoptosis: a new perspective for cure, J. Essent. Oil Res. 33 (2021) 53–62. https://doi.org/10.1080/10412905.2020.1839586.

[164] S.E. Nigjeh, S.K. Yeap, N. Nordin, B. Kamalideghan, H. Ky, R. Rosli, Citral induced apoptosis in MDA-MB-231 spheroid cells, BMC Complement. Altern. Med. 18 (2018) 56. https://doi.org/10.1186/s12906-018-2115-y.

[165] P. Choudhury, A. Barua, A. Roy, R. Pattanayak, M. Bhattacharyya, P. Saha, Chemico-Biological Interactions Eugenol restricts Cancer Stem Cell population by degradation of β-catenin via N-terminal Ser37 phosphorylation-an in vivo and in vitro experimental evaluation, Chem. Biol. Interact. 316 (2020) 108938. https://doi.org/10.1016/j.cbi.2020.108938.

[166] M. Krifa, H. El Mekdad, N. Bentouati, A. Pizzi, K. Ghedira, M. Hammami, S.E. El Meshri, L. Chekir-Ghedira, Immunomodulatory and anticancer effects of Pituranthos tortuosus essential oil, Tumor Biol. 36 (2015) 5165–5170. https://doi.org/10.1007/s13277-015-3170-3.

[167] T. Jamali, G. Kavoosi, S.K. Ardestani, In-vitro and in-vivo anti-breast cancer activity of

OEO (Oliveria decumbens vent essential oil) through promoting the apoptosis and immunomodulatory effects, J. Ethnopharmacol. 248 (2020) 112313. https://doi.org/10.1016/j.jep.2019.112313.

[168] α-Pinene Enhances the Anticancer Activity of Natural Killer Cells via ERK-AKT Pathway.pdf, (n.d.).

[169] J. Jampilek, K. Kralova, Anticancer Applications of Essential Oils Formulated into Lipid-Based Delivery Nanosystems, Pharmaceutics. 14 (2022) 30–35. https://doi.org/10.3390/pharmaceutics14122681.

[170] P.M. Albuquerque, S.G. Azevedo, C.P. de Andrade, N.C. de S. D'Ambros, M.T.M. Pérez, L. Manzato, Biotechnological Applications of Nanoencapsulated Essential Oils: A Review, Polymers (Basel). 14 (2022). https://doi.org/10.3390/polym14245495.

[171] W. Weisany, S. Yousefi, N.A. Tahir, N. Golestanehzadeh, Targeted delivery and controlled released of essential oils using nanoencapsulation : A review, Adv. Colloid Interface Sci. 303 (2022) 102655. https://doi.org/10.1016/j.cis.2022.102655.

[172] T.N. Barradas, K.G. de Holanda e Silva, Nanoemulsions of essential oils to improve solubility, stability and permeability: a review, Environ. Chem. Lett. 19 (2021) 1153–1171. https://doi.org/10.1007/s10311-020-01142-2.

[173] G. Rajivgandhi, K. Saravanan, G. Ramachandran, J. Li, L. Yin, International Journal of Biological Macromolecules Enhanced anti-cancer activity of chitosan loaded Morinda citrifolia essential oil against A549 human lung cancer cells, Int. J. Biol. Macromol. 164 (2020) 4010–4021. https://doi.org/10.1016/j.ijbiomac.2020.08.169.

[174] P. Panyajai, F. Chueahongthong, N. Viriyaadhammaa, W. Nirachonkul, S. Tima, S. Chiampanichayakul, S. Anuchapreeda, S. Okonogi, Anticancer activity of Zingiber ottensii essential oil and its nanoformulations, PLoS One. 17 (2022). https://doi.org/10.1371/journal.pone.0262335.

[175] T.L.K. Ryeziu, E.H. Aloci, A.L.O. Hala, U.B.A.Ǧ Ci, A.O. Ral, G.J.S. Tefkov, A.Z. Immer, M.B.A. Alihu, Nanoencapsulation of Origanum vulgare essential oil into liposomes with anticancer potential, 77 (2022) 172–178. https://doi.org/10.1691/ph.2022.1230.

[176] P. Singh, S.K. Sahoo, Piperlongumine loaded PLGA nanoparticles inhibit cancer stem-like cells through modulation of STAT3 in mammosphere model of triple negative breast cancer, Int. J. Pharm. 616 (2022). https://doi.org/10.1016/j.ijpharm.2022.121526.

[177] F. Danhier, E. Ansorena, J.M. Silva, R. Coco, A. Le Breton, V. Préat, PLGA-based nanoparticles: An overview of biomedical applications, J. Control. Release. 161 (2012) 505–522. https://doi.org/10.1016/j.jconrel.2012.01.043.

[178] E. Ercin, S. Kecel-Gunduz, B. Gok, T. Aydin, Y. Budama-Kilinc, M. Kartal, Laurus nobilis L. Essential Oil-Loaded PLGA as a Nanoformulation Candidate for Cancer Treatment, Molecules. 27 (2022). https://doi.org/10.3390/molecules27061899.

[179] K.B. Almeida, A.S. Ramos, J.B.B. Nunes, B.O. Silva, E.R.A. Ferraz, A.S. Fernandes, I. Felzenszwalb, A.C.F. Amaral, V.G. Roullin, D.Q. Falcão, PLGA nanoparticles optimized by Box-Behnken for efficient encapsulation of therapeutic Cymbopogon citratus essential oil, Colloids Surfaces B Biointerfaces. 181 (2019) 935–942. https://doi.org/10.1016/j.colsurfb.2019.06.010.

[180] M. Almnhawy, M. Jebur, M. Alhajamee, M.H. Tabrizi, PLGA-Based Nano-Encapsulation

of Trachyspermum Ammi Seed Essential Oil (TSEO- PNP) as a Safe , Natural , Efficient , Anticancer Compound in Human HT-29 Colon Cancer Cell Line PLGA-Based Nano-Encapsulation of Trachyspermum Ammi Seed Essential Oil, Nutr. Cancer. 73 (2021) 2808–2820. https://doi.org/10.1080/01635581.2020.1862256.

[181]   S. Bao, H. Zheng, J. Ye, H. Huang, B. Zhou, Q. Yao, G. Lin, H. Zhang, L. Kou, R. Chen, Dual Targeting EGFR and STAT3 With Erlotinib and Alantolactone Co-Loaded PLGA Nanoparticles for Pancreatic Cancer Treatment, Front. Pharmacol. 12 (2021) 1–12. https://doi.org/10.3389/fphar.2021.625084.

[182]   Dual AO / EB Staining to Detect Apoptosis in Osteosarcoma Cells Compared with Flow Cytometry, (2015) 15–20. https://doi.org/10.12659/MSMBR.893327.

[183]   A. Suarez-Arnedo, F.T. Figueroa, C. Clavijo, P. Arbeláez, J.C. Cruz, C. Muñoz-Camargo, An image J plugin for the high throughput image analysis of in vitro scratch wound healing assays, PLoS One. 15 (2020) 1–14. https://doi.org/10.1371/journal.pone.0232565.

[184]   T.C. Chou, Drug combination studies and their synergy quantification using the chou-talalay method, Cancer Res. 70 (2010) 440–446. https://doi.org/10.1158/0008-5472.CAN-09-1947.

[185]   S. Bhattacharjee, DLS and zeta potential - What they are and what they are not?, J. Control. Release. 235 (2016) 337–351. https://doi.org/10.1016/j.jconrel.2016.06.017.

[186]   A.S. Choudhari, P.C. Mandave, M. Deshpande, P. Ranjekar, O. Prakash, Phytochemicals in cancer treatment: From preclinical studies to clinical practice, Front. Pharmacol. 10 (2020) 1–17. https://doi.org/10.3389/fphar.2019.01614.

[187]   T. Naka, T. Ohkawara, Signal Transduction Pathways in Development: the JAK/STAT Pathway, ELS. (2006) 1–7. https://doi.org/10.1038/npg.els.0004188.

[188]   R. Garcia, T.L. Bowman, G. Niu, H. Yu, S. Minton, C.A. Muro-Cacho, C.E. Cox, R. Falcone, R. Fairclough, S. Parsons, A. Laudano, A. Gazit, A. Levitzki, A. Kraker, R. Jove, Constitutive activation of Stat3 by the Src and JAK tyrosine kinases participates in growth regulation of human breast carcinoma cells, Oncogene. 20 (2001) 2499–2513. https://doi.org/10.1038/sj.onc.1204349.

[189]   S.L. Furtek, D.S. Backos, C.J. Matheson, P. Reigan, Strategies and Approaches of Targeting STAT3 for Cancer Treatment, ACS Chem. Biol. 11 (2016) 308–318. https://doi.org/10.1021/acschembio.5b00945.

[190]   A.G. Porter, R.U. Ja, Emerging roles of caspase-3 in apoptosis, (1999) 99–104.

[191]   J. Chun, R.J. Li, M.S. Cheng, Y.S. Kim, Alantolactone selectively suppresses STAT3 activation and exhibits potent anticancer activity in MDA-MB-231 cells, Cancer Lett. 357 (2015) 393–403. https://doi.org/10.1016/j.canlet.2014.11.049.

[192]   C. Zhao, H. Li, H.J. Lin, S. Yang, J. Lin, G. Liang, Feedback Activation of STAT3 as a Cancer Drug-Resistance Mechanism, Trends Pharmacol. Sci. 37 (2016) 47–61. https://doi.org/10.1016/j.tips.2015.10.001.

[193]   I. Rivolta, A. Panariti, B. Lettiero, S. Sesana, P. Gasco, M.R. Gasco, M. Masserini, G. Miserocchi, Cellular uptake of coumarin-6 as a model drug loaded in solid lipid nanoparticles, J. Physiol. Pharmacol. 62 (2011) 45–53.

[194]   S. Kim, C.H. Kaschula, N. Priedigkeit, A. V Lee, S. V Singh, Forkhead Box Q1 Is a Novel Target of Breast Cancer Stem Cell Inhibition by Diallyl Trisulfide *, 291 (2016) 13495–

13508. https://doi.org/10.1074/jbc.M116.715219.

[195] M. Lois, R. De Antueno, K. Mila, M. Sultan, B. Marie, A. Giacomantonio, C. Anthony, R. Duncan, P. Marcato, ScienceDirect Citral reduces breast tumor growth by inhibiting the cancer stem cell marker ALDH1A3, 0 (2016) 0–11.

[196] J.F. Bromberg, M.H. Wrzeszczynska, G. Devgan, Y. Zhao, R.G. Pestell, C. Albanese, J.E. Darnell, Stat3 as an oncogene, Cell. 98 (1999) 295–303. https://doi.org/10.1016/S0092-8674(00)81959-5.

[197] R.M. De Queiroz, C.M. Takiya, L.P. Tavares, P. Guimarães, G. Rocha, D.S. Alviano, F. Blank, C.S. Alviano, C.R. Gattass, R.M. De Queiroz, C.M. Takiya, Apoptosis-Inducing Effects of Melissa officinalis L . Essential Oil in Glioblastoma Multiforme Cells Apoptosis-Inducing Effects of Melissa officinalis L . Essential Oil in Glioblastoma Multiforme Cells, 7907 (2014). https://doi.org/10.3109/07357907.2014.905587.

[198] M.R. Loizzo, R. Tundis, F. Menichini, A.M. Saab, G.A. Statti, F. Menichini, Antiproliferative effects of essential oils and their major constituents in human renal adenocarcinoma and amelanotic melanoma cells, (2008) 1002–1012. https://doi.org/10.1111/j.1365-2184.2008.00561.x.

[199] A. Venditti, A.M. Serrilli, S. Vittori, F. Papa, F. Maggi, M. Di Cecco, G. Ciaschetti, M. Bruno, S. Rosselli, A. Bianco, R. La Sapienza, C. Piazzale, A. Moro, V.S. Agostino, P. Nazionale, V. Occidentale, P. Sciences, S. Chemistry, O. Ii, Secondary Metabolites from Pinus mugo Turra subsp . mugo Growing in the Majella National Park (Central Apennines , Italy), 10 (2013) 2091–2100.

[200] P. Mag, N.T. Hoai, H.V. Duc, D.T. Thao, A. Orav, A. Raal, Selectivity of Pinus sylvestris extract and essential oil to estrogen - insensitive breast cancer cells Pinus sylvestris against cancer cells, 11 (2015) 290–295. https://doi.org/10.4103/0973-1296.166052.

[201] E. Oil, A. Activity, C.C. Evaluation, Original article : PINUS ROXBURGHII ESSENTIAL OIL ANTICANCER ACTIVITY, (2018) 233–245.

[202] P. Ren, X. Ren, L. Cheng, L. Xu, Frankincense, pine needle and geranium essential oils suppress tumor progression through the regulation of the AMPK/mTOR pathway in breast cancer, Oncol. Rep. (2017) 129–137. https://doi.org/10.3892/or.2017.6067.

[203] J. Jo, J.U.S. Park, Y. Park, Y.Z.O.O. Chae, G. Lee, G. Park, B. Jang, Pinus densiflora leaf essential oil induces apoptosis via ROS generation and activation of caspases in YD-8 human oral cancer cells, (2012) 1238–1245. https://doi.org/10.3892/ijo.2011.1263.

[204] S. Cho, E. Lee, S. Kim, H. Lee, Essential oil of Pinus koraiensis inhibits cell proliferation and migration via inhibition of p21-activated kinase 1 pathway in HCT116 colorectal cancer cells, (2014) 1–9.

[205] Y. Zhang, C. Xin, C. Cheng, Z. Wang, Antitumor activity of nanoemulsion based on essential oil of Pinus koraiensis pinecones in MGC-803 tumor-bearing nude mice, Arab. J. Chem. 13 (2020) 8226–8238. https://doi.org/10.1016/j.arabjc.2020.09.058.

[206] Chemistry Biodiversity - 2016 - Bojovi - Essential-Oil Variability in Natural Populations of Pinus mugo Turra from the.pdf, (n.d.).

[207] Modulation of STAT3 Signaling, Cell Redox Defenses and Cell Cycle Checkpoints by β-Caryophyllene in Cholangiocarcinoma Cells-Possible Mechanisms Accounting for Doxorubicin Chemosensitization and Chemoprevention.pdf, (n.d.).

[208] P.P. Approach, Essential Oil Phytocomplex Activity , a Review with a, (n.d.) 1–15.

[209] J. Kim, J.S. Won, A.K. Singh, A.K. Sharma, I. Singh, STAT3 regulation by S-nitrosylation: Implication for inflammatory disease, Antioxidants Redox Signal. 20 (2014) 2514–2527. https://doi.org/10.1089/ars.2013.5223.

[210] M. Carballo, M. Conde, R. El Bekay, J. Martı, J. Monteseirı, F.J. Bedoya, F. Sobrino, Oxidative Stress Triggers STAT3 Tyrosine Phosphorylation and Nuclear Translocation in Human Lymphocytes * ´ s, 274 (1999) 17580–17586. https://doi.org/10.1074/jbc.274.25.17580.

[211] E. Butturini, A.C. de Prati, S. Mariotto, Redox regulation of STAT1 and STAT3 signaling, Int. J. Mol. Sci. 21 (2020) 1–18. https://doi.org/10.3390/ijms21197034.

[212] C. Kim, F. Arfuso, R.P. Samym, A. Deivasigamanim, L. Hsiu, K. Lim, L. Wang, B.C. Goh, A.P. Kumar, K.M. Hui, Nimbolide-Induced Oxidative Stress Abrogates STAT3 Signaling Cascade and Inhibits Tumor Growth in Transgenic Adenocarcinoma of Mouse Prostate Model, 24 (2016) 575–589. https://doi.org/10.1089/ars.2015.6418.

[213] H.M.E. Azzazy, A. Abdelnaser, H. Al Mulla, A.M. Sawy, S.N. Shamma, M. Elhusseiny, S. Alwahibi, N.K. Mahdy, S.A. Fahmy, Essential Oils Extracted from Boswellia sacra Oleo Gum Resin Loaded into PLGA − PCL Nanoparticles : Enhanced Cytotoxic and Apoptotic Effects against Breast Cancer Cells, (2023) 2–10. https://doi.org/10.1021/acsomega.2c06390.

[214] M.A. Thalappil, E. Butturini, A. Carcereri de Prati, I. Bettin, L. Antonini, F.U. Sapienza, S. Garzoli, R. Ragno, S. Mariotto, Pinus mugo Essential Oil Impairs STAT3 Activation through Oxidative Stress and Induces Apoptosis in Prostate Cancer Cells, Molecules. 27 (2022) 4834. https://doi.org/10.3390/molecules27154834.

9. ACKNOWLEDGEMENTS